

LIFE Integrated Projects 2016

Optimising the implementation of the 2nd RBMP in the Malta River Basin District

LIFE 16 IPE MT 008



Action A.9:

***Development of Groundwater Models to Support Groundwater Management in the
Maltese Islands***

Deliverable D.6.1: Modelling Manual – Part 3: Scenarios

Development of Groundwater Models to Support Groundwater Management in the Maltese Islands

Deliverable D6.1: Modelling Manual
Part 3: Scenarios

Contracting Authority	Government of Malta Ministry for Energy and Water Management The Energy & Water Agency
Contractor	TEA SISTEMI SpA (TEA) STEAM Srl. (STEAM) University of Siena-Centre of Geotechnologies (CGT)
Sub-contractor	Adi Associates Environmental Consultants Ltd (ADI)
Contract no.	CT 3068/2018
Project Manager	Iacopo Borsi (TEA)
Title	Development of groundwater models to support groundwater management in the Maltese island, Inception Report
Authors	Iacopo Borsi, Francesca Lotti (TEA) Paolo Basile, Tiziana Mazzoni (STEAM) Enrico Guastaldi, Alessio Barbagli (CGT)
QC check	Riccardo Corsi (STEAM) Adrian Mallia (ADI)
Document history	Version 1, June 2020 – Sent to EWA for approval.

Table of Contents

Acronyms and abbreviations.....	5
Executive Summary	6
Introduction.....	Error! Bookmark not defined.
Part 1: Models for Malta	13
Malta Mean Sea Level Aquifer	14
Introduction	14
Hydrogeological Scenario 1 (HG_S1).....	16
Abstraction Scenario 1 (ABS_S1).....	18
Abstraction Scenario 2 (ABS_S2).....	21
Abstraction Scenario 3 (ABS_S3).....	22
Abstraction Scenario 4 (ABS_S4).....	23
Abstraction Scenario 5 (ABS_S5).....	24
Abstraction Scenario 6 (ABS_S6).....	25
Recharge Scenario 1 (RCH_S1).....	27
Recharge Scenario 2 (RCH_S2).....	28
Alternative Development Scenario 1 (AD_S1).....	30
Method.....	30
Application	32
Climate Change Scenario 1 (CC_S1).....	36
Climate Change Scenario 2 (CC_S2).....	38
Climate Change Scenario 3 (CC_S3).....	39
Artificial Recharge Scenario 1 (AR_S1).....	40
Artificial Recharge Scenario 2 (AR_S2).....	41
Artificial Recharge Scenario 3 (AR_S3).....	42
Comments.....	44
Mizieb and Pwales	46
Hydrogeological Scenario 1 (HG_S1).....	46
Domain and discretization	47
Boundary condition	47
Initial properties and heads.....	48
Results	50
Zone calibration.....	50

PP calibration	53
Water budget and head distribution	57
Aquifer Management Scenario 1 (AM_S1).....	60
Aquifer Management Scenario 2 (AM_S2).....	61
Aquifer Management Scenario 3 (AM_S3).....	62
Comments.....	63
Part 2: Models for Gozo.....	64
Gozo Mean Sea Level Aquifer.....	65
Introduction	65
Hydrogeological Scenario 1 (HG_S1).....	67
Abstraction Scenario 1 (ABS_S1).....	69
Abstraction Scenario 2 (ABS_S2).....	71
Abstraction Scenario 3 (ABS_S3).....	72
Climate Change Scenario 1 (CC_S1).....	74
Ghajnsielem Perched Aquifer	76
Introduction	76
Abstraction Scenario 1 (ABS_S1).....	77
References.....	78
Appendix 1 - Density of fresh and seawater	79

Acronyms and abbreviations

BC	Blue Clay
BRGM	Bureau de Recherches Géologiques et Minières
EC	Electric Conductivity (of water)
EWA	Energy and Water Agency
GHB	General Head Boundary
GUI	Graphical User Interface
GL	Globigerina Limestone
LCL	Lower Coralline Limestone
MSLA	Mean Sea Level Aquifer
UCL	Upper Coralline Limestone
WSC	Water Services Corporation

Executive Summary

Scenario modelling is the activity that shows the usage of numerical models in a dynamic approach, namely the application of models as effective tools to assess future (or alternative) settings due to the variation of anthropic or natural conditions, such as management of resources, abstraction policy, land use variation, changing in climate conditions, etc.

This report describes the work done during Activity 6 to apply transient models (as results of Activity 4) in the picture above depicted. Transient models have been slightly modified to be used as reference (or base) model in scenarios simulation: the relevant change, with respect to Activity 4, regard the time discretization which was simplified in a compact form to be consistent with the long-term timeframe assumed for future scenarios. On the other hand, the finer time discretization defined in Activity 4 was necessary mainly for the calibration procedure, which is not the aim of Activity 6.

The methodology started by defining a classification of different kind of scenarios, depending on the main changes applied, for instance: abstraction, recharge, management, etc.

This methodology was applied to all the aquifer systems considered in the study.

The scenarios development at the present stage does not include the uncertainty analysis that would be necessary to associate the degree of reliability to the results obtained. Given the high number of assumptions of the reference models and the missing of important details which influence some of the prediction outcome, the uncertainty is likely to be relatively high. This is also due to the fact that a “all purposes model” cannot exist and every kind of scenario would require a specifically built model with assumptions and details important to the specific prediction to be provided (see for instance Doherty and Moore, 2017 for a summary of related concepts).

Due to the high interest on Malta MSLA as the main aquifer system of the Maltese archipelago, 16 scenarios have been performed for this aquifer; 4 were devoted to Mizieb-Pwales system, 5 to Gozo MSLA and 1 to Ghajnsielem, for a total of 26 scenarios. The following list summarizes the model runs classified by category and the code used to identify it.

Malta MSLA:

- Hydrogeological Scenario - HG (1)
- Abstraction Scenario - ABS (6).
- Recharge Scenario – RCH (2)
- Alternative Development Scenario - AD (1)
- Climate Change Scenario - CC (3)
- Artificial Recharge Scenario - AR (3)

Mizieb & Pwales:

- Hydrogeological Scenario – HG (1)
- Aquifer Management Scenario – AM (3)

Gozo MSLA:

- Hydrogeological Scenario – HG (1)
- Abstraction Scenarios – ABS (3)
- Climate Change Scenario – CC (1)

Ghajnsielem perched aquifer:

- Abstraction Scenario – ABS (1)

The main conclusions for each model run are reported hereunder. The adjectives “worse” and “better” are intended with respect to the reference situation, and are to be considered in terms of groundwater head and related freshwater-seawater surface.

Malta MSLA:

- **HG_S1:** worse than the reference situation. The scenario is focused on the overall aquifer thickness reduction (to a half) and consequent hydraulic conductivity (K) increase (to the double) which is a reliable possibility, since the first parameter is unknown and the second is affected by estimate errors. Simulation with the SAA approach would not highlight main differences, while the SWI2 simulation (which takes into account even more assumed variables), presents an extremely different situation. The use of SWI2 (which includes time, K, aquifer thickness and storage coefficient) is recommended when a better understanding of the physical parameters will be available through new investigations and monitoring.
- **ABS_S1:** worse than the reference situation. The scenario is focused to represent a more reliable amount of private abstraction trying to keep the parameter field acceptably calibrated. In order to better evaluate the effect of the private abstraction, the volume abstracted should be known more in details, not only as an overall amount but associated to each single well average abstraction. When this information will be complete, a new round of calibration of the parameter field is recommended.
- **ABS_S2:** worse than the reference situation. Private abstraction is stopped and the public groundwater abstraction is increased. This scenario does not seem to be sustainable, regardless of the parameter field applied with high local and general rise of the interface.
- **ABS_S3:** not so different from the reference situation. Public borehole abstraction is stopped. Private abstraction is kept as in the reference model, as well as pumping stations abstraction.
- **ABS_S4:** better than the reference situation. Public abstraction is completely stopped, commercial abstraction is kept as in the reference model and groundwater resources allocated to the agricultural sector are increased by 2.5 times.
- **ABS_S5:** not so different from the reference situation. Commercial abstraction is completely stopped, with agricultural and public abstraction kept as in the reference model.
- **ABS_S6:** worse than the reference situation, but with an additional water volume that can be saved from other pumping sources. Draining water at an elevation higher than 0 m asl would in general be a preferable option than pumping. A proper representation of this scenario would

require further information about the hydraulic conductivity in the selected position of the gallery through pumping tests.

- RCH_S1: worse than the reference situation. A 30% reduction of losses with respect to the 99-2015 period average is applied, keeping other stresses same as in the reference model.
 - RCH_S2: extremely worse than the reference situation. This scenario is not even thinkable and demonstrates the importance of a wise urbanization that, even in already built up areas, should imply the recommendation provided by a wide literature about the urban hydrogeology (see for instance the review on the matter by Schirmer et al., 2012).
 - AD_S1: this scenario qualitatively simulates the effect of a deep well-field located at the center of the island, abstracting seawater from beneath the freshwater-saltwater interface. Pumping from below the interface would move it downward. As a consequence, the hydraulic head (which rests as a pillow over the saltwater) would move down accordingly. If the final head goes below 0 m asl, the result would be an increase in seawater intrusion from the coast; this is very likely to happen given the very low head elevation in the example area (< 1 m asl) and of the MSLA in general (< 2 m asl). Feasibility of such a well is highly questionable, at risk of failure because of probable low K, at risk of high impact because of the variation of the classical reference sea level from 0 m asl to a lower elevation (in a measure which is function of K, which is not known). The idea should be abandoned, moving to alternative solutions, such as lifting the sea water from the sea (and not from hundreds of meters below ground surface) on the west coast, having the same advantages in terms of concentrating the RO treatment plant in a single location and of the high topographic elevation to distribute water by gravity. The potential energy required for the lifting in this case would be much lower, rising the volume of water of about 180 m instead of more than 300 m.
 - CC_S1: worse than the reference situation. In general, impact of climate change seems to be extremely less threatening with respect to wrong groundwater management practices.
 - CC_S2: worse than the reference situation. In general, impact of climate change seems to be extremely less threatening with respect to wrong groundwater management practices.
 - CC_S3: not so different from the reference situation. In general, impact of climate change seems to be extremely less threatening with respect to wrong groundwater management practices.
 - AR_S1: locally better than the reference situation.
 - AR_S2: better than the reference situation, with important effects over the whole system.
 - AR_S3: not so different from the reference situation. Furthermore, the model assumes that the creation of new dams does not interfere with the recharge capacity of the existing ones, but this is not reliable, since the flow intercepted by an upstream dam is likely to reduce the flow to the downstream dam along the same valley. Estimates of the dams effect could be performed by hydrological modelling through surface water flow simulations. This would also give some inputs to the groundwater counterpart in terms of a better spatial distribution of recharge.
- Recharge Scenario – RCH (2)

Mizieb & Pwales: the preliminary results obtained for the Mizieb-Pwales model are mostly based on assumptions and observations affected by a high uncertainty. The whole process needs to be revised as

soon as further and updated data are made available. Nevertheless, some points can be commented both regarding the model calibration and the scenarios:

- in order to calibrate the heads, the model adjust the parameters in order to get more water from outside the system, since it does not “receive” enough water from direct recharge;
- this can be interpreted with an additional recharge provided by runoff over the Blue Clay and/or local discontinuities in BC and faults. Some insights from the calibration process would suggest a lateral exchange from Mizieb to Pwales in that area;
- AM_S1: better than the reference situation, but the effect of single boreholes injection is strongly affected by the local hydraulic conductivity and degree of fracturing. If K is high, the raise in head would be small and spread in a wide area, if K is low the head would raise only locally, with little effect over wide areas. Furthermore, a critical K in points near the coast (for instance W4 in Figure 44. Potentiometric surface deformation due to the 4 injection wells.) would make the difference between creating a hydraulic barrier to seawater intrusion (hard to achieve) and throwing away freshwater to the sea (easier to happen).
- AM_S2: better than the reference situation and AM_S1. Shaft B, closer to the coast, does not play a fundamental role in the overall management, vice versa could increase the outflow of freshwater to the sea.
- AM_S3: better than the reference situation and AM_S1. It seems to be more efficient than AM_S2.

Gozo MSLA:

- HG_S1: this new model run features different Hydraulic Conductivity values, loosely based on the experience acquired by EWA from the operation of groundwater abstraction wells. In particular, the western zone of the island is now represented to have a conductivity halving the value found through calibration for the entire northern part. The model run shows that the piezometry mainly changes in the northern part of the aquifer, as expected, while this difference slight influences the head elevation in the high exploitation zone (south part): therefore, this scenario confirms the suggestion (already pointed out in Deliverable D4.1) that additional investigations on transmissivity and piezometry level of the northern zone are needed to get a deeper understanding of the whole flow regime in Gozo MSLA.
- ABS_S1: the abstraction conditions for private usage are taken the same, while the public abstraction (pumping stations and boreholes) is reduced by 3000 m³/day which will instead be sourced from the new RO desalination plant at Hondoq ir-Rummien. Results show that this abstraction setting is more sustainable than the current one (SP3): the piezometry level is always positive even in the high exploitation region (the minimum value is 0.161 m), and even the saltwater interface is never reaching the critical value (maximum level is -5.31 m).
- ABS_S2: the private pumping is reduced by 25% with respect to ABS_S1, thus lowering also the private abstraction compared to the existing management. This reduction mimics the impact of the New Water project in Gozo, as well as the adoption of water storage techniques by farmers. This further reduction of withdrawal will improve the status of MSLA, especially for what concerns the distribution of drawdown zone and of the interface, consequently.

- **ABS_S3:** the last abstraction scenario deals with a complete stopping of abstraction for public purposes, allocating groundwater to the agricultural sector. Model run shows that the great impact on the aquifer is given by the public pumping, since in this case the depletion zone is vanishing and no problems of seawater upcoming appear anymore.
- **CC_1:** this version simulates the impact of reduction of recharge due to changing precipitation characteristics and higher evapotranspiration, represented by reducing the recharge term by 10%. Results show that even in this scenario the assumed management for public abstraction (as set out in ABS_S1) is still able to guarantee a status better than the existing one (reference model).

Ghajnsielem perched aquifer:

- **ABS_1:** this scenario simulates the impact of doubling the abstraction in future 50 years. The overall picture shows a reduction of about 4 m of the piezometric surface. Furthermore, the model suggests that this doubled pumping rate is not feasible for all the abstraction points: the one in the southern zone seems to create dry zone larger than in the reference scenario, namely the pumping rate might be too high for the water storage available. In the meantime, the northern part referred as Through in the region classification identified in (Costain, 1958) seems to be not negatively impacted by this increased withdrawal.

Introduction

This report describes the modelling exercise carried out during Activity 6 of the project, dealing with simulations of 26 groundwater management scenarios. The overall objective of this activity is to demonstrate the usage of models defined in Activity 2 and 4, as effective tools to test or verify the impact of different management practices. Furthermore, some of the scenarios are useful to test hydrological settings (for instance bottom elevation, conductivity field, etc.) that differ from the reference ones applied in transient models (namely models delivered as results of Activity 4).

A unique methodology has been applied to all the aquifers considered in the modelling exercise, that summarizes as follows:

- a) Select a reference model.
- b) Define one or more scenarios to be applied, after classifying it (them) in one of the categories defined to qualify the scenario, namely:
 - i. Hydrogeological Scenario: changes regard the hydrodynamic parameters and/or the geometry of the model. These are actually “alternative models” which should be subject of further calibration. However, the simulation can give a first insight on the model sensitivity to these variations.
 - ii. Abstraction Scenario: changes dealing with variation of abstraction due to public or private infrastructure, or both of them.
 - iii. Recharge Scenario: variations to the recharge term, not due to climate variations.
 - iv. Climate Change Scenario: variations to the recharge term arising from long-period variations in temperature and precipitations.
 - v. Artificial Recharge Scenario: testing Managed Aquifer recharge scheme envisaged by the Authority.

Definition of each scenario was achieved in collaboration with EWA, including the establishment of the timeframe to be simulated.

Due to the high interest on Malta MSLA as the main aquifer system of the Maltese archipelago, 16 scenarios have been performed for this aquifer; 4 were devoted to Mizieb-Pwales system, 5 to Gozo MSLA and 1 to Ghajnsielem, for a total of 26 scenarios. The following list summarizes the model runs classified by category, for each base model, and the code used to identify it.

Malta MSLA:

- Hydrogeological Scenario - HG (1)
- Abstraction Scenario - ABS (6).
- Recharge Scenario – RCH (2)
- Alternative Development Scenario - AD (1)

-
- Climate Change Scenario - CC (3)
 - Artificial Recharge Scenario - AR (3)

Mizieb & Pwales:

- Hydrogeological Scenario – HG (1)
- Aquifer Management Scenario – AM (3)

Gozo MSLA:

- Hydrogeological Scenario – HG (1)
- Abstraction Scenarios – ABS (3)
- Climate Change Scenario – CC (1)

Ghajnsielem perched aquifer:

- Abstraction Scenario – ABS (1)

As done for Activity 2 and 4, the report is organized in two parts, one dealing with aquifer systems belonging to Malta (Malta MSLA and Pwales-Mizieb) and one regarding aquifers in Gozo (Gozo MSLA and Ghajnsielem).

Model files to be run through FREEWAT user interface are attached to this report as electronic annex.

Part 1: Models for Malta

Malta Mean Sea Level Aquifer

Introduction

The version of the model used to simulate the interface behavior is described in Delivery 4.1; it makes use of a time discretization of four main periods which cover the same years of the calibrated version as shown in Table 1. Comparison of the stress periods definition used in the calibrated version of the model and in the reference version used to simulate the scenarios.. The hydraulic head distribution of the “reference state” (i.e., Stress Period 3) is reported in Figure 1. Simulated heads (m asl) of Stress Period 3 (1999-2012) used as reference..

Simulation SP	Calibration SP	Start	End	Time (d)
1	1-2	≈ 100 b.C.	31/12/1943	750000
2	3-4	01/01/1944	31/12/1998	20089
3	5-18	01/01/1999	31/12/2012	5114
--	19-42	01/01/2013	31/12/2014	730
4	--	Scenario time frame		20000

Table 1. Comparison of the stress periods definition used in the calibrated version of the model and in the reference version used to simulate the scenarios.

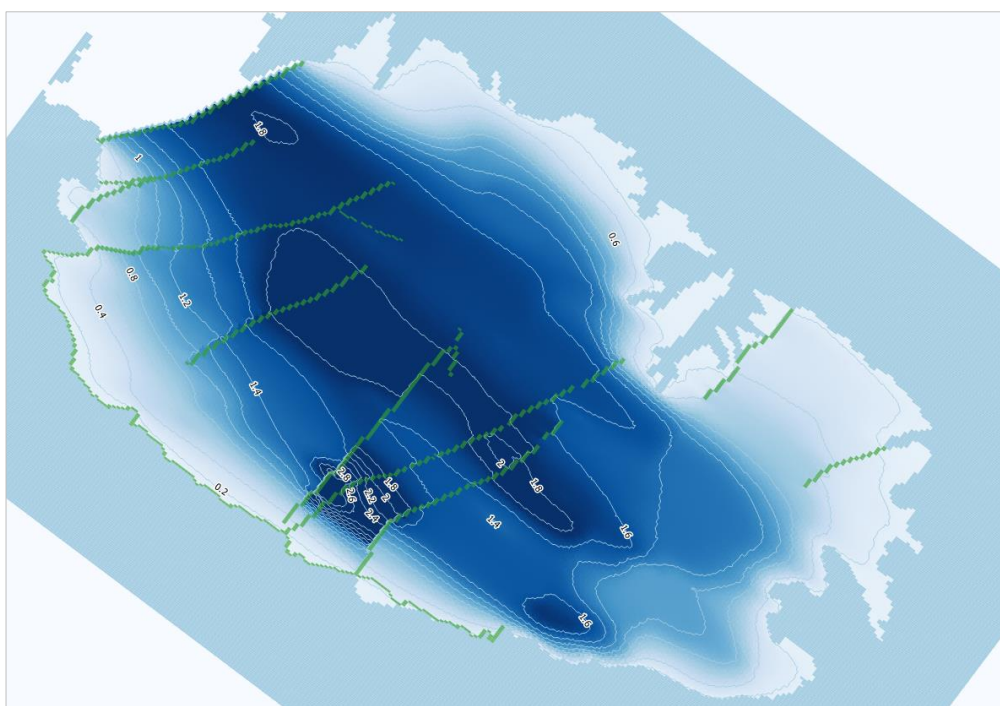


Figure 1. Simulated heads (m asl) of Stress Period 3 (1999-2012) used as reference.

In order to test the most reliable method to represent the interface response to the environmental and anthropic stresses, different simulations of the seawater interface were performed. The first approach was to use the same code applied to the steady state version of the model, i.e. SWI2 (Bakker et al. 2013). The second set of the interface simulations was attained starting from the simulated heads in each stress period and the Ghyben-Herzberg relationship was applied on a cell-by-cell basis, considering a density ratio equal to 0.028 ($\alpha = 36$), as reported in literature in the case of Malta (Morris, 1952; further consideration about the parameter α are reported in Appendix 1).

This semi-analytical approach (SAA) is independent by the possible error on the aquifer thickness and aquifer storage coefficient and only relies on the simulated head distribution, which is function of recharge, hydraulic conductivity and pumping rates. Considering the present knowledge of the system, it seems to be the preferable approach to test the different scenarios.

Anyway, both methods suffer of the wide model grid cells (50x100m) with a punctual underestimate of the upconing in the well cells, which is compensated by a more general diffuse rising of the interface. Results relative to the reference SP3 are shown in Figure 2. Interface contours, SP3 (SAA) used as reference..

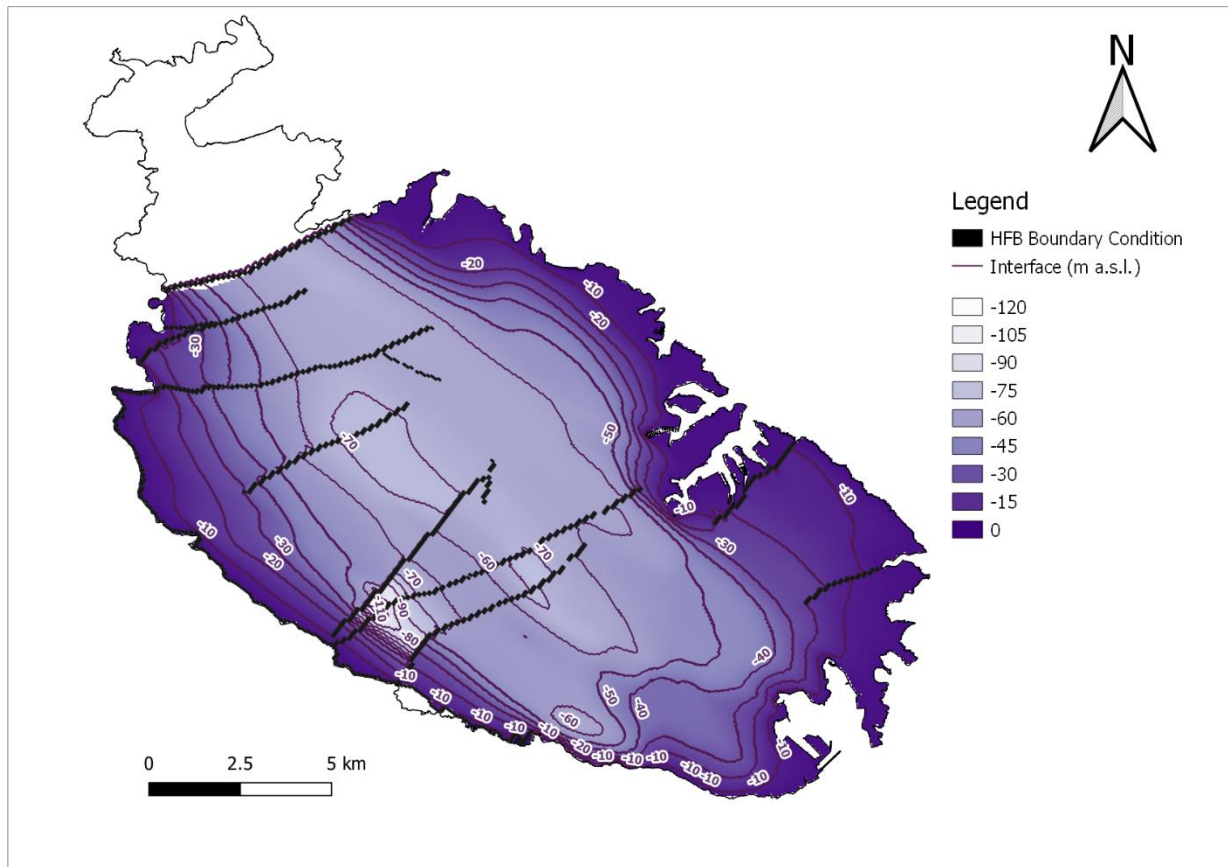


Figure 2. Interface contours, SP3 (SAA) used as reference.

Hydrogeological Scenario 1 (HG_S1)

This scenario highlights the importance of the conceptual model and the initial assumption of aquifer bottom depth. Calibrating just against heads, the estimated hydraulic conductivity (K) is perfectly correlated to the aquifer thickness (b) to provide the aquifer transmissivity which dominated the flow field. This leads to an infinite number of combinations providing the same degree of “calibration”.

Calibrating just against heads does not provide information to constraint correlated parameters (as widely discussed in literature, for instance Hill & Tiedeman 2007, p. 82); for this reason, *prior information* were “searched” among the data as much as possible to limit the non-uniqueness of the numerical solution.

Nevertheless, the prior information about K , estimated from pumping tests, tide tests and chloride concentration, come from estimates of transmissivity and relies on the borehole length intercepting the saturated thickness. The information of the borehole depth is not available for many points, and an intercepted thickness of 20 m was assumed (average of the available information, see Table 18 in Deliverable D4.1 Part 2). If the assumed thickness is 10 instead of 20 m, K value would result doubled ($2.11\text{E-}04$ m/s would be $4.22\text{E-}04$ m/s and so on).

The present scenario is focused on the overall aquifer thickness reduction (to a half) and consequent K increase (to the double) which is a reliable possibility, since the first parameter is unknown and the second is affected by estimate errors.

The effect of doubling the K does not affect the simulated heads (both static and dynamic) if the model bottom is halved (since transmissivity remains the same), but it has a dramatic effect over the simulation of the seawater interface with SWI2, as can be seen from Figure 3. Results from SP3 of HG_S1 (model bottom = -100 m asl) simulated with SWI2, to be compared with of the same SP of the reference model (model bottom = -180 m asl) (Figure 2. Interface contours, SP3 (SAA) used as reference.)..

As stated in the Introduction, we suggest postponing the use of SWI2 (which includes time, K , b , S_y) to when a better understanding of the physical parameters will be available through monitoring.

To this end the application of the SAA “skip” the problem at the moment and can be applied to the reference model version with no “risks” to commit gross errors due to the aquifer thickness uncertainty.

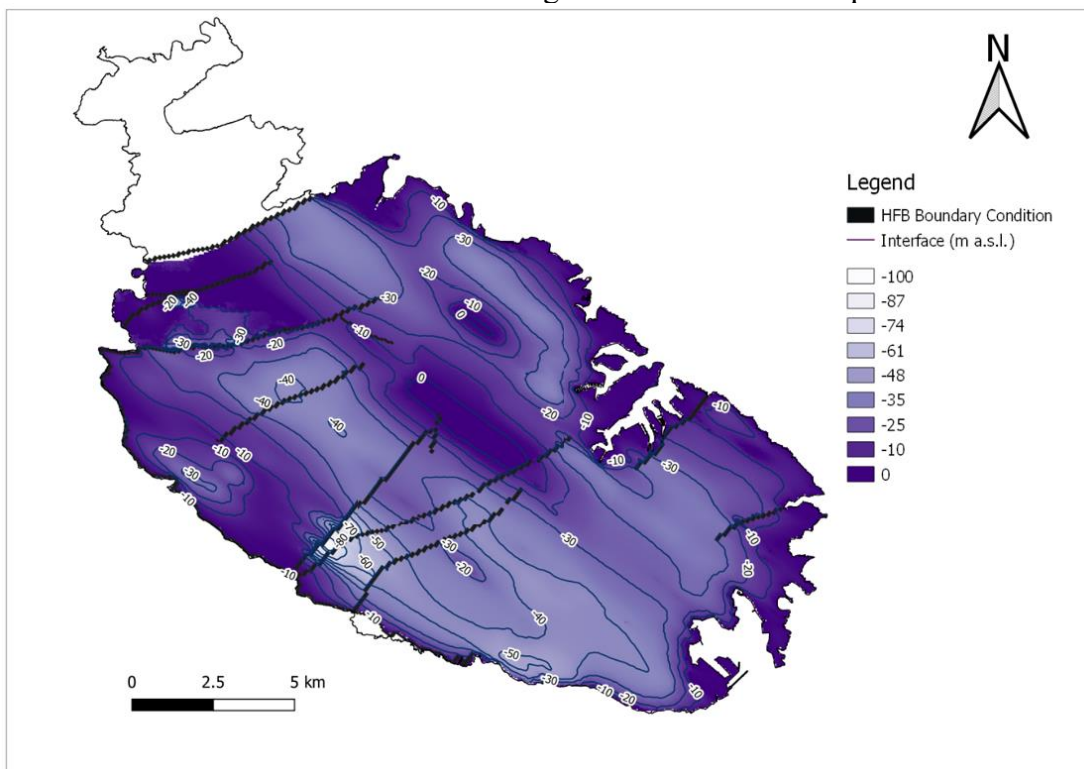


Figure 3. Results from SP3 of HG_S1 (model bottom = -100 m asl) simulated with SWI2, to be compared with of the same SP of the reference model (model bottom = -180 m asl) (Figure 2. Interface contours, SP3 (SAA) used as reference.).

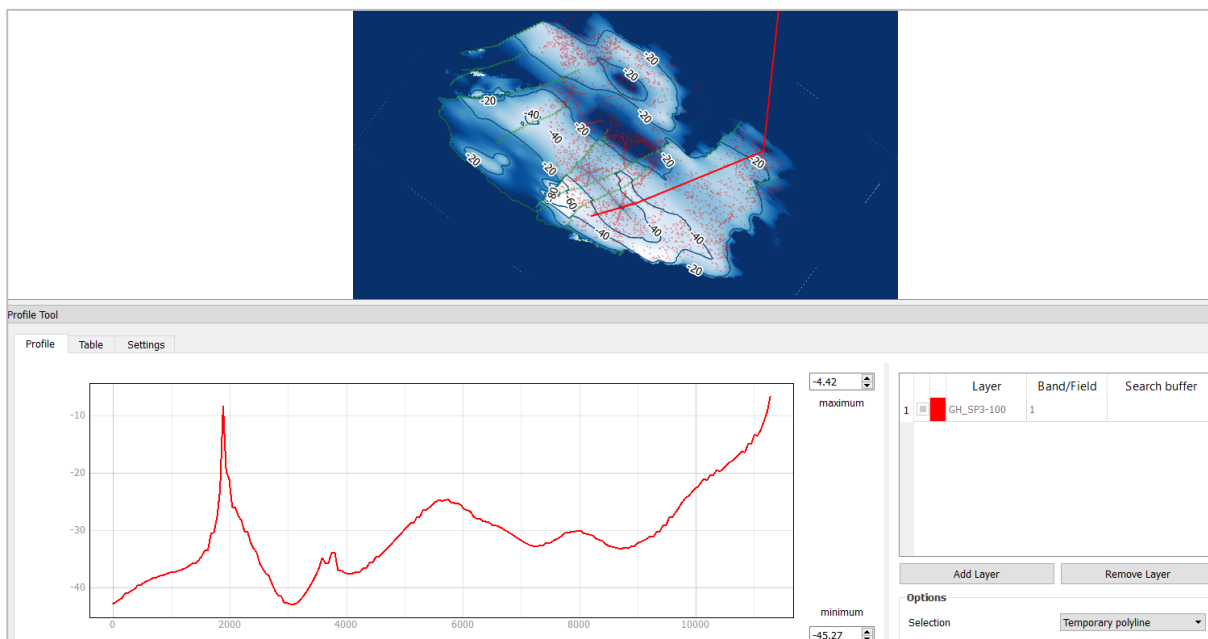
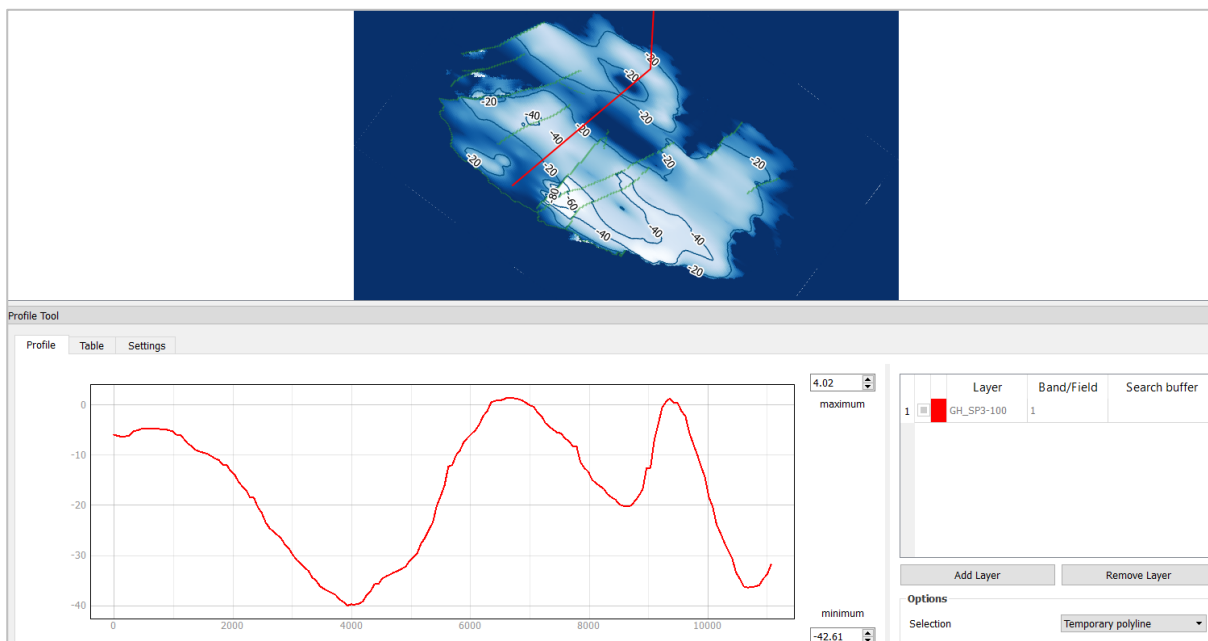


Figure 4. Example of cross-section representing the interface depth in SP3 for HG_S1 (model bottom = -100 m asl).

Abstraction Scenario 1 (ABS_S1)

The first Abstraction Scenario tries to represent the impact of private groundwater abstraction at 2020 levels – that is 10.5 million m³/y. Data used to calibrate the model till 2014 underestimated the abstracted volume by about 50%, producing an estimate of the hydraulic conductivity which is underestimated by a rate proportional to the overall difference in abstracted volumes. This scenario (with doubled private abstraction) applies the *K* reference parameter field (ABS_S1a) and a fictitious increase of 25% to *K* (ABS_S1b) with the aim to approximate the 2020 situation.

Groundwater production is set at 33,750 m³/day, artificial groundwater recharge from municipal distribution system leakages is unchanged.

As also in the following Abstraction Scenarios, Private wells have been distinguished between Agricultural and Commercial (Figure 5. Distinction of Private well types: Agricultural (pink), Commercial (red)).

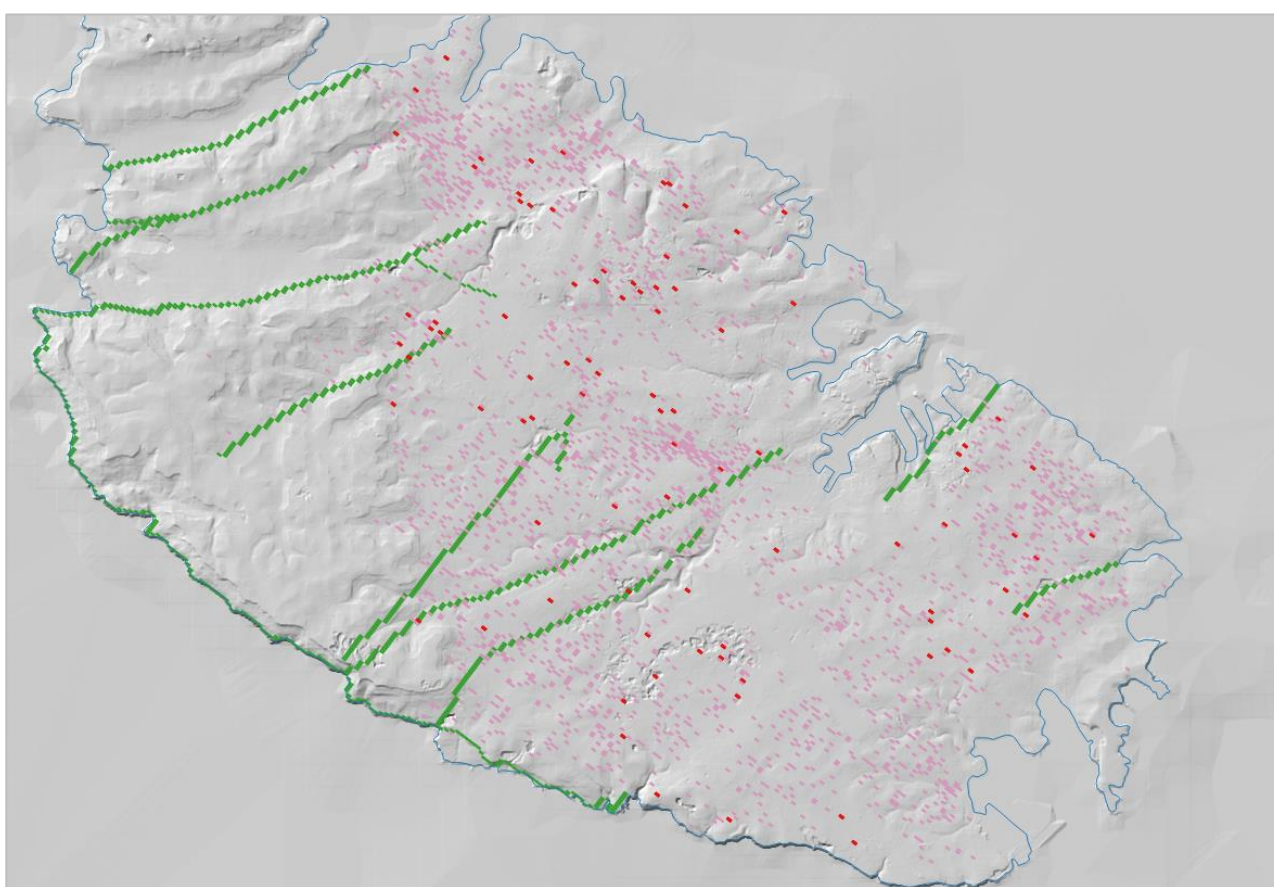


Figure 5. Distinction of Private well types: Agricultural (pink), Commercial (red).

Results are reported in Figure 6. ABS_S1a potentiometric surface and freshwater-seawater interface (*K* as reference model). and Figure 7. ABS_S1b potentiometric surface and freshwater-seawater interface (*K* raised by 25%). If the interface is compared to Figure 2. Interface contours, SP3 (SAA) used as reference., in both cases the effect is a considerable rise of the interface.

In order to better evaluate the effect of the private abstraction, the volume abstracted should be known more in details, not only as an overall amount but associated to each single well average abstraction. When this information will be complete, a new round of calibration of the parameter field is recommended.

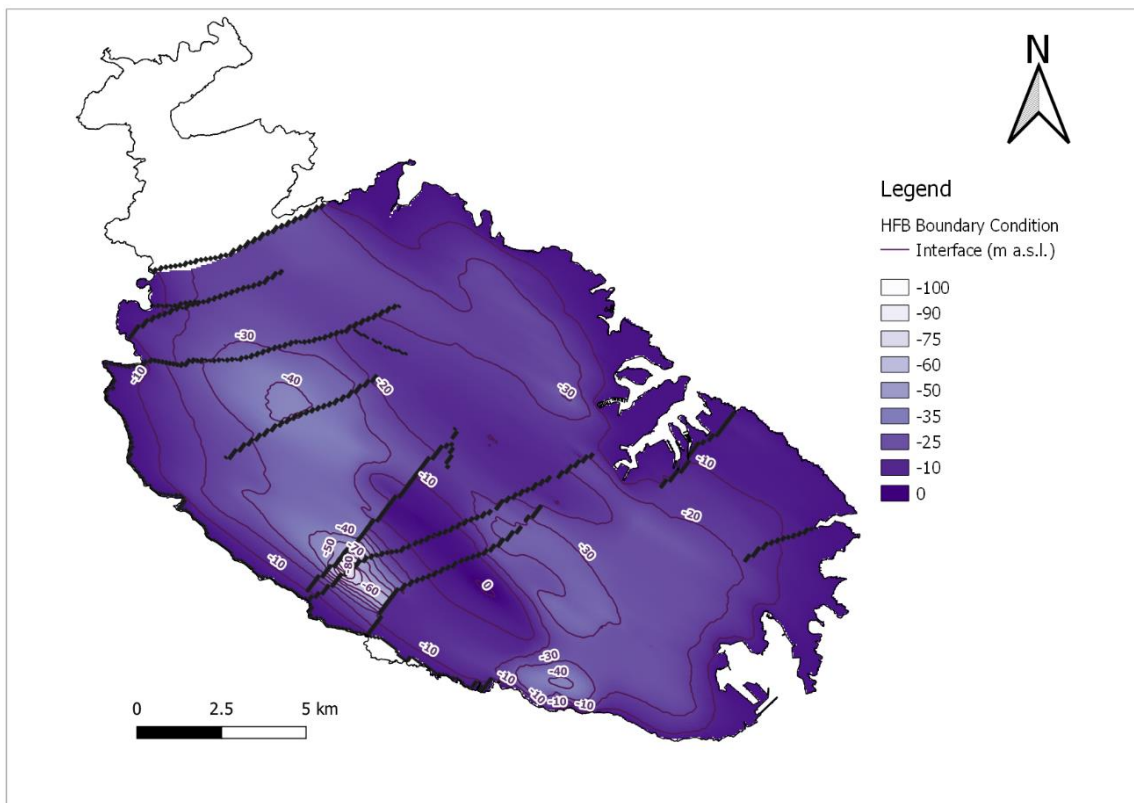
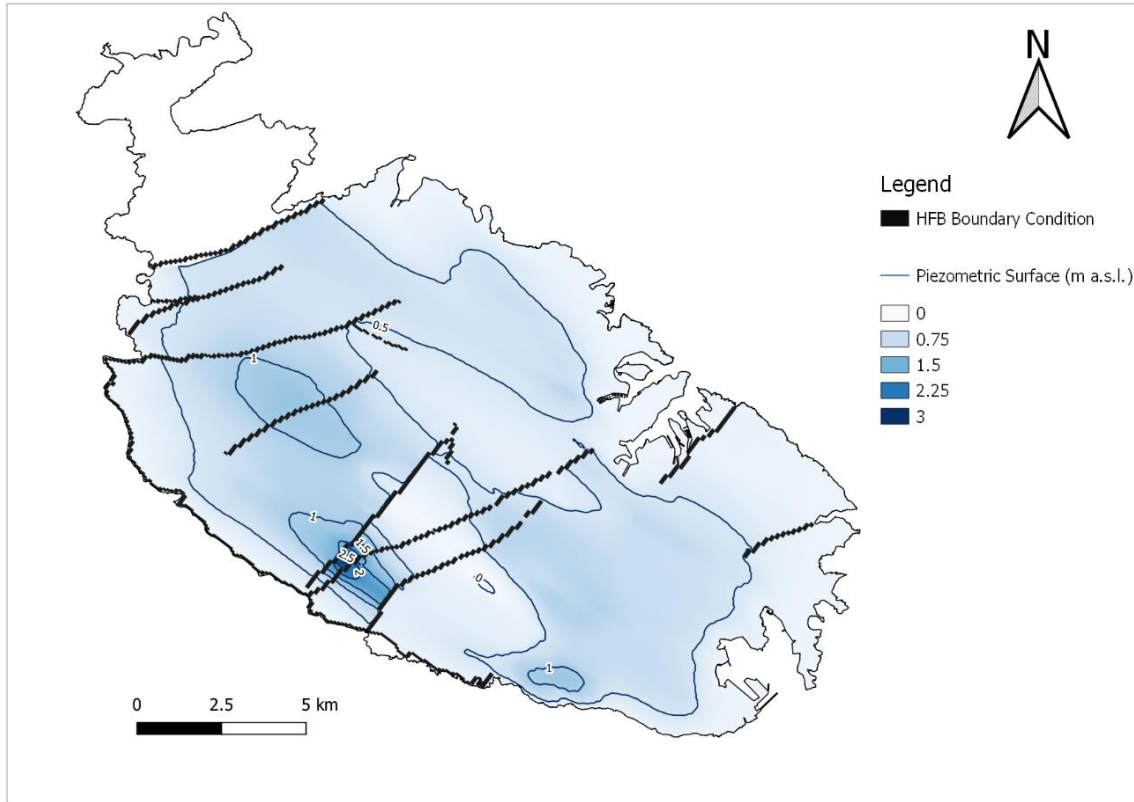


Figure 6. ABS_S1a potentiometric surface and freshwater-seawater interface (K as reference model).

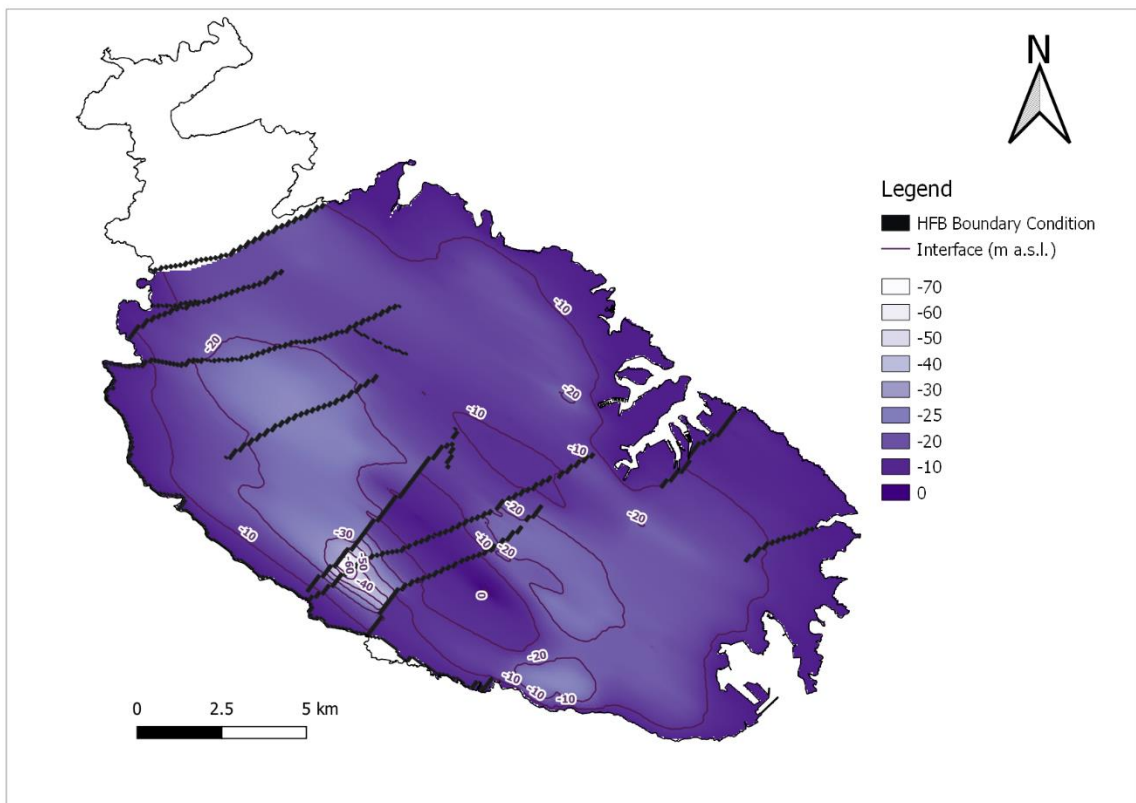
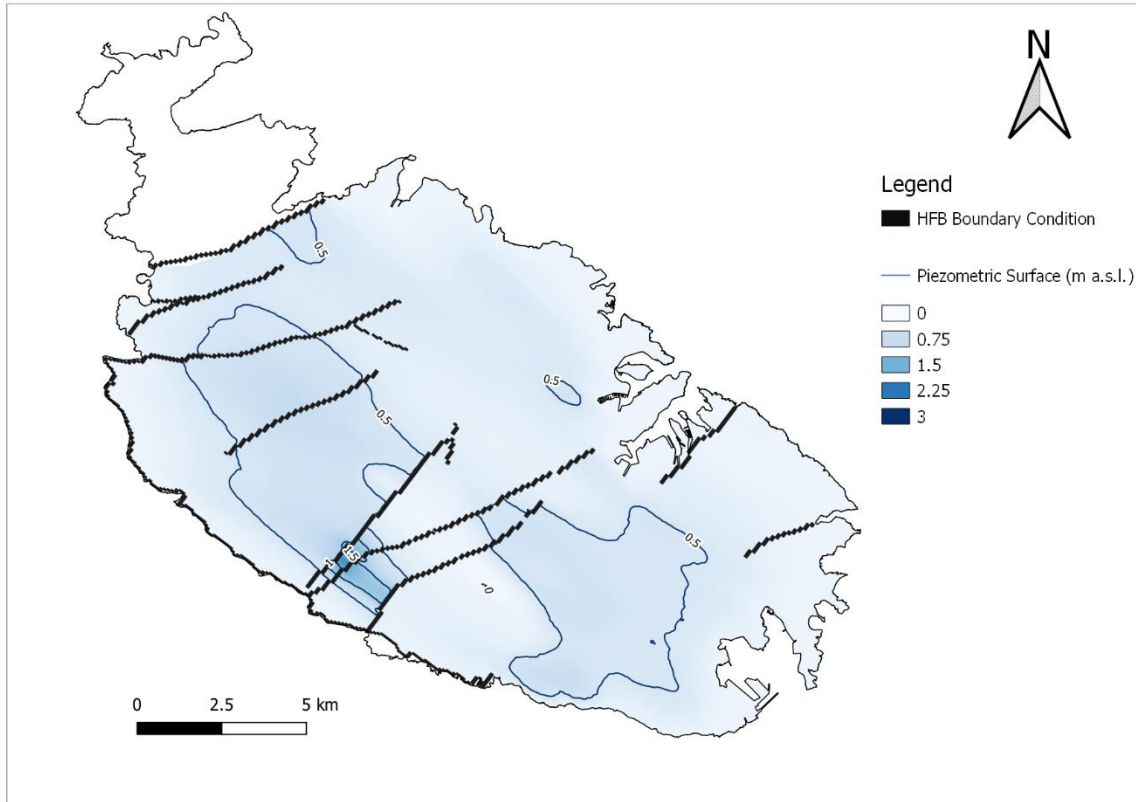


Figure 7. ABS_S1b potentiometric surface and freshwater-seawater interface (K raised by 25%).

Abstraction Scenario 2 (ABS_S2)

In the second Abstraction scenario (ABS_S2) all private abstraction are halted and the abstraction from public groundwater sources is increased to 53,500 m³/d, leakages from municipal distribution system are maintained constant at reference levels.

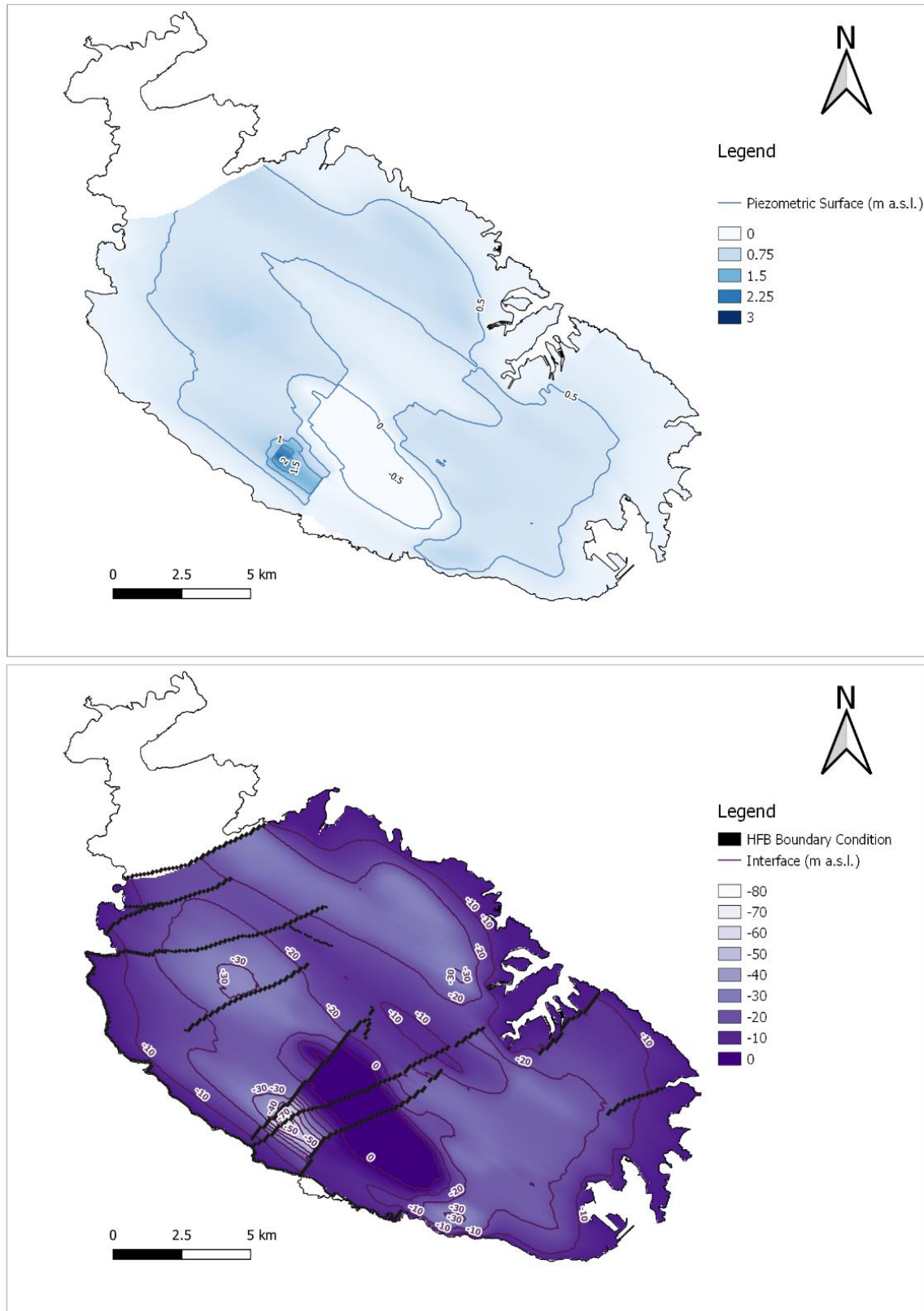


Figure 8. ABS_S2 potentiometric surface and freshwater-seawater interface.

Abstraction Scenario 3 (ABS_S3)

Under this scenario Public abstraction from boreholes is stopped, whilst the pumping stations are operated under the production capacity of 21,000 m³/day. Private groundwater abstraction is assumed to remain at the level of the reference model.

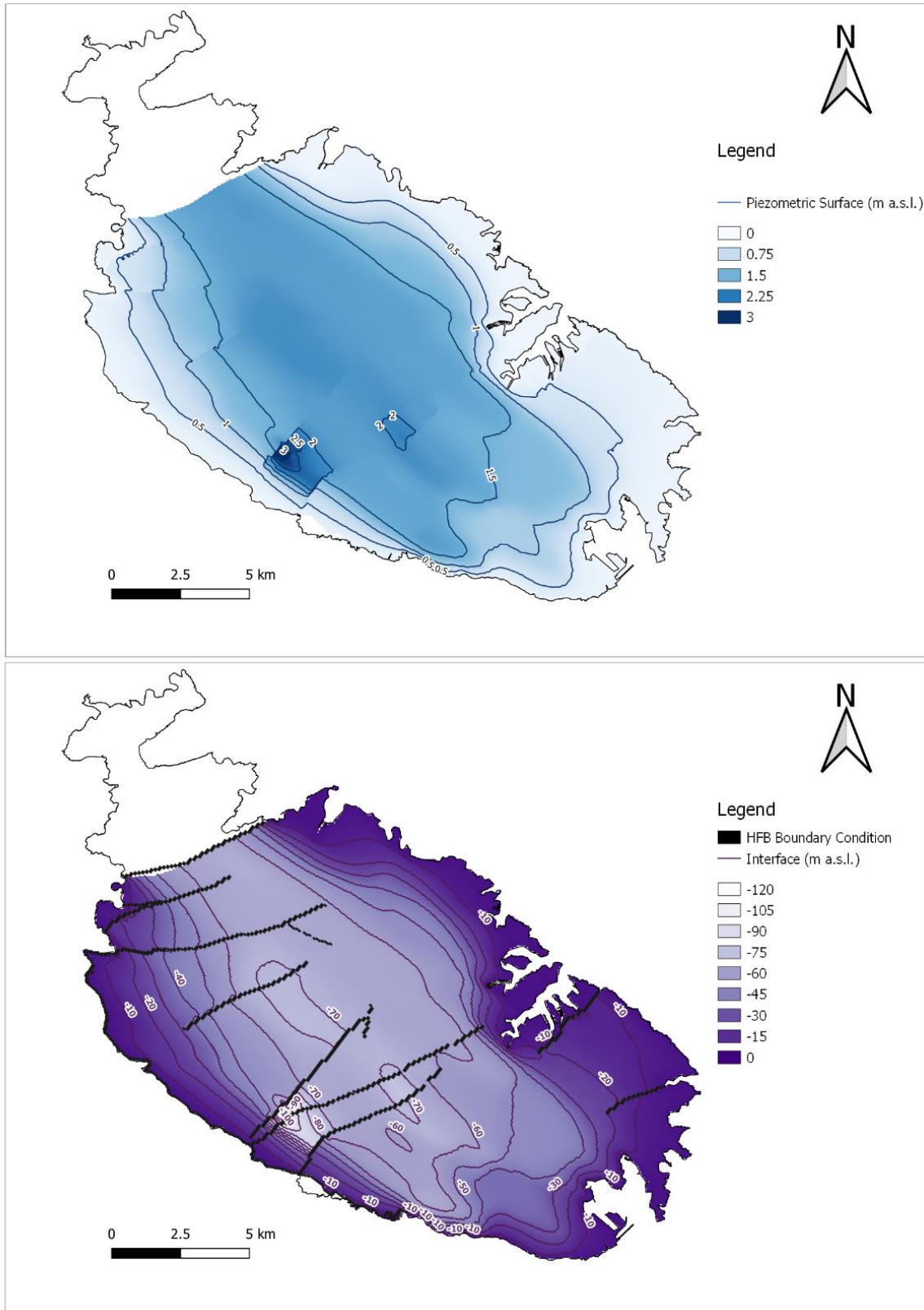


Figure 9. ABS_S3 potentiometric surface freshwater-seawater interface.

Abstraction Scenario 4 (ABS_S4)

In this scenario, abstraction for public purposes is completely stopped and groundwater resources are allocated to the agricultural sector assuming to be at 2.5 times the current level of abstraction. Abstraction from commercial abstraction is maintained at the reference levels.

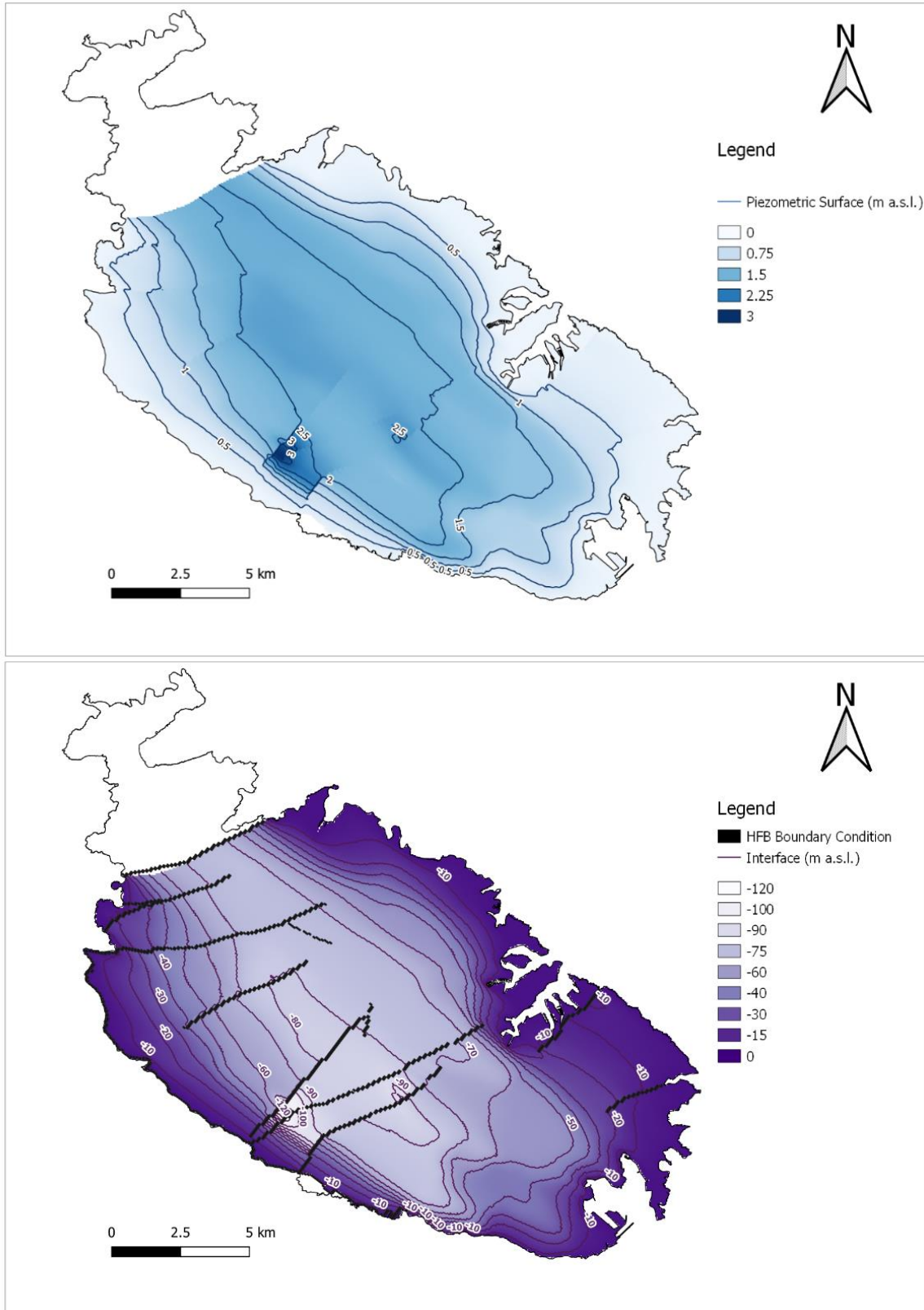


Figure 10. ABS_S4 potentiometric surface and freshwater-seawater interface.

Abstraction Scenario 5 (ABS_S5)

The scenario assumes the stopping of abstraction for commercial purposes, with agricultural and public abstraction kept as in the reference model.

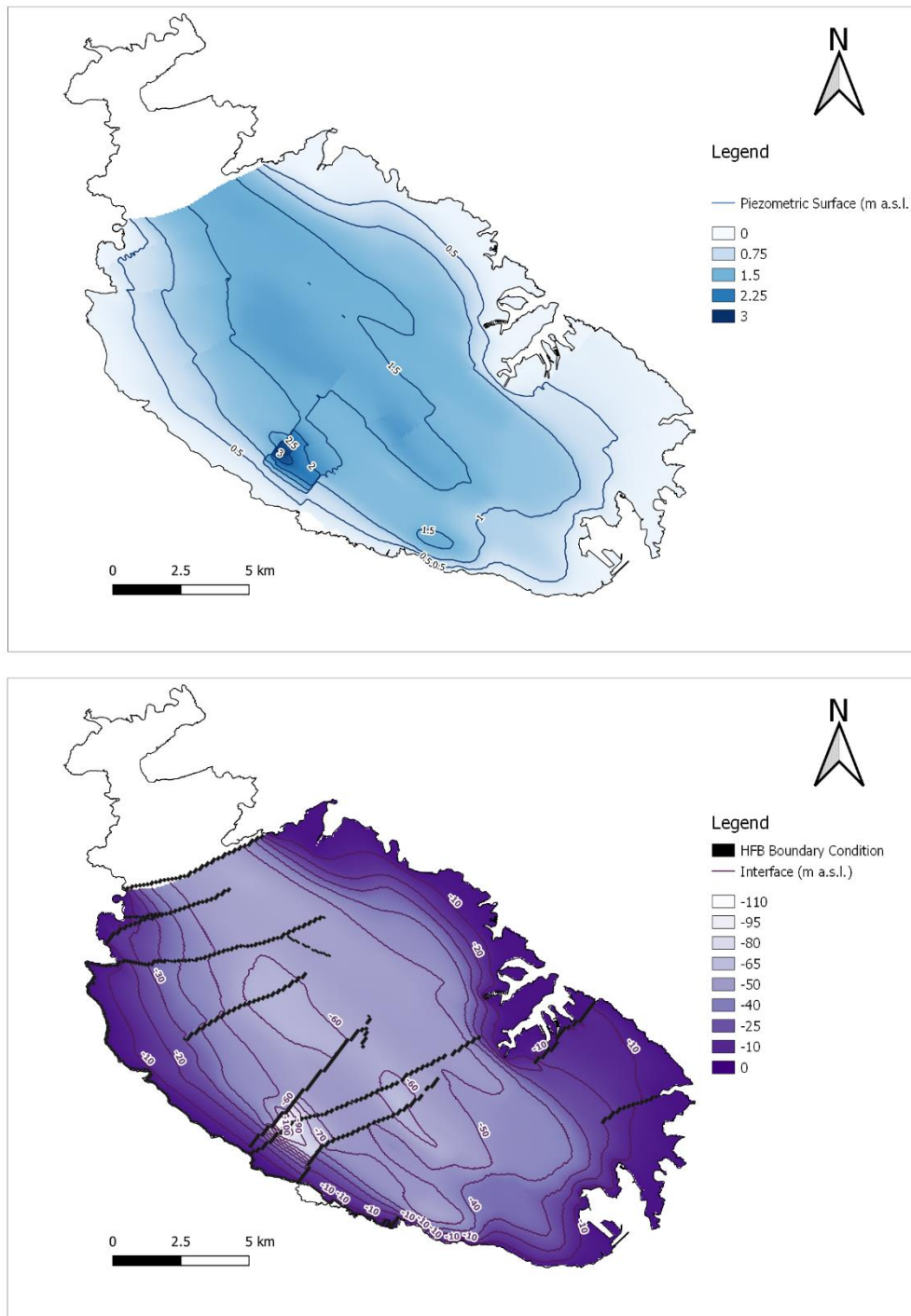


Figure 11. ABS_S5 potentiometric surface and freshwater-seawater interface.

Abstraction Scenario 6 (ABS_S6)

In this scenario, the development of a gallery system in the MSLA under the Rabat-Dingli perched aquifer is simulated, keeping other abstracted volumes as in the reference model. The L shaped abstraction gallery has been represented with the DRAIN boundary condition (Figure 12. Representation of the new gallery as Drain boundary condition.) with a total length of 3000 m, with a 1x1 m cross section and a constant bottom elevation equal to 1 m asl; the drain conductance has been set to 50 m/d. Under this assumption, the total outflow from the drain is equal to 54 L/s.

Results shown in Figure 13. ABS_S6 potentiometric surface and freshwater-seawater interface. strongly rely on the local parameter field of K , which under Rabat Plateau has just been estimated through the model calibration process, without much information from investigations. A proper representation of this scenario would require further information about the hydraulic conductivity in the selected position of the gallery through pumping tests.

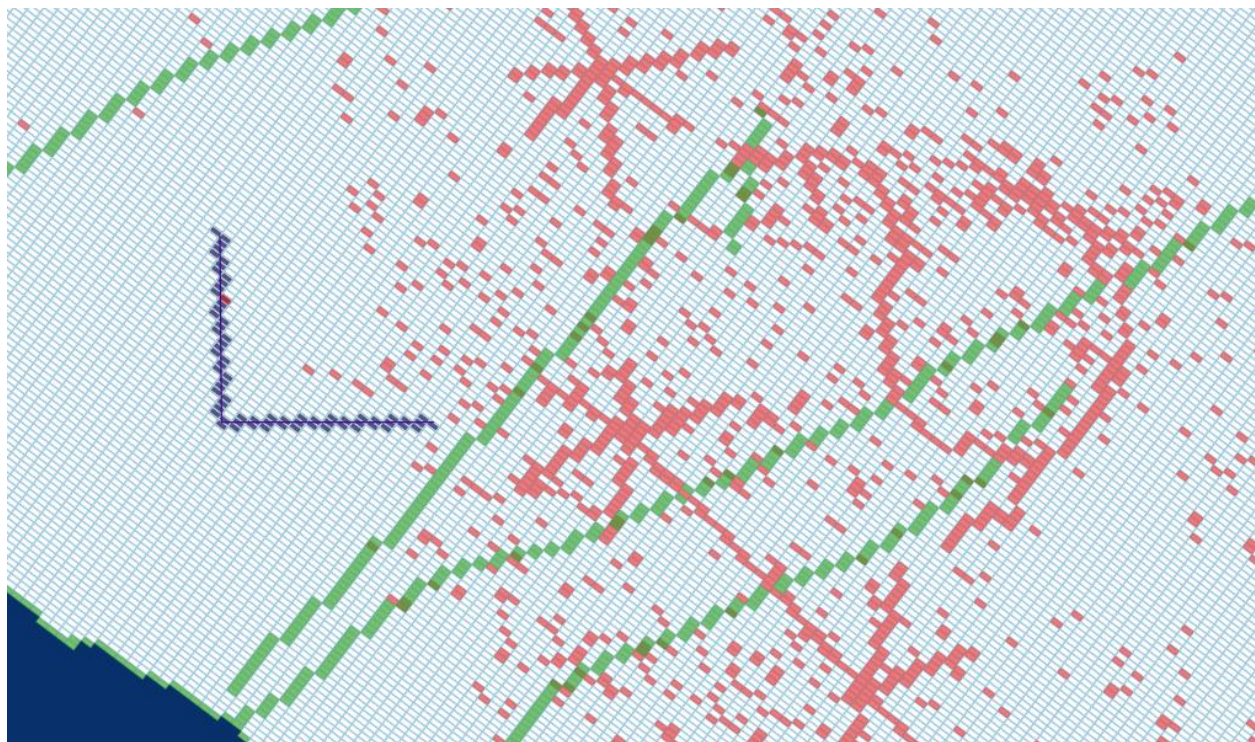


Figure 12. Representation of the new gallery as Drain boundary condition.

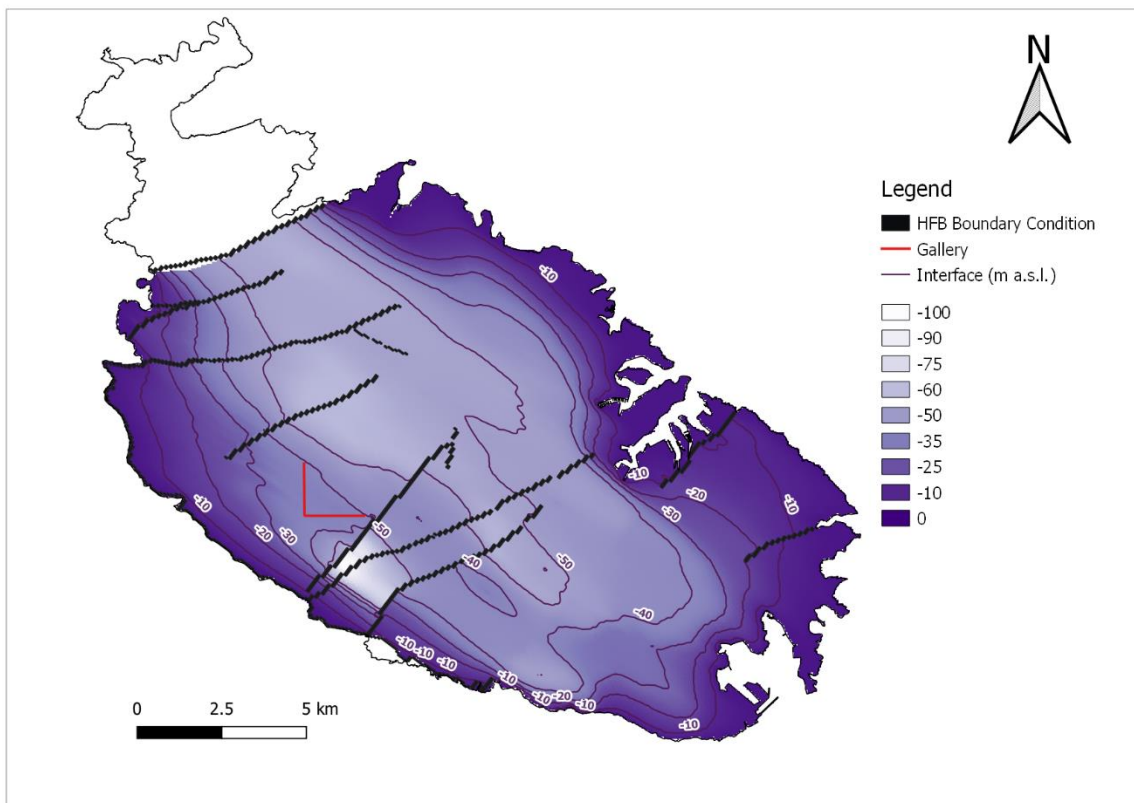
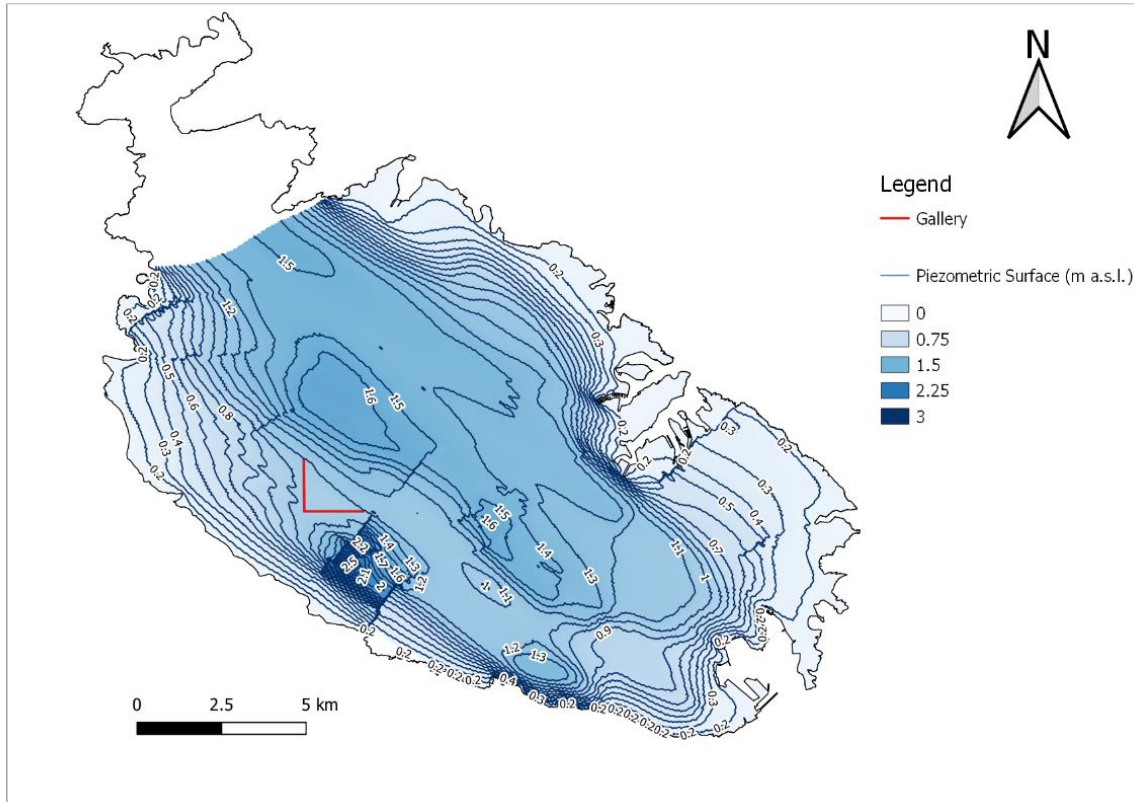


Figure 13. ABS_S6 potentiometric surface and freshwater-seawater interface.

Recharge Scenario 1 (RCH_S1)

The scenario simulates the effect of reducing water losses in supply and sewage network as a consequence of the improvement of the pipes network. A 30% reduction of losses with respect to the 99-2015 period average is applied, keeping other stresses same as in the reference model.

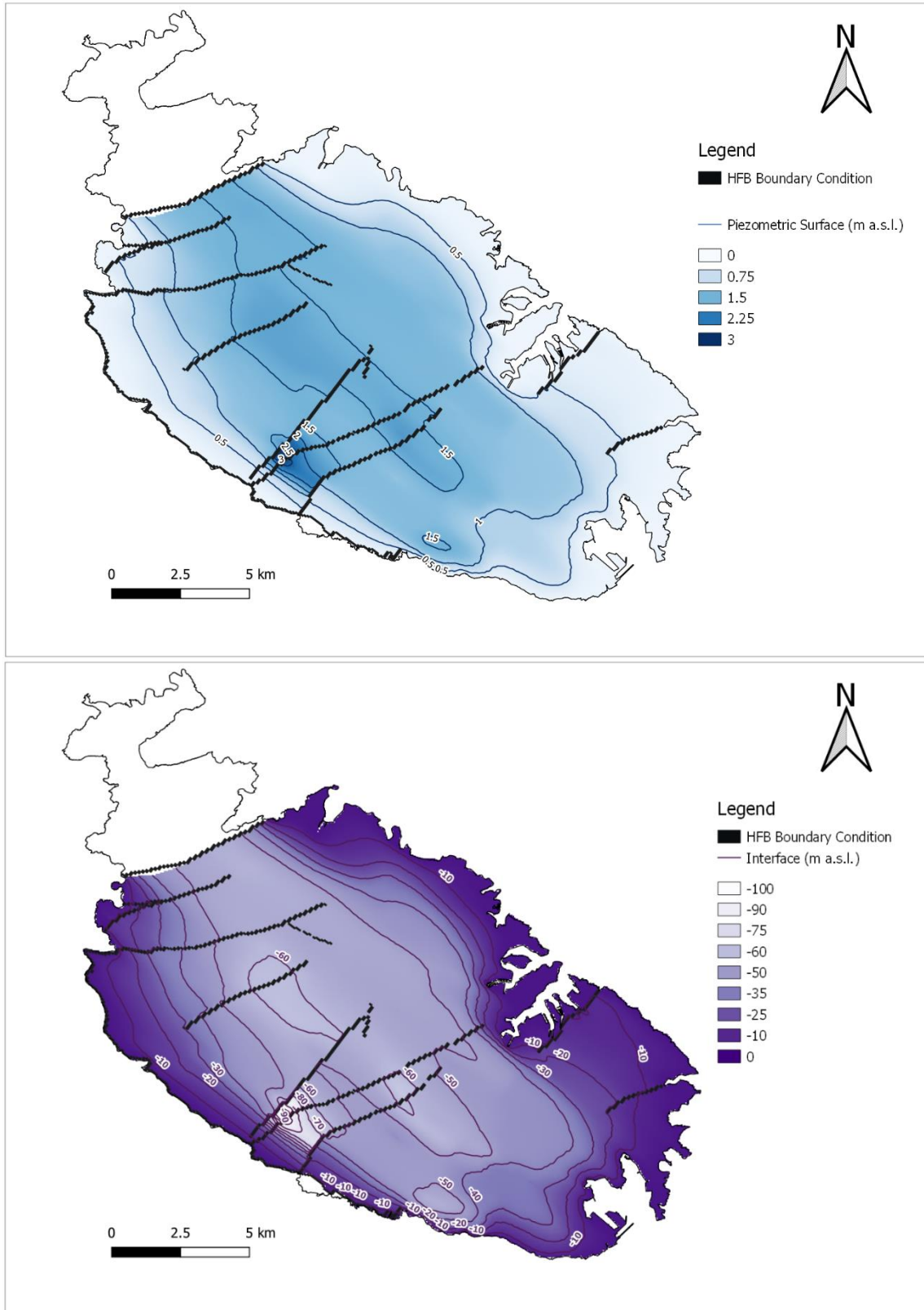


Figure 14. RCH_S1 potentiometric surface and freshwater-seawater interface.

Recharge Scenario 2 (RCH_S2)

In this scenario the natural recharge is diminished because of the increase in land-sealing due to the extension of the development/build up zones. Urban land area over the MSLA is approximately doubled, with the consequent decrease in infiltration rates. No compensation for artificial recharge from network leakages is included, assuming that such leakages are minimal in a new distribution network.

The reference urban area covers about 60 km²; this surface is approximately doubled to 120 km² in the scenario recharge distribution, as shown in Figure 15. Recharge distribution in the reference model (above) and in RCH_S2 (below)..

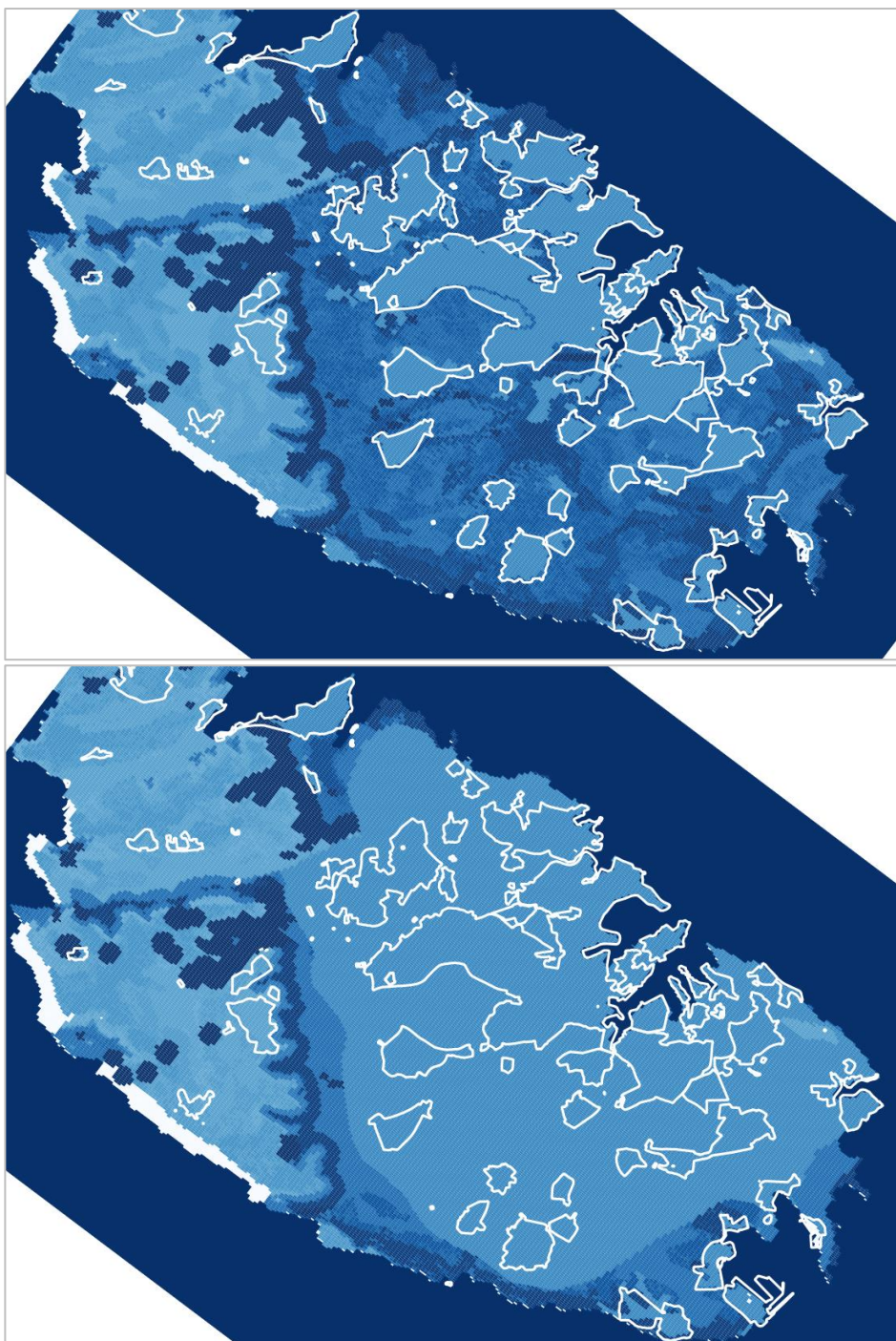


Figure 15. Recharge distribution in the reference model (above) and in RCH_S2 (below).

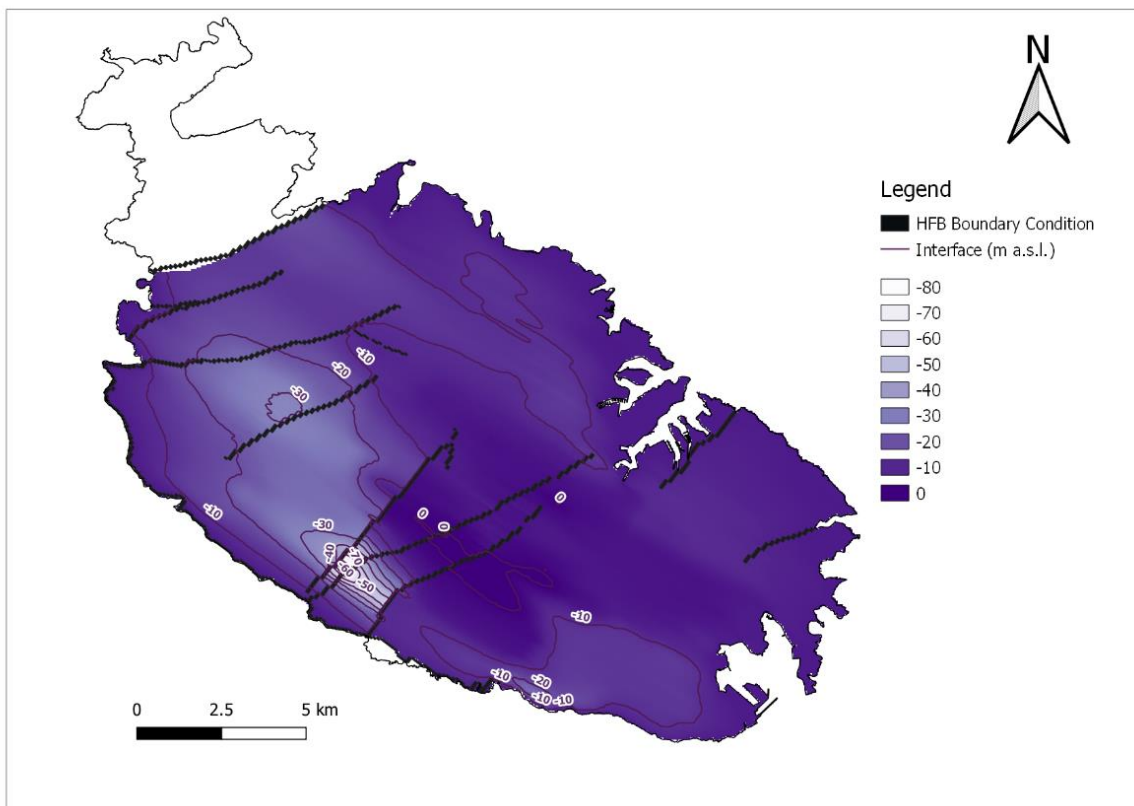
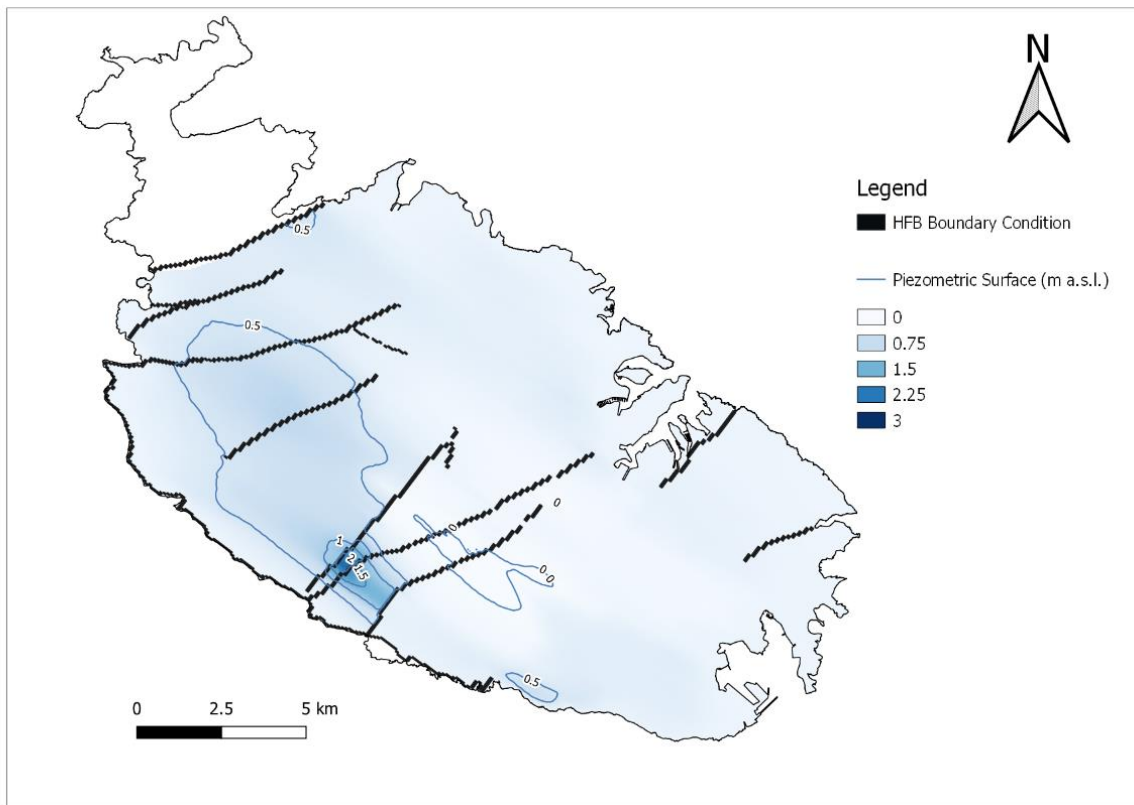


Figure 16. RCH_S2 potentiometric surface and freshwater-seawater interface.

Alternative Development Scenario 1 (AD_S1)

Method

From a flow dynamic point of view, the freshwater lens floating on seawater can be seen as a single multi-layered aquifer system composed by 2 layers. As reported in Kruseman & de Ridder (1994), multi-layered aquifer systems may be one of three kinds. The first consists of two or more aquifer layers, separated by aquicludes, the second consists of two or more aquifer layers, separated by aquitards.

The third multi-layered aquifer system consists of two or more aquifers, each with its own hydraulic characteristics (included fluid density), and separated by interfaces that allow unrestricted crossflow (i.e., the interface can move up and down with no physical constraints) (Figure 17. Two layered aquifer system separated by an interface (Kruseman & de Ridder, 1994)).

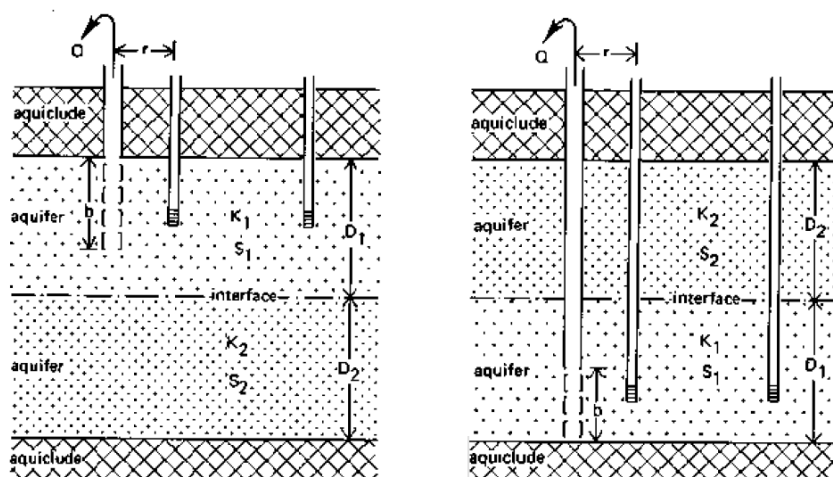


Figure 17. Two layered aquifer system separated by an interface (Kruseman & de Ridder, 1994).

This system response to pumping will be analogous to that of a single-layered aquifer whose properties are equal to the combination of the hydraulic properties of the individual layers. Hence, in an aquifer with unrestricted crossflow, the same methods as used for single-layered aquifers can be applied (Kruseman & de Ridder, 1994).

The flow field deformation operated by a pumping well in an unconfined single-layered aquifer is shown in the schematic cross section of Figure 18. Cross section of a pumped unconfined aquifer (Kruseman & de Ridder, 1994). If an interface is added to the scheme, it would be represented by a flow line perpendicular to the equipotential lines, since no vertical flow exchanges are allowed across the interface itself. Deformation of the flow field can only move up and down the interface.

The water lens, floating over the seawater layer in static condition, would move accordingly under the effect of the depressurization of the seawater layer operated by pumping, following a local new reference elevation which is now lower than 0 m asl (Figure 19. Schematic behavior of an unconfined aquifer characterized by an upper layer with freshwater and a lower layer with saltwater in undisturbed conditions (left) and under the effect of pumping from the lower layer (right)).

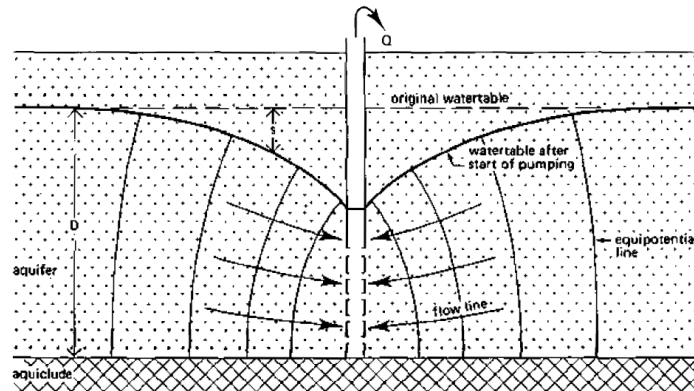


Figure 18. Cross section of a pumped unconfined aquifer (Kruseman & de Ridder, 1994).

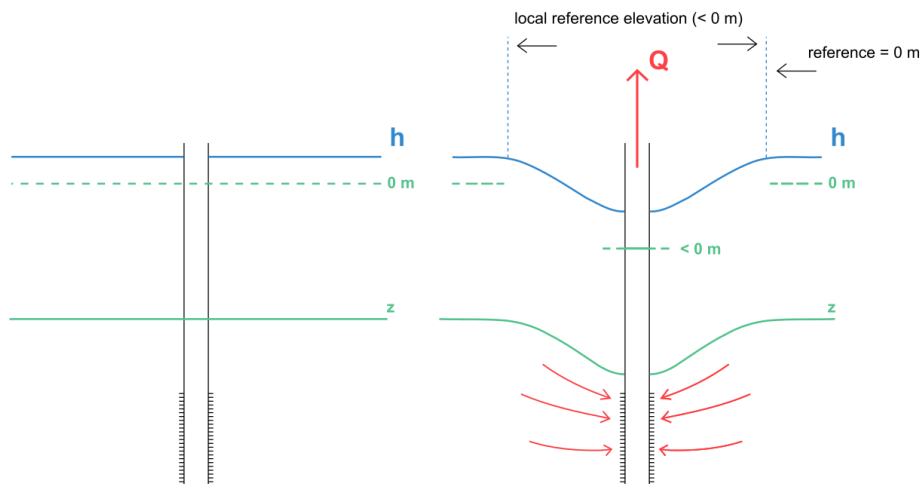


Figure 19. Schematic behavior of an unconfined aquifer characterized by an upper layer with freshwater and a lower layer with saltwater in undisturbed conditions (left) and under the effect of pumping from the lower layer (right).

An analytical estimate of the distance covered by the interface displacement under the effect of pumping in freshwater is available through the relation of Schmorak and Mercado (1969):

$$\Delta z = \frac{Q \rho_f}{2\pi d K (\rho_s - \rho_f)} \quad (1)$$

Where Δz is the difference in z elevation between the static conditions and the new equilibrium elevation, Q is the pumping rate, d is the distance from the bottom of the well to the original interface (Figure 20 Effect of pumping from the freshwater layer). The relation applies up to a critical elevation at which the interface is no longer stable and saltwater flows into the well. Dagan and Bear (1968) suggest that the interface will be stable for upconed heights that do not exceed $1/3 d$, thus if Δz is put equal to $0.3d$, the maximum permitted pumping rate should not exceed:

$$Q_{max} \leq 0.6\pi d^2 K \frac{(\rho_s - \rho_f)}{\rho_f} \quad (2)$$

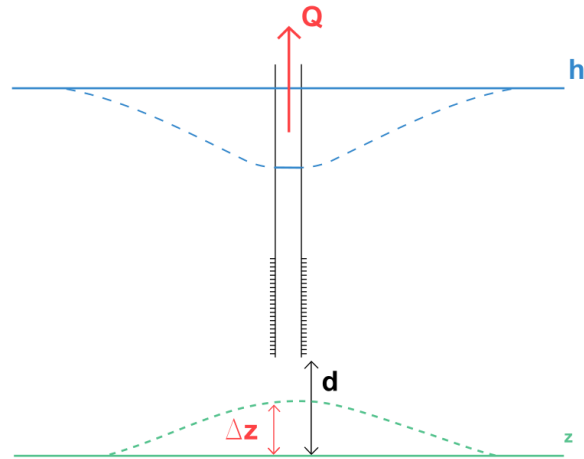


Figure 20 Effect of pumping from the freshwater layer

Let's assume that the analytical relationships (1) can be applied even if pumping is operated in the seawater layer (below the original interface). To this end, d would be measured between the static interface and the elevation at the top screen of the well (Figure 21. Effect of pumping from the saltwater layer (to be further investigated with other approaches).). As in case of the specular problem, a critical Q would exist in this case as well that, if exceeded, would make freshwater flow into the well.

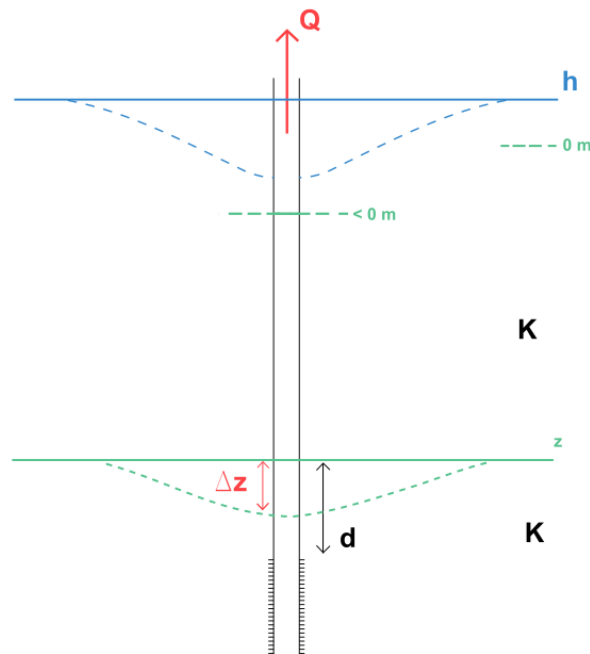


Figure 21. Effect of pumping from the saltwater layer (to be further investigated with other approaches).

In the specific case of the deep well, due to increased confining pressure with depth, decreased rock mass permeability with depth is to be expected as widely reported in literature (e.g., Carlsson and Olsson 1993; Lee and Farmer 1993; Meng et al. 2011; Zhang 2013).

Different empirical relationships have been found between permeability and depth. While some equations estimate the hydraulic conductivity simply as a function of depth, others include the hydraulic conductivity close to the top of the aquifer K_0 (e.g., Snow 1968, 1970; Lewis and Burgy 1964; Louis 1974; Lee and Farmer 1993, Wei et al. 1995).

For example, in Wei et al. (1995) the following relationship is found:

$$K_p = K_0 \left(1 - \frac{p}{58+1.02 p} \right)^3 \quad (3)$$

Where K_p is the estimated hydraulic conductivity at depth p , K_0 is the one measured at the top of the aquifer, p is the depth measured from the top of the aquifer.

Application

This scenario simulates the effect of a deep well-field located at the center of the island, abstracting seawater from beneath the freshwater-saltwater interface. The aim of such a work would be to concentrate the seawater RO treatment plant in a single location with relevant advantages on the scale effect efficiency of the treatment. The assumed pumping rate is 250 m³/d (sufficient to produce 100 m³/d of freshwater). The position would be at a high topographic elevation so that the network distribution would happen by gravity towards most of the island towns.

A possible position could be at the margin of the Rabat-Plateau, in a place where there is no excessive pumping from freshwater and where K is not too low, for instance in the area reported in Figure 22. Possible position of the deep well (yellow box) and trace of cross-section (yellow box). The cross-section with indication of head and interface elevation is shown in Figure 23. Cross-section and possible position of the deep well, together with a possible borehole scheme with a depth of 340 m (till -160 m asl) and screens from -120 m asl till the borehole bottom.

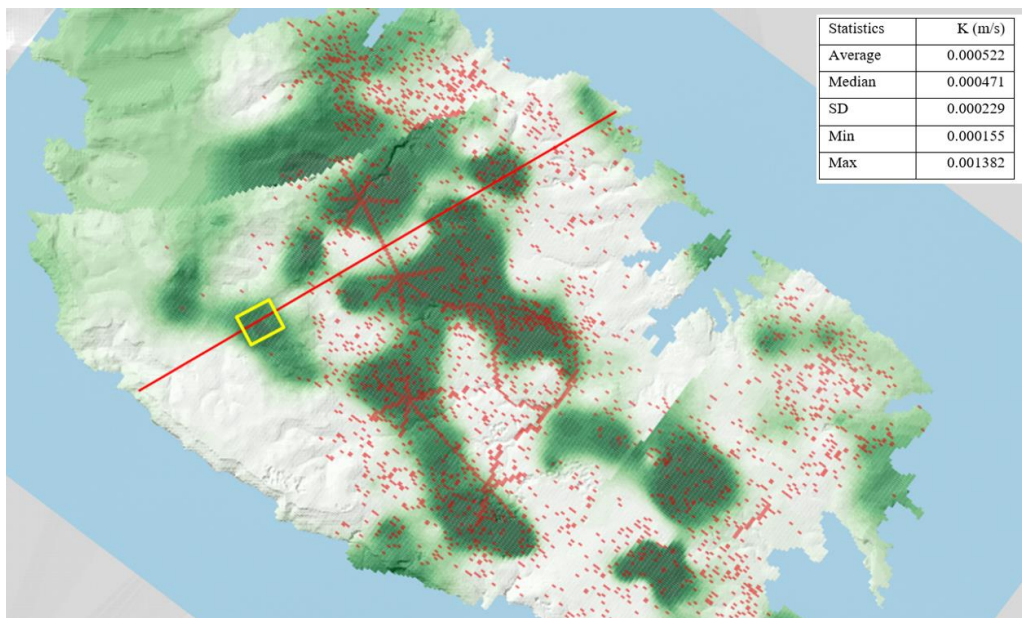


Figure 22. Possible position of the deep well (yellow box) and trace of cross-section.

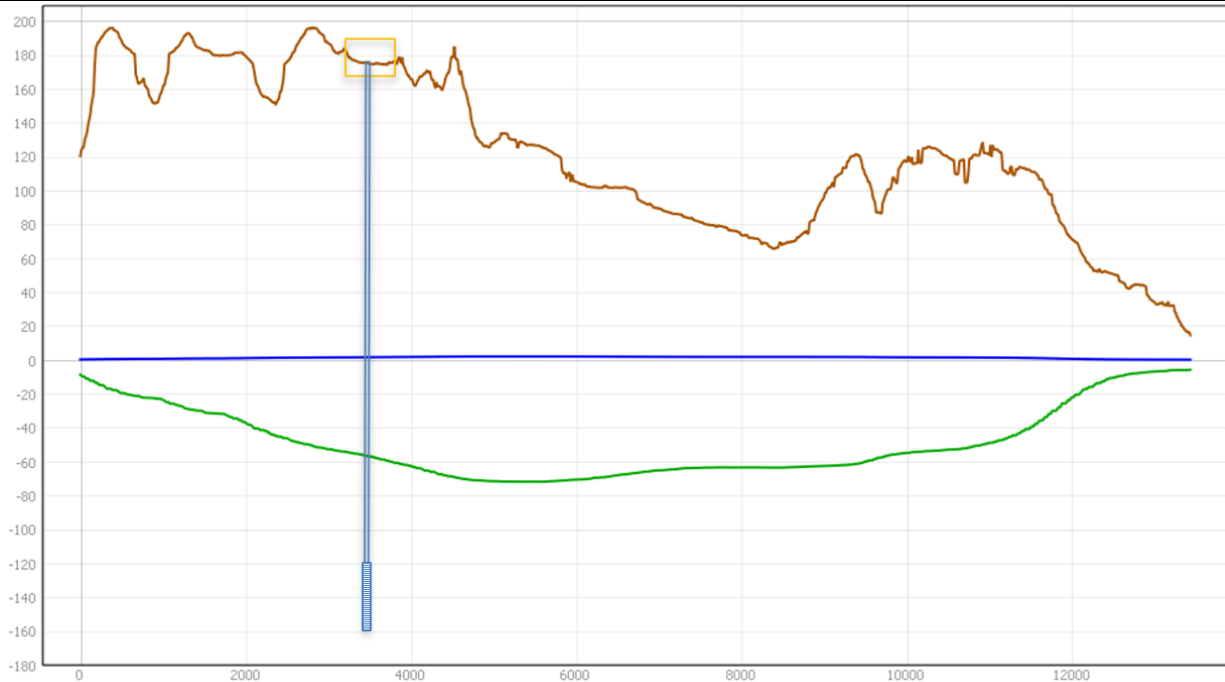


Figure 23. Cross-section and possible position of the deep well.

Conceptually, if the previous relationships are considered, the effect of pumping from the saltwater layer would generate the situation reported in Figure 24. Conceptual scheme (not in scale) of the stabilized equilibrium due to pumping from the saltwater layer; 1: position of well as in Figure 22. Possible position of the deep well (yellow box) and trace of cross-section; 2: ground surface; 3: ante-operam potentiometric surface; 4: ante-operam interface; 5: stabilized post-operam potentiometric surface; 6: stabilized post-operam interface; 7: flow to the well; 8: borehole and its screened length, where the lowering of the interface elevation is followed by a lowering of the freshwater hydraulic heads.

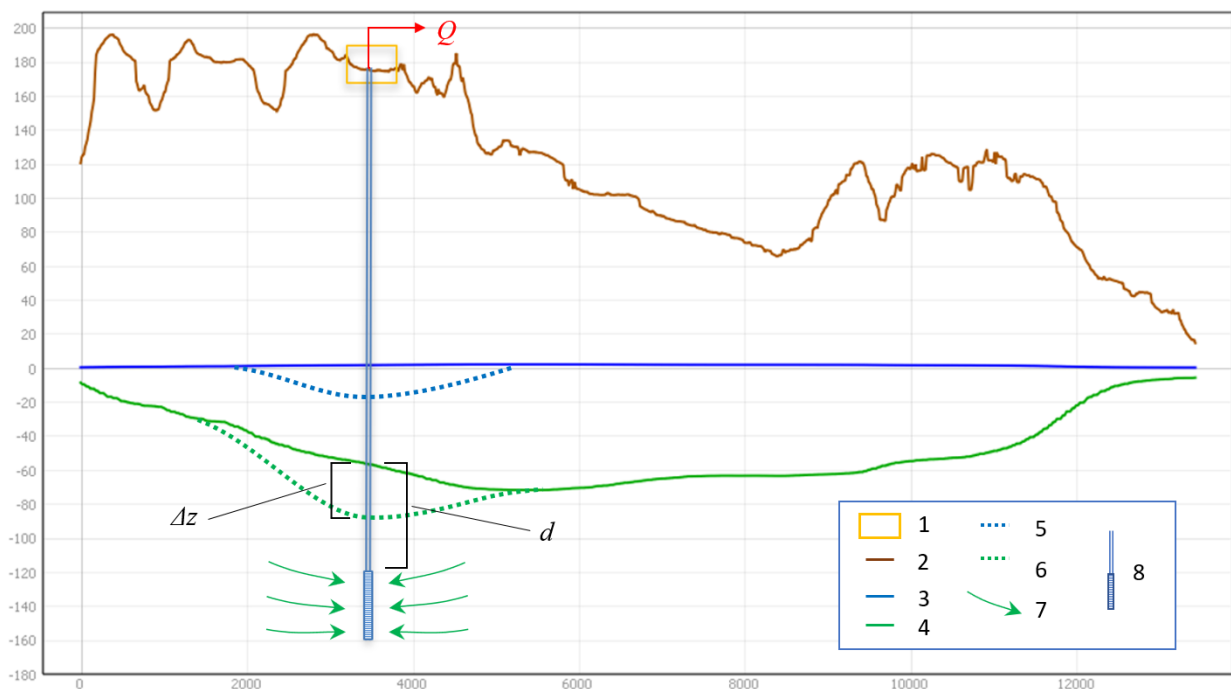


Figure 24. Conceptual scheme (not in scale) of the stabilized equilibrium due to pumping from the saltwater layer; 1: position of well as in Figure 22. Possible position of the deep well (yellow box) and trace of cross-section; 2: ground surface; 3: ante-operam potentiometric surface; 4: ante-operam interface; 5: stabilized post-operam potentiometric surface; 6: stabilized post-operam interface; 7: flow to the well; 8: borehole and its screened length.

If this completely hypothetical example is analyzed through (Equ. 1), different results in terms of interface displacement are obtained according to the assumed hydraulic conductivity, with Q kept constant.

The calibrated hydraulic conductivities inside the yellow box in Figure 22. Possible position of the deep well (yellow box) and trace of cross-section are in line with the values of K obtained through pumping tests in Lower Coralline Limestone (LCL) which indagated the upper portion of the freshwater layer (average value $5.22E-4$ m/s).

Combining the results from (Equ. 3) and (Equ. 1), different hypothesis can be done concerning d and K_p on the basis of the model results to estimate Δz . Also, assuming the selected Q close to the Q_{max} of (2), a K threshold (K_t) for the proposed $Q = 0.003$ m³/s can be found; if the local K results lower than K_t the pumping is likely to recall freshwater and not only saltwater at a given distance interface-top screen d . Results are reported in Table 2. Results of analytical relationship to estimate Δz , consequent head lowering ($\Delta h = \Delta z/36$) and K_t .

Hypothesis	Q (m ³ /s)	K_0 (m/s)	p (m)	K_p (m/s) (Wei et al. 1995)	D (m)	Δz (m)	Δh (m)	K_t (m/s) (Dagan & Bear 1968)
Hyp1	0.003	5.22E-04	160	1.11E-05	-60	25	0.71	1.58E-05
Hyp2	0.003	1.00E-04	160	2.12E-06	-60	134	3.72	1.58E-05
Hyp3	0.003	5.00E-05	160	1.06E-06	-60	268	7.45	1.58E-05
Hyp4	0.003	5.22E-04	120	1.96E-05	-20	44	1.21	1.42E-04
Hyp5	0.003	5.22E-04	100	2.75E-05	-10	62	1.72	5.68E-04

Table 2. Results of analytical relationship to estimate Δz , consequent head lowering ($\Delta h = \Delta z/36$) and K_t .

If the final head ($h_0 - \Delta h$) goes below 0 m asl, the result would be an increase in seawater intrusion from the coast; this is very likely to happen given the very low head elevation in the example area (< 1 m asl) and of the MSLA in general (< 2 m asl).

Climate Change Scenario 1 (CC_S1)

This scenario takes into account the foreseen climate change effects on the water balance, with reference to an estimated decrease of infiltration caused by the existing trends in rainfall decrease and temperature rise. Applying the foreseen variation of precipitation, temperature and evapotranspiration reported in Table 3. Estimated variation of the water balance term as a consequence of the Climate Change scenarios available for the Malta aera (provided by EWA). an overall reduction of about 10% of the reference recharge has been calculated for the year 2050.

Temperature (Deg C)	Oct.	Nov.	Dec.	Jan.	Feb.	Mar.	Apr.	May.	Jun.	Jul.	Aug.	Sep.
Average temperature (1980-2010)	21.5	17.6	14.2	12.7	12.5	13.9	16.0	19.7	23.8	26.6	27.1	24.6
T change under 3 deg C global change (max)	2.0	1.8	1.9	1.7	1.7	1.7	1.8	2.0	2.1	2.3	2.1	2.1
Projected Temperature (2050) for scenario	23.5	19.4	16.1	14.4	14.2	15.6	17.8	21.6	25.9	28.8	29.2	26.7

Precipitation (mm/month)	Oct.	Nov.	Dec.	Jan.	Feb.	Mar.	Apr.	May	Jun.	Jul.	Aug.	Sep.
Average PR (1980-2010)	68.6	102.9	108.6	92.9	56.9	37.9	20.8	8.5	4.0	0.2	5.6	56.0
Change in PR under 3 deg global change (min)	0.924	0.814	0.683	0.686	0.503	0.745	0.930	0.677	0.500	1.000	0.762	0.701
Projected Precipitation for scenario (2050)	63.43	83.75	74.22	63.72	28.63	28.26	19.35	5.77	2.01	0.21	4.26	39.29

Potential Evapotranspiration (mm/month)	Oct.	Nov.	Dec.	Jan.	Feb.	Mar.	Apr.	May	Jun.	Jul.	Aug.	Sep.
Average PET (1980-2010)	97.6	66.9	46.0	36.0	29.5	37.2	44.5	64.2	87.6	116.6	131.3	114.4
Change in PET under 3 deg global change (max)	1.052	1.050	1.060	1.056	1.056	1.053	1.053	1.052	1.051	1.051	1.046	1.048
Projected PET for scenario (2050)	102.7	70.3	48.8	38.0	31.1	39.2	46.8	67.5	92.1	122.6	137.4	119.9

Table 3. Estimated variation of the water balance term as a consequence of the Climate Change scenarios available for the Malta aera (provided by EWA).

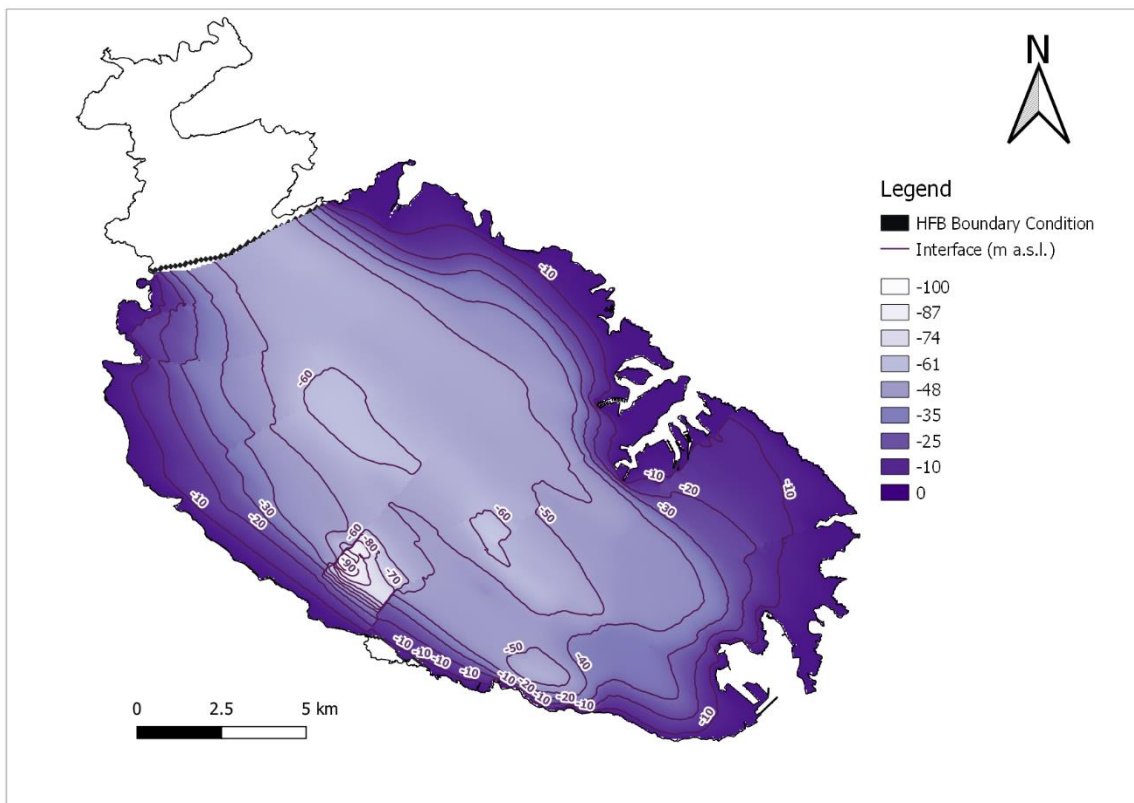
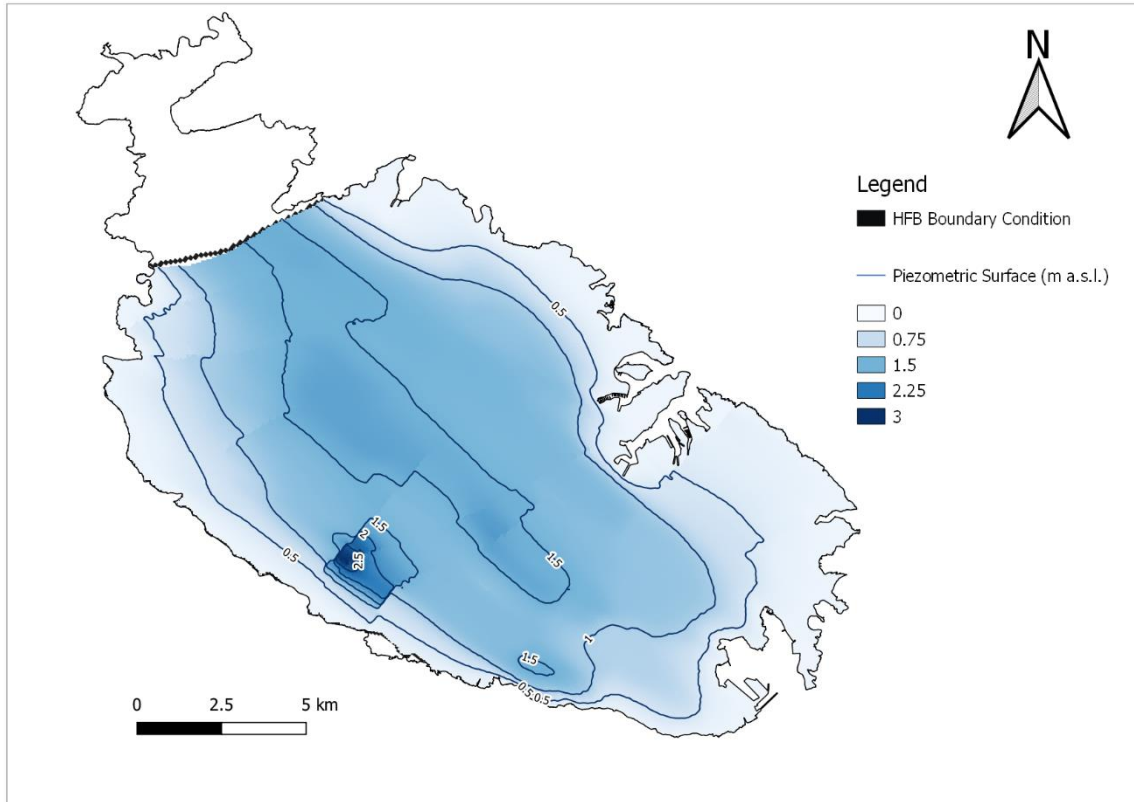


Figure 25. CC_S1 potentiometric surface and freshwater-seawater interface.

Climate Change Scenario 2 (CC_S2)

Starting from CC_S1, an increasing abstraction for agriculture is assumed, to compensate the demand due to higher losses by evapotranspiration. In this case the recharge is decreased by 10% with respect to the reference model and the agricultural abstraction increased by 10%. Other stresses are kept unchanged.

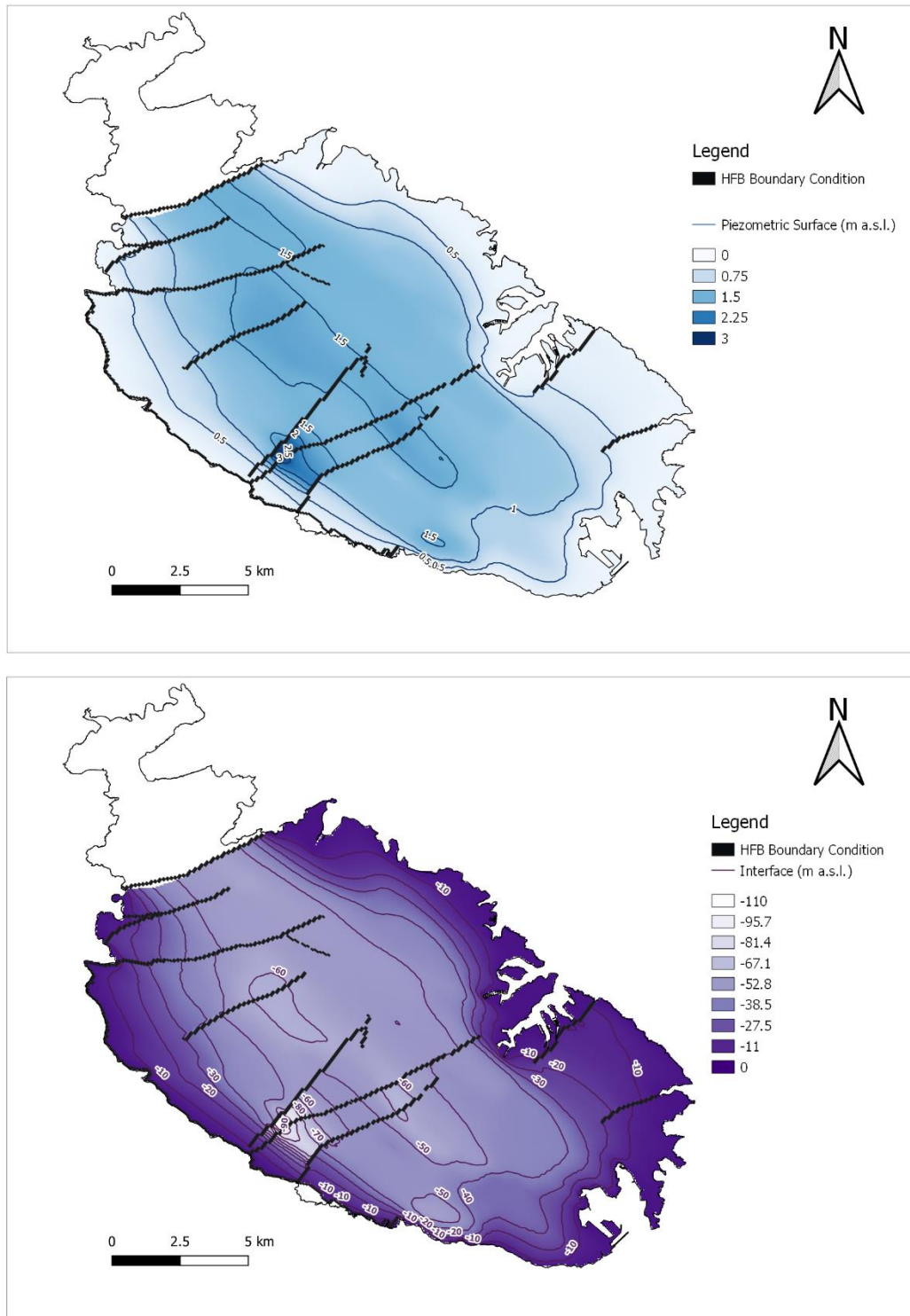


Figure 26. CC_S2 potentiometric surface and freshwater-seawater interface.

Climate Change Scenario 3 (CC_S3)

In this scenario the increase in sea level till the elevation of 0.40 m. To do so, the reference elevation of the GHB boundary condition has been raised. What is observed is a consequent rise of the interface elevation of +0.40 m and of the potentiometric surface elevation of +0.40 m. The only effect over the overall aquifer volume is a boundary reduction along the coast generated by the reduction of emerged land. Given the grid cells of the present model version, this effect cannot be appreciated.

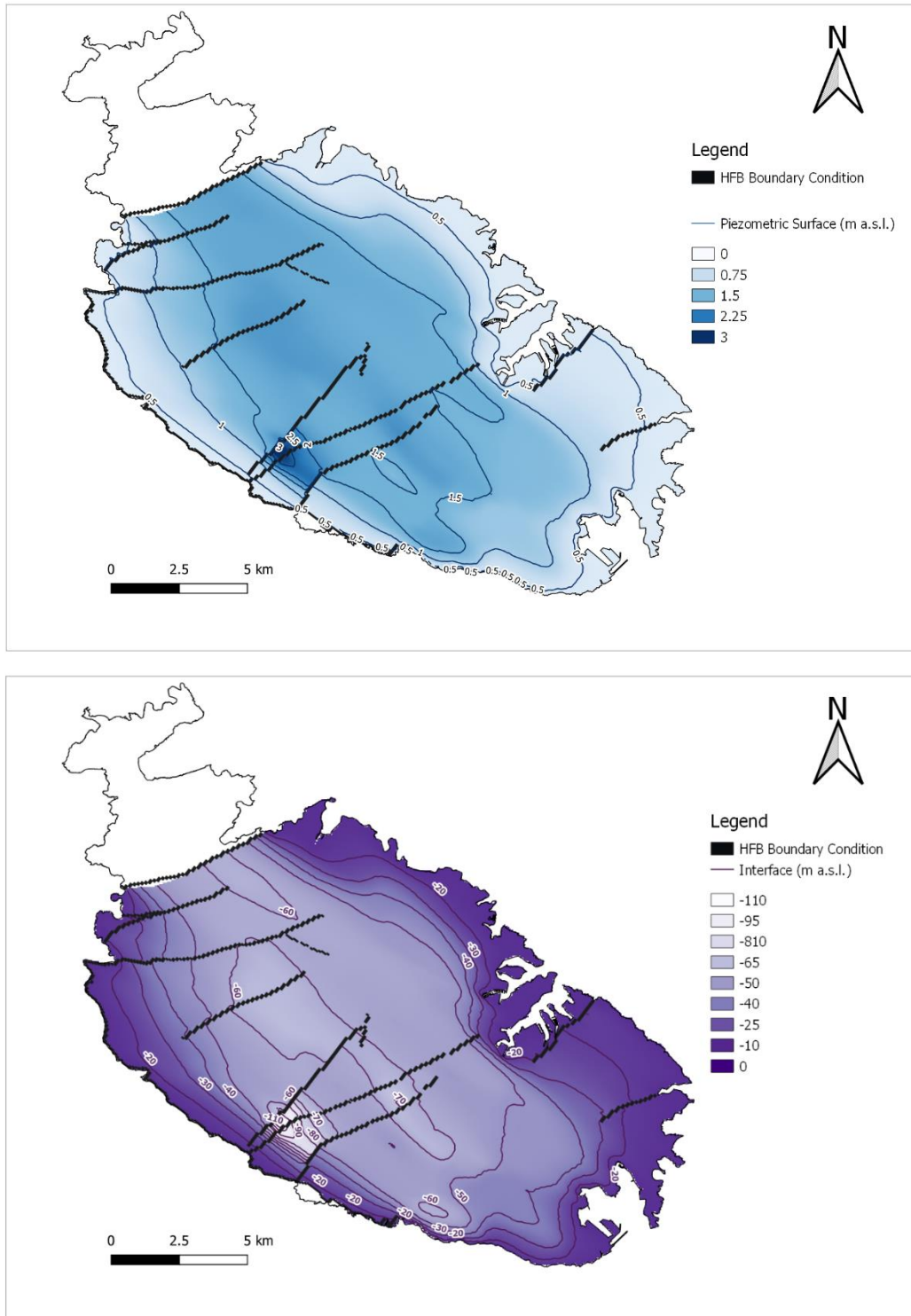


Figure 27. CC_S3 potentiometric surface and freshwater-seawater interface.

Artificial Recharge Scenario 1 (AR_S1)

The scenario simulates the effect of a MAR Scheme at the South-Eastern region of the aquifer system through 10 injection boreholes with an injection rate of 1,000 m³/d for each borehole.

The injection boreholes would be active during the wet season (from October till April) when polished water would be available from the closest sewage treatment plant and they would be inactive during the dry season (from May till September). Results are expressed in the long term applying the yearly average volume of injection per well, i.e. 583 m³/d (7 months active, 5 inactive).

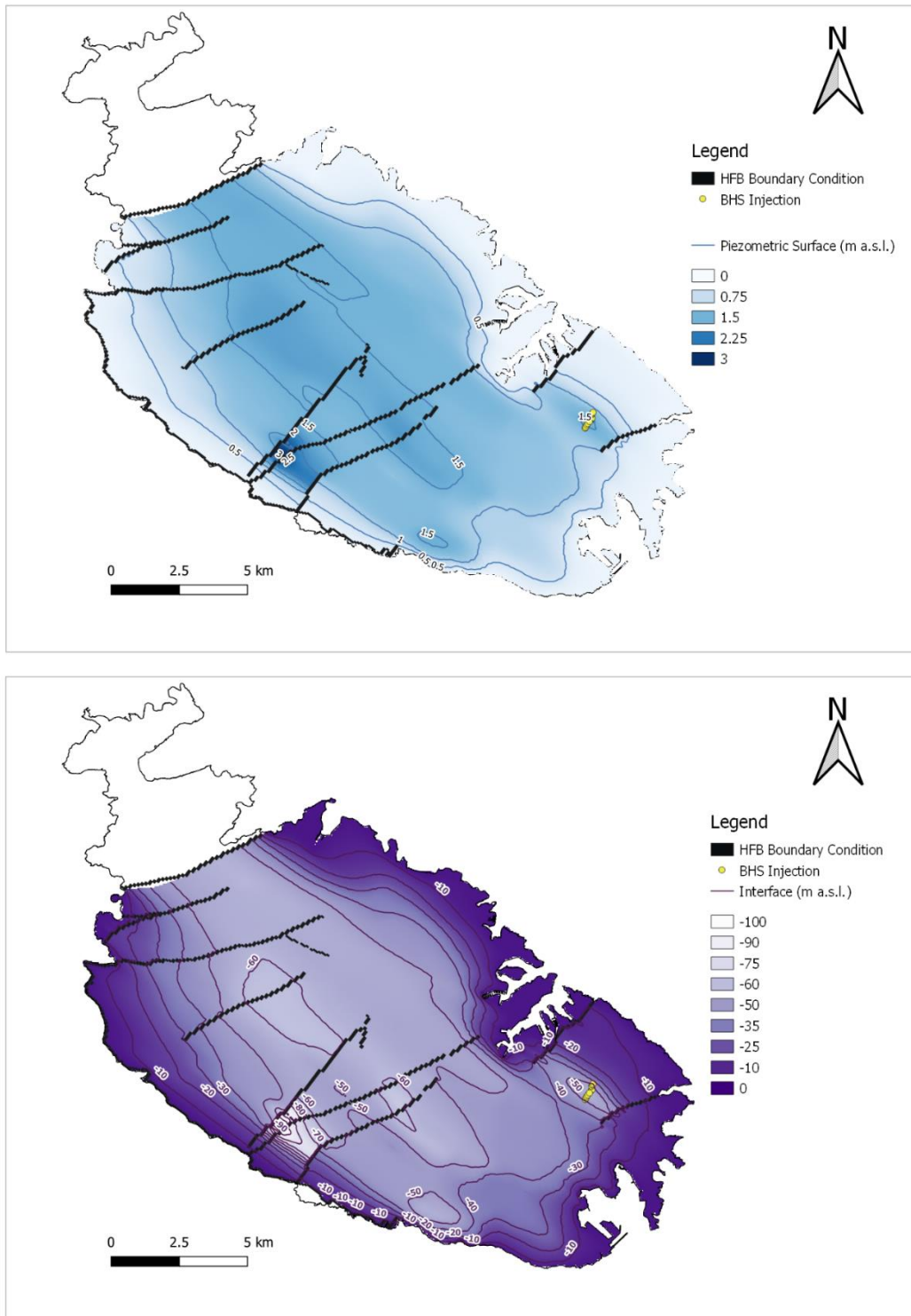


Figure 28. AR_S1 potentiometric surface and freshwater-seawater interface.

Artificial Recharge Scenario 2 (AR_S2)

The scenario simulates the effect of a MAR Scheme at the Central Region of the aquifer system aligned to Qali-Speranza gallery axis. The “Atiga” gallery would be drilled through the unsaturated zone with an injection rate of 15,000 m³/d along all the year. The gallery has been simulated as 147 injection wells and the volume has been distributed equally (+104 m³/d each).

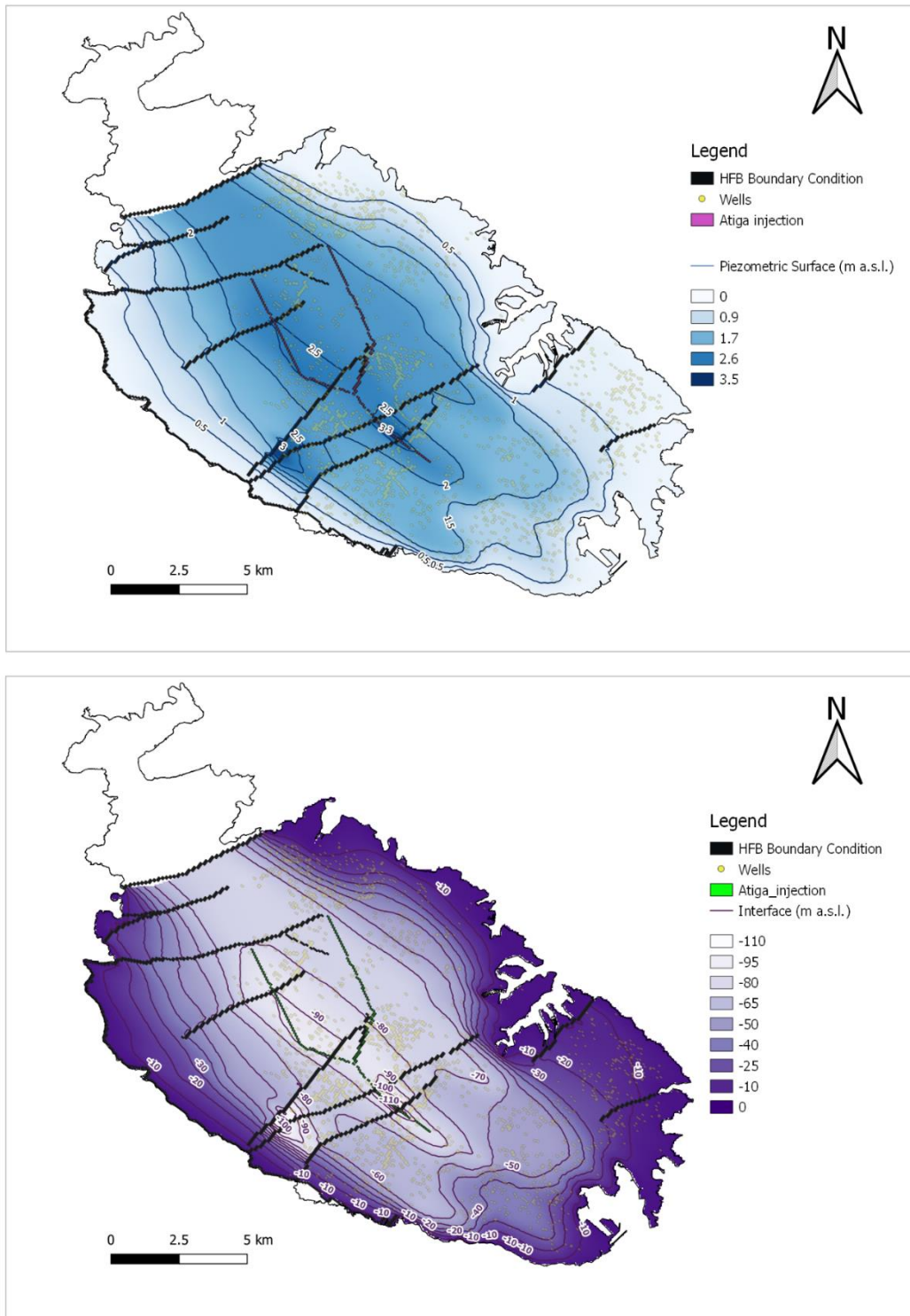


Figure 29. AR_S2 potentiometric surface and freshwater-seawater interface.

Artificial Recharge Scenario 3 (AR_S3)

This scenario represents an increased number of dams in valley systems through the rehabilitation of existing and the development of new dam structures, with an overall increase of the recharge capacity. The new dam recharge effect has been simulated as described for the existing ones in Deliverable D2.1, assuming $0.002 \text{ m}^3/\text{d}$ per cell in a buffer around the dam as shown in Figure 30. Existing (blue) and new dams (beige) with buffer of increased recharge shown for the existing dams (figure below) – the same has been applied to the new points..



Figure 30. Existing (blue) and new dams (beige) with buffer of increased recharge shown for the existing dams (figure below) – the same has been applied to the new points.

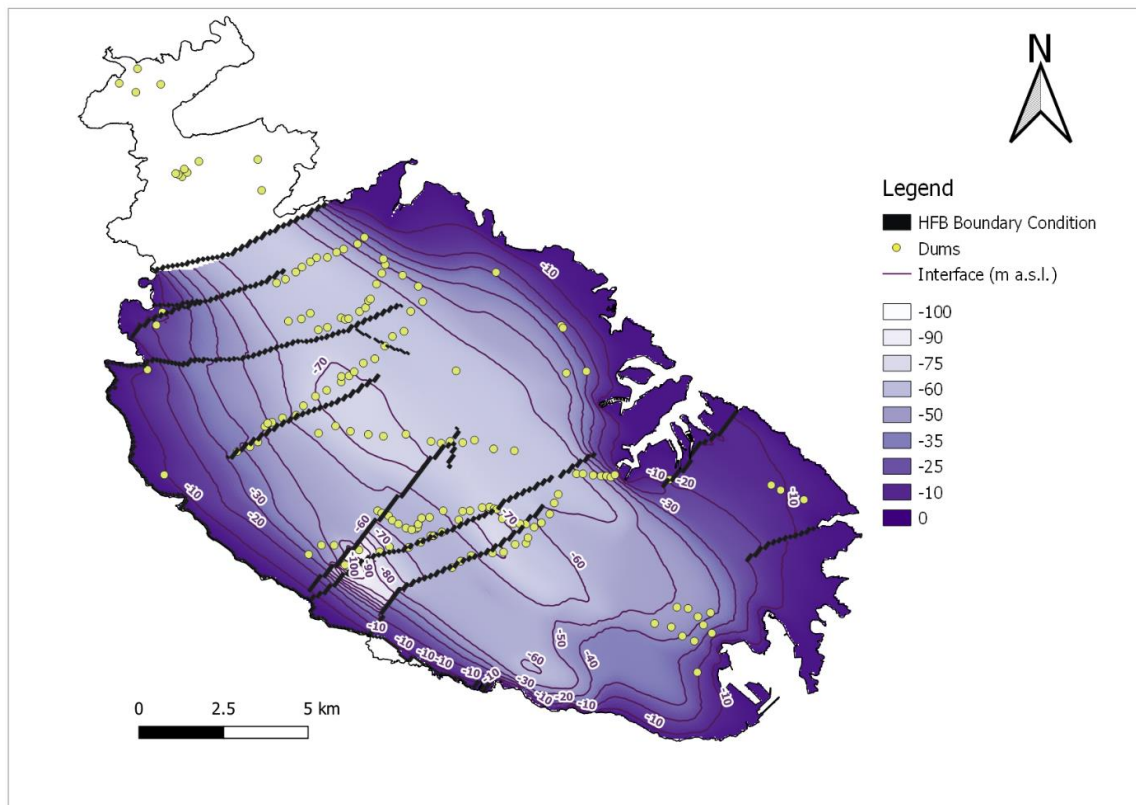
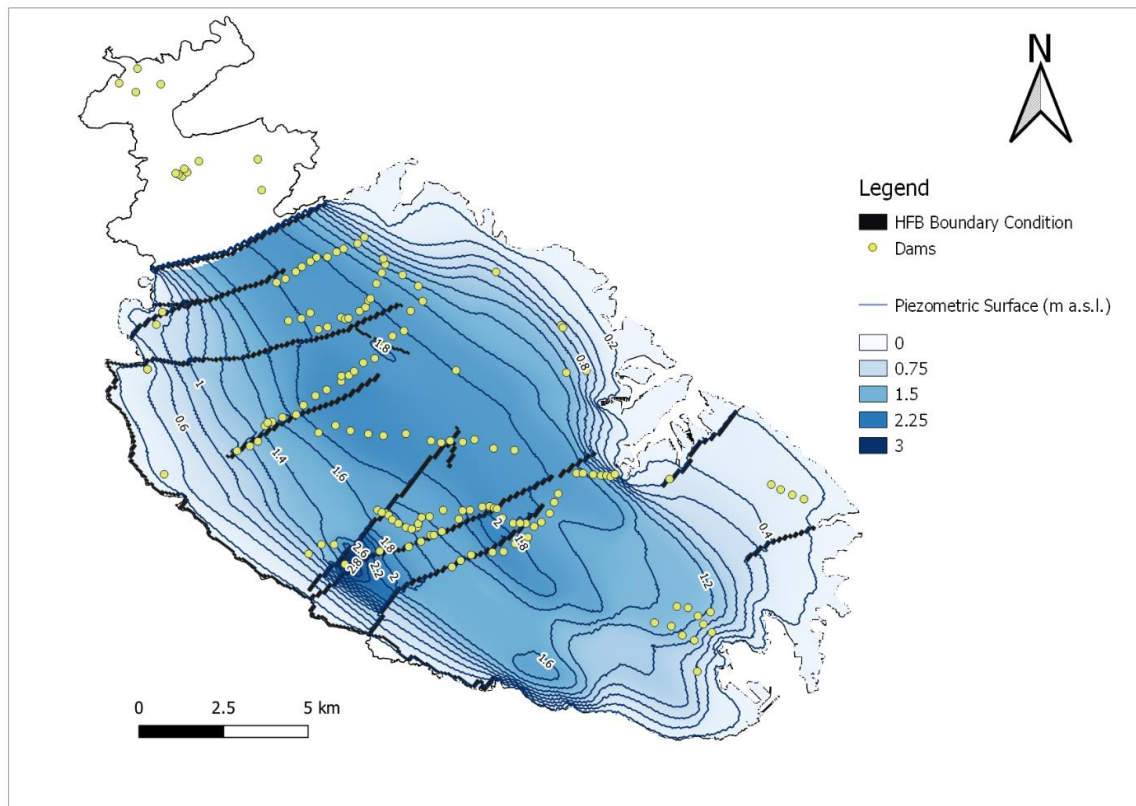


Figure 31. AR_S3 potentiometric surface and freshwater-seawater interface.

Comments

A synthetic comment is herein summarized for each MSLA scenario, with comparison to the reference present situation (Figure 2. Interface contours, SP3 (SAA) used as reference.):

- **HG_S1:** worse than the reference situation. The scenario is focused on the overall aquifer thickness reduction (to a half) and consequent K increase (to the double) which is a reliable possibility, since the first parameter is unknown and the second is affected by estimate errors. Simulation with the SAA approach would not highlight big differences, while the SWI2 simulation (which takes into account more assumed variables), presents an extremely different situation. The use of SWI2 (which includes time, K , aquifer thickness and storage coefficient) is recommended when a better understanding of the physical parameters will be available through new investigations and monitoring.
- **ABS_S1:** worse than the reference situation. The scenario is focused to represent a more reliable amount of private abstraction trying to keep the parameter field acceptably calibrated. In order to better evaluate the effect of the private abstraction, the volume abstracted should be known more in details, not only as an overall amount but associated to each single well average abstraction. When this information will be complete, a new round of calibration of the parameter field is recommended.
- **ABS_S2:** worse than the reference situation. Private abstraction is stopped and the public groundwater abstraction is increased. This scenario does not seem to be sustainable, regardless of the parameter field applied with high local and general rise of the interface.
- **ABS_S3:** not so different from the reference situation. Public borehole abstraction is stopped. Private abstraction is kept as in the reference model, as well as pumping stations abstraction.
- **ABS_S4:** better than the reference situation. Public abstraction is completely stopped, commercial abstraction is kept as in the reference model and groundwater resources allocated to the agricultural sector are increased by 2.5 times.
- **ABS_S5:** not so different from the reference situation. Commercial abstraction is completely stopped, with agricultural and public abstraction kept as in the reference model.
- **ABS_S6:** worse than the reference situation, but with an additional water volume that can be saved from other pumping sources. Draining water at an elevation higher than 0 m asl would in general be a preferable option than pumping. A proper representation of this scenario would require further information about the hydraulic conductivity in the selected position of the gallery through pumping tests.
- **RCH_S1:** worse than the reference situation. A 30% reduction of losses with respect to the 99-2015 period average is applied, keeping other stresses same as in the reference model.
- **RCH_S2:** extremely worse than the reference situation. This scenario is not even thinkable and demonstrates the importance of a wise urbanization that, even in already built up areas, should imply the recommendation provided by a wide literature about the urban hydrogeology (see for instance the review on the matter by Schirmer et al. 2012).
- **AD_S1:** this scenario qualitatively simulates the effect of a deep well-field located at the center of the island, abstracting seawater from beneath the freshwater-saltwater interface. Pumping

from below the interface would move it downward. As a consequence, the hydraulic head (which rests as a pillow over the saltwater) would move down accordingly. If the final head goes below 0 m asl, the result would be an increase in seawater intrusion from the coast; this is very likely to happen given the very low head elevation in the example area (< 1 m asl) and of the MSLA in general (< 2 m asl). Feasibility of such a well is highly questionable, at risk of failure because of probable low K , at risk of high impact because of the variation of the classical reference sea level from 0 m asl to a lower elevation (in a measure which is function of K , which is not known). The idea should be abandoned, moving to alternative solutions, such as lifting the sea water from the sea (and not from hundreds of meters below ground surface) on the west coast, having the same advantages in terms of concentrating the RO treatment plant in a single location and of the high topographic elevation to distribute water by gravity. The potential energy required for the lifting in this case would be much lower, rising the volume of water of about 180 m instead of more than 300 m.

- CC_S1: worse than the reference situation. In general, impact of climate change seems to be extremely less threatening with respect to wrong groundwater management practices.
- CC_S2: worse than the reference situation. In general, impact of climate change seems to be extremely less threatening with respect to wrong groundwater management practices.
- CC_S3: not so different from the reference situation. In general, impact of climate change seems to be extremely less threatening with respect to wrong groundwater management practices.
- AR_S1: locally better than the reference situation.
- AR_S2: better than the reference situation, with important effects over the whole system.
- AR_S3: not so different from the reference situation. Furthermore, the model assumes that the creation of new dams does not interfere with the recharge capacity of the existing ones, but this is not reliable, since the flow intercepted by an upstream dam is likely to reduce the flow to the downstream dam along the same valley. Estimates of the dams effect could be performed by hydrological modelling through surface water flow simulations. This would also give some inputs to the groundwater counterpart in terms of a better spatial distribution of recharge.

The scenarios development at the present stage does not include the uncertainty analysis that would be necessary to associate the degree of reliability to the results obtained. Given the high number of assumptions of the reference model and the missing of important details which influence some of the prediction outcome, the uncertainty is likely to be relatively high.

This is also due to the fact that a “all purposes model” cannot exist and every kind of scenario would require a specifically built model with assumptions and details important to the specific prediction to be provided (see for instance Doherty and Moore, 2017 for a summary of related concepts).

Mizieb and Pwales

Hydrogeological Scenario 1 (HG_S1)

The conceptual models of Mizieb and Pwales aquifers are described in the Deliverable D1.3. They are separated one each other by a low conductivity fault, and are separated from the MSLA by Pwales fault, assumed to be perfectly impermeable. Elevations of top and bottom of the two aquifers allows to include them into a unique model, even if hydrogeological behaviour is quite different. In both cases measured data are scarce, but an attempt of model calibration was performed on the basis of head data reported in the Royal maps, in Constain (1958) for Mizieb and collected in the 1940 census for Pwales (data provided by EWA in electronic format). The work of Constain reports hydraulic head elevations measured in different months between 1957 and 1958 during the Mgarr gallery works (started in 1957 and completed in 1962). The present scenario includes the introduction of head data in the version of the model described in Deliverable D2.1 and the consequent parameter calibration to fit the data. The dataset used, anyway, is affected by high uncertainty for the following reasons:

1. Heads are based on a single measurement;
2. Borehole elevation approximation is not known;
3. Pumping active in the measurement period are unknown;
4. Measurements are taken in different seasons and years;
5. The bottom of the aquifers is not exactly known.

These premises make all the modelling processing described in the following pages completely hypothetical and results should not be used to take any groundwater management decision.

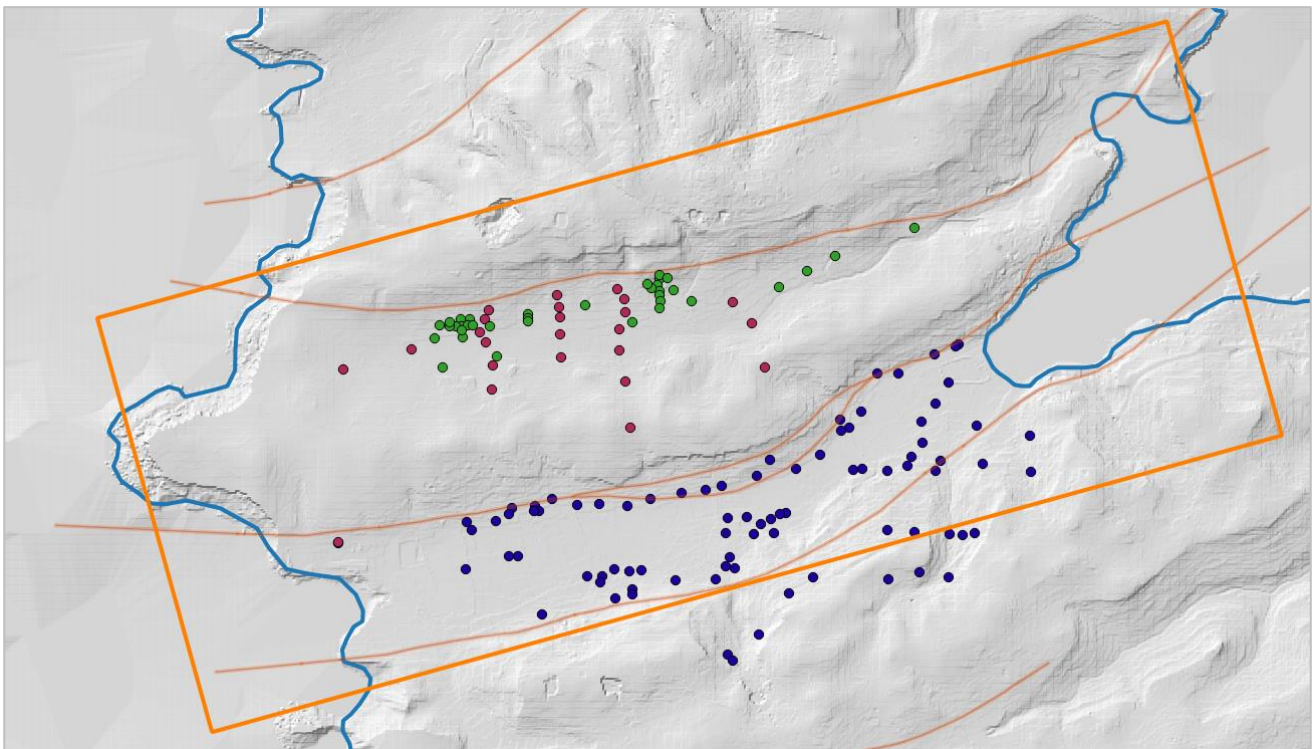


Figure 32. Available data from the Royal maps (red), Constain (1958) (green) and 1940 census (blue).

Domain and discretization

The Mizieb-Pwales (MP) model grid covers an area of about 15 km², divided into 47616 cells with dimension 12.5x25 m, rotated by 15.5 degree (Figure 33. MP model grid.). The Mizieb aquifer surface occupies 16000 cells, Pwales 8350, the sea 3200 cells, while the southern and western portions of the domain are limited by low conductivity formations, assuming that groundwater exchanges are extremely scarce in those directions.

The model is single-layer, with a variable thickness. The bottom elevation of the model was set according to the stratigraphic interpretation of the Blue Clay top, nevertheless the bottom surface needed to be smoothed and deepened in some portions in order to control numerical instability.

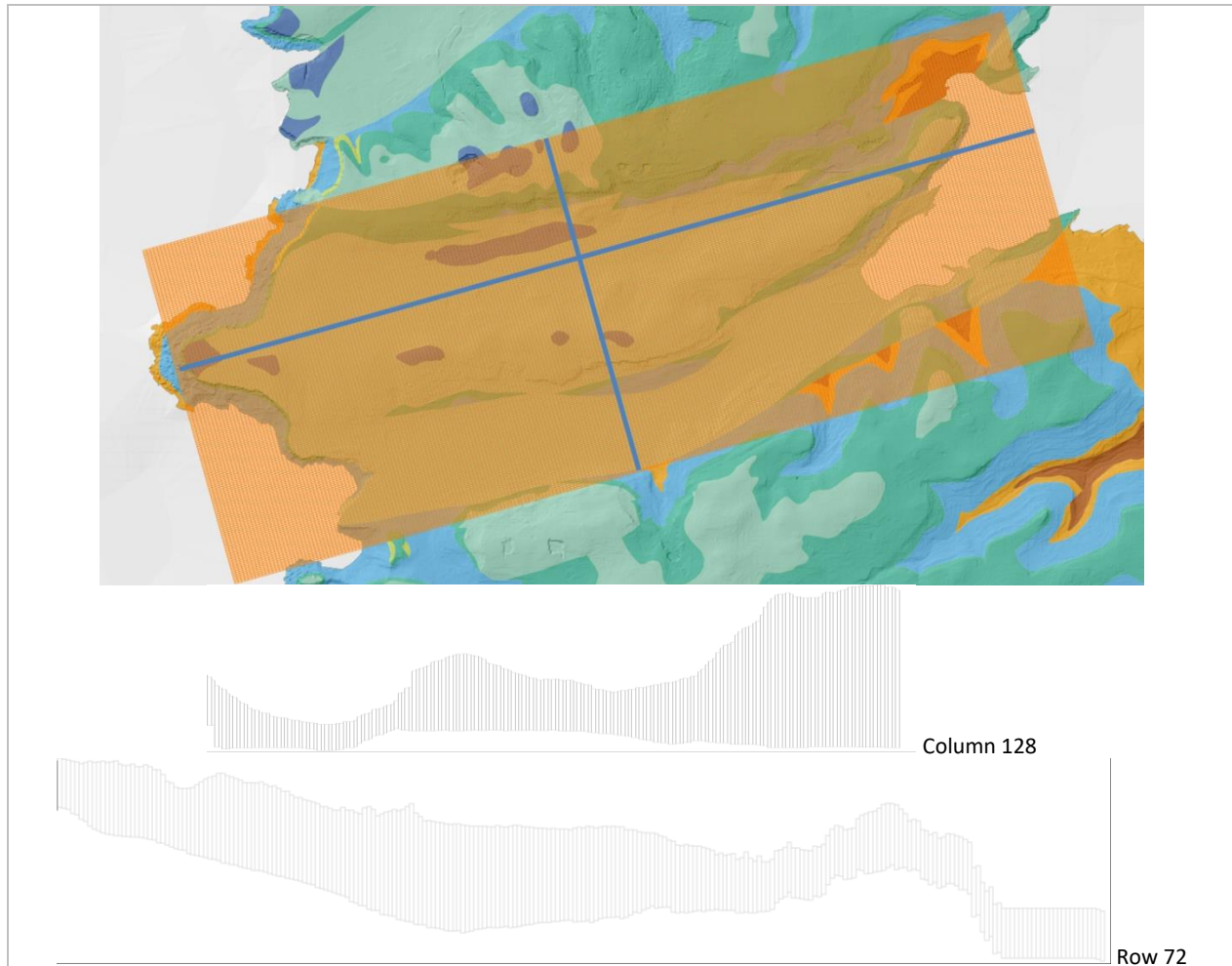


Figure 33. MP model grid.

Boundary condition

The preliminary (and probably wrong) configuration of boundary conditions presently includes (Figure 34. Boundary conditions of MP model.):

1. General head boundary (GHB) to represent the sea, characterized by head elevation = 0 m asl;
2. General head boundary (GHB) to represent the sinkholes at the aquifer bottom in Mizieb, characterized by head elevation = 0 m asl and conductance which was varied in the calibration process;
3. Hydraulic flow barrier (HFB) to represent the main faults discontinuities with an initial low hydraulic conductivity (1E-8 m/s);

4. Drain boundary to represent a possible outflow from the aquifer along the northern breccia fault, characterized by head elevation = 0 m asl and conductance which was varied in the calibration process;
5. Wells (WELL) to represent the 81 private wells that are supposed to be active during the period of reference (1940-1960) characterized by an estimated average discharge of about 10,000 m³/y each.

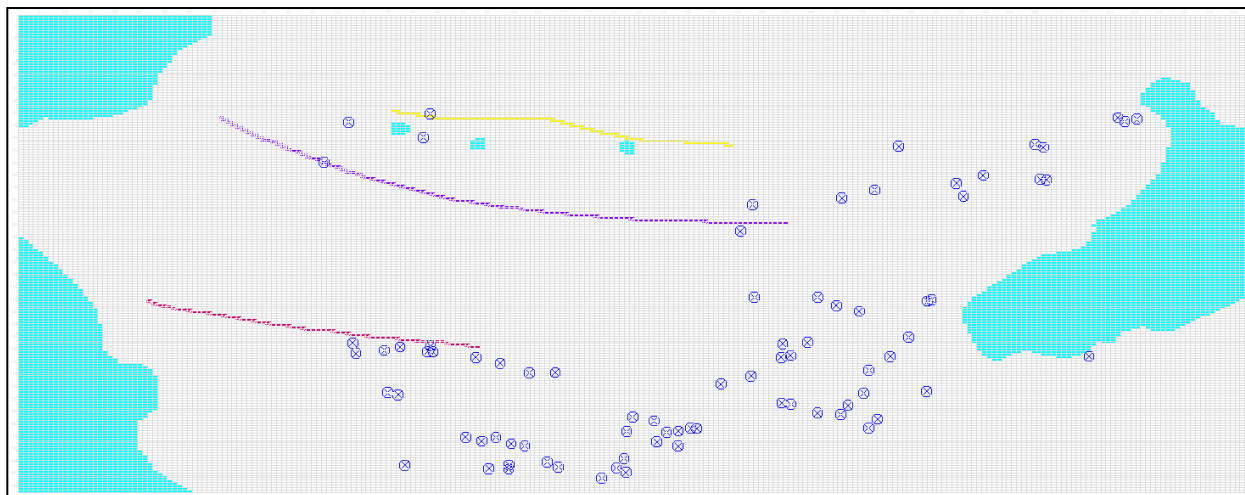
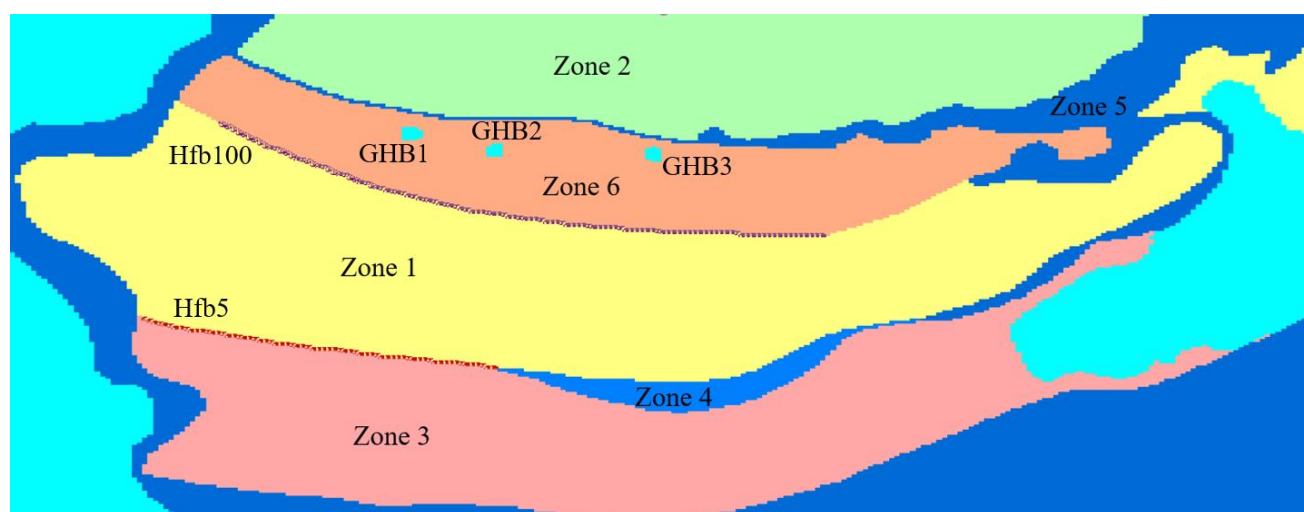


Figure 34. Boundary conditions of MP model.

Initial properties and heads

Initial hydraulic conductivity values were assigned on the basis of results obtained in the MSLA model calibration and preliminarily adjusting the values using uniform zones (Figure 35. Initial hydraulic conductivity distribution.). The available heads and their position are shown in Table 4. Available data from the Royal maps, Constain (1958) and 1940 census. and Figure 32. Available data from the Royal maps (red), Constain (1958) (green) and 1940 census (blue)..



	Kx	Ky	Kz	Color
1	0.0005	0.0005	5e-005	Yellow
2	0.0005	0.0005	5e-005	Light Green
3	0.0005	0.0005	5e-005	Light Red
4	1e-007	1e-007	1e-008	Blue
5	1e-007	1e-007	1e-008	Dark Blue
6	0.0005	0.0005	5e-005	Orange

Figure 35. Initial hydraulic conductivity distribution.

ID	X	Y	Ground elevation (m asl)	Borehole depth (m)	Depth to water (m)	Water head (m asl)	Date
10000	441798.8	3978405	48.768	45.72	dry	dry	Apr_1958
10001	442381	3978360	43.5864	54.864	40.8432	2.7432	Jun_1958
10002	442713.5	3978480	47.8536	62.1792	45.1104	2.7432	Jun_1958
10003	443200.9	3978559	37.4904	41.148	32.004	5.4864	Jun_1958
10004	443957.2	3978888	28.6512	30.7848	16.4592	12.192	Jun_1958
10005	442118.7	3978458	51.5112	58.5216	46.9392	4.572	Apr_1958
10006	443357.5	3978645	37.7952	42.672	dry	dry	Jun_1958
10007	443515.7	3978733	43.2816	49.3776	38.4048	4.8768	Jun_1958
10008	441799.2	3978381	46.9392	50.292	43.2816	3.6576	May_1958
10009	441800	3978368	46.6344	58.2168	43.2816	3.3528	May_1958
1074	442532.6	3978601	66.7512	78.0288	59.1312	7.62	Sept_1957
1075	442525.7	3978568	58.5216	83.82	55.4736	3.048	Sept_1957
1076	442533.1	3978537	53.6448	99.6696	49.9872	3.6576	Oct_1957
1078	442490.8	3978553	57.3024	86.5632	54.2544	3.048	Nov_1957
1079	442538.9	3978477	45.72	68.8848	42.3672	3.3528	Nov_1957
1090	441364.7	3978339	52.1208	70.104	48.1584	3.9624	Nov_1957
1096	441321.4	3978110	44.8056	44.8056	33.8328	10.9728	Jun_1958
1097	441278.2	3978273	47.8536	51.816	39.0144	8.8392	Jun_1958
1098	441629.2	3978168	44.5008	53.0352	39.3192	5.1816	Jun_1958
1099	441589.2	3978338	49.3776	63.3984	45.72	3.6576	Jun_1958
B.H 160	441583.9	3978431	62.08	61.87	58.22	2.87	
B.H 144	441561.6	3978380	54.51	65.84	49.99	3.85	
B.H 133	441530.1	3978304	47.23	61.57	43.28	4.27	
B.H 138	441564.1	3978248	44.76	55.17	38.89	6.72	
B.H 142	441602.7	3978119	47.07	53.34	43.28	3.53	
B.H 146	441148.8	3978207	45.88	44.5	30.78	15.53	
B.H 157	441962.4	3978510	61.39	63.09	55.47	4.69	
B.H 153	441976.9	3978447	52.4	60.05	47.55	4.32	
B.H 156	441981	3978388	47.87	56.39	43.89	3.87	
B.H 139	441597.6	3977984	51.38	52.73	41.42	10.73	
B.H 161	441987.9	3978166	42.53	51.51	38.1	4.58	
B.H 159	441979.8	3978293	44.77	52.12	40.72	3.14	
B.H 131	442308	3978324	43.88	53.34	40.42	2.53	
B.H 137	442311.7	3978206	40.54	50.29	36.76	3.76	
B.H 136	442341.6	3978415	48.63	58.22	44.5	2.75	
B.H 135	442343.6	3978028	47.14	34.44	29.26	19.44	
B.H 150	442371.9	3977772	74.7	58.83	54.25	21.07	
B.H 147	442297.4	3978546	58.34		54.25	3.02	
B.H 140	442337.5	3978492	53.93	71.93	50.29	3.05	
B.H 134	440766.7	3978097	54	39.62	32	21.52	
B.H 152	443125.5	3978110	60.39	45.72	42.37	18.95	
B.H 132	442946.6	3978472	40.27	49.99	37.19	3.78	
B.H 141	443053	3978358	34.91	39.62	30.91	4.65	
B.H 29	440743.7	3977135	32.47 (from DEM)	31.09	24.69	7.78	
318	444277.7	3978420	3.069	4.0132	3.302	0.712	1940
368	444260.6	3978408	2.327	3.3528	3.0734	0.28	1940
317	444145.2	3978366	2.032	3.7338	3.3528	0.381	1940
369	444219	3978210	2.538	1.8288	1.6256	0.203	1940
370	444151	3978090	3.809	6.2992	4.572	1.727	1940
342	444380.5	3977969	12.409	8.3312	7.874	0.457	1940
340	444069.4	3977991	4.893	6.5024	6.0198	0.483	1940
327	443942.1	3978262	1.502	2.0066	1.5494	0.458	1940
326	443822.9	3978260	5.884	6.3246	6.0452	0.28	1940
319	443732.1	3978045	2.12	4.8768	4.6228	0.254	1940
315	443613.9	3978001	7.043	7.493	7.3406	0.153	1940
316	443667.3	3977957	2.597	4.3688	3.9624	0.406	1940
314	443622.9	3977938	3.156	5.4864	5.1308	0.356	1940
378	443887.3	3977112	93.052	27.8384	27.2796	0.559	1940
308	444058.3	3977150	90.566	27.813	26.416	1.397	1940

ID	X	Y	Ground elevation (m asl)	Borehole depth (m)	Depth to water (m)	Water head (m asl)	Date
341	444076.3	3977875	10.925	10.1854	9.779	0.407	1940
301	444014.9	3977796	14.534	9.906	9.3472	0.559	1940
302	444176.1	3977770	18.728	17.9832	17.526	0.458	1940
372	444145.6	3977715	24.238	22.4536	21.9964	0.457	1940
373	443992.7	3977741	20.309	15.875	15.113	0.762	1940
296	443878.1	3977716	15.264	12.8016	12.192	0.609	1940
294	443738.1	3977724	12.149	9.7536	8.7376	1.016	1940
330	443690.9	3977721	10.461	4.2418	4.0386	0.204	1940
331	443505.2	3977806	3.946	6.9088	6.2992	0.61	1940
323	443371.2	3977727	4.48	6.7564	5.5372	1.219	1940
322	443225.6	3977778	20.808	23.4696	23.0378	0.432	1940
345	443149.9	3977689	10.115	12.954	12.192	0.762	1940
344	442952.6	3977634	11.473	12.954	12.192	0.762	1940
337	443313.4	3977480	9.05	7.9756	7.3152	0.66	1940
338	443282	3977474	9.408	8.4582	7.6962	0.762	1940
289	443227.5	3977445	10.457	9.779	8.3566	1.422	1940
290	443171.1	3977421	12.514	11.5062	9.779	1.727	1940
339	443094.9	3977460	9.025	9.7536	8.8392	0.915	1940
343	442985.8	3977449	11.278	12.7508	12.2936	0.457	1940
346	442728.5	3977594	11.211	13.1826	12.192	0.991	1940
286	442978	3977370	15.486	15.2654	13.462	1.803	1940
279	442694.7	3977106	23.943	21.4376	20.3454	1.092	1940
284	442917.9	3977112	29.639	28.2448	26.5176	1.727	1940
285	443028.8	3977173	33.223	27.432	26.7462	0.685	1940
280	442974.7	3977181	27.17	26.035	24.8158	1.219	1940
288	443000.6	3977236	23.036	22.86	21.6408	1.219	1940
274	443135.1	3977362	20.206	25.3238	24.1554	1.168	1940
297	442989.5	3976689	79.241	2.0574	1.778	0.279	1940
363	442504.3	3977163	15.028	15.113	13.1318	1.981	1940
352	442435.7	3977155	14.155	15.6464	14.7828	0.864	1940
351	442351.9	3977168	12.391	13.0302	12.4206	0.61	1940
353	442288.8	3977128	14.56	13.7922	13.1064	0.686	1940
274	442360.9	3977004	28.497	25.3238	24.1554	1.168	1940
276	442453.8	3977052	24.299	22.352	21.2344	1.117	1940
277	442457.2	3977028	29.877	24.6888	23.7744	0.915	1940
350	442272.9	3977530	13.069	13.8684	13.1826	0.686	1940
349	442428.8	3977521	11.046	12.8524	12.065	0.788	1940
348	442553.6	3977560	12.769	13.843	13.1064	0.737	1940
354	442148.1	3977528	14.505	15.367	14.7066	0.66	1940
359	442204.2	3977126	14.568	16.5354	15.621	0.915	1940
367	441948.5	3976912	29.09	29.083	28.6512	0.432	1940
355	442005.3	3977557	18.454	20.5486	20.3708	0.177	1940
356	441911	3977521	19.349	20.7264	20.2692	0.458	1940
357	441931.1	3977493	16.116	17.0688	16.4592	0.61	1940
371	441906.9	3977490	17.018	18.4404	18.2118	0.228	1940
358	441781.4	3977507	21.85	22.5298	21.7678	0.762	1940
360	441766.9	3977474	18.728	22.3266	21.5646	0.762	1940
365	441764.8	3977237	15.431	16.5354	16.0528	0.482	1940
361	441529.1	3977430	21.008	24.13	22.606	1.524	1940
362	441559.6	3977383	17.658	18.4658	18.288	0.177	1940
bh28	441525.7	3977168	20.635	30.48	24.384	6.096	1940
bh29	440812	3977314	30.304	28.956	30.296	4.267	1940
bh25	442276.8	3977092	16.097	19.812	14.0208	5.791	1940

Table 4. Available data from the Royal maps, Constrain (1958) and 1940 census.

Results

Zone calibration

The adjustable parameters of this calibration run included zones of hydraulic conductivity, the GHB conductance (sinkholes), HFB conductivity (low permeability faults), drain conductance (breccia fault), recharge multiplier. Sensitivities are reported in Figure 36. Parameter sensitivities; all parameters (above) and hf5 excluded (below). and Table 5. Parameter sensitivities and preliminary values.. The highest values of sensitivity is associated to the HFB conductivity of the fault that separates Mizieb from Pwales (hf5).

The scatterplot with the comparison of the simulated heads with the available data is shown in Figure 37. Scatterplot of calculated and observed heads. and Table 6. Comparison of observed and simulated heads (zone calibration)..

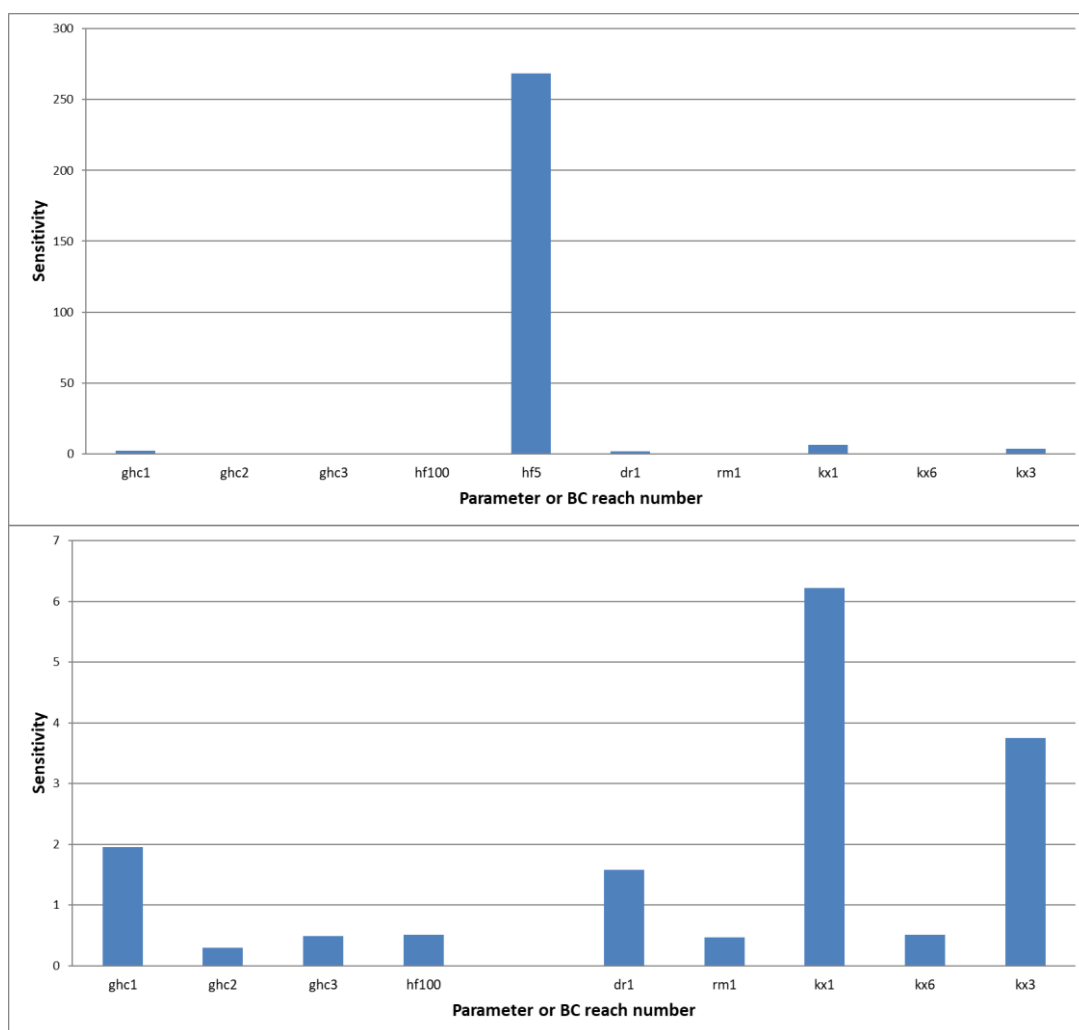


Figure 36. Parameter sensitivities; all parameters (above) and hf5 excluded (below).

Name	type	Value	Unit	Sensitivity
ghc1	Sinkhole conductance	6.88E-04	m/s	1.95399
ghc2	Sinkhole conductance	8.31E-06	m/s	0.299683
ghc3	Sinkhole conductance	4.02E-04	m/s	0.487705
hf100	Fault hydraulic conductivity	4.20E-09	m/s	0.51565

Name	type	Value	Unit	Sensitivity
hf5	Fault hydraulic conductivity	1.26E-09	m/s	268.649
dr1	Breccia Fault hydraulic conductivity	9.27E-06	m/s	1.57563
rm1	Recharge multiplier	0.824099	--	0.463828
kx1	Hydraulic conductivity, zone 1	4.97E-05	m/s	6.22476
kx6	Hydraulic conductivity, zone 6	4.45E-05	m/s	0.513294
kx3	Hydraulic conductivity, zone 3	6.53E-04	m/s	3.75376

Table 5. Parameter sensitivities and preliminary values.

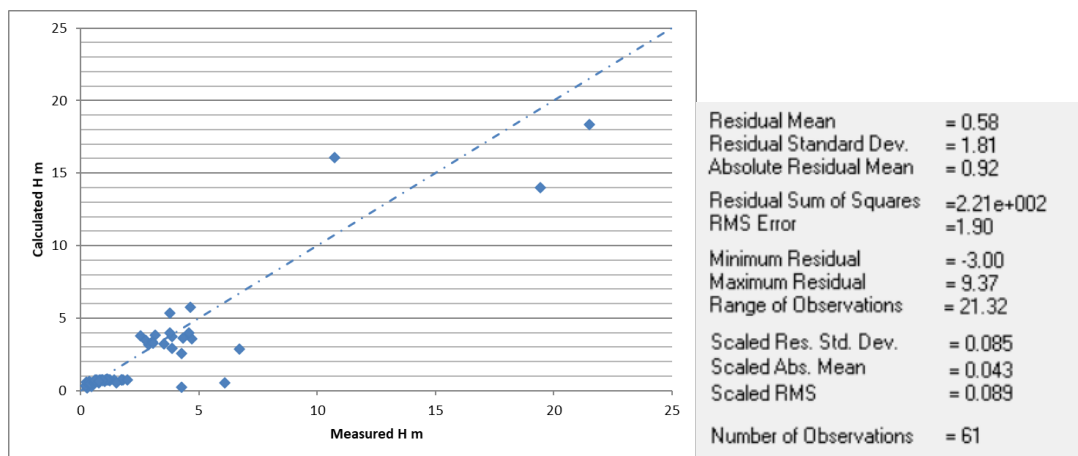


Figure 37. Scatterplot of calculated and observed heads.

Name	Group	Measured	Modelled	Residual
o1	Mizieb	2.87	3.1715	-0.3015
o2	Mizieb	3.85	2.90562	0.94438
o3	Mizieb	4.27	2.54216	1.72784
o4	Mizieb	6.72	2.84835	3.87165
o5	Mizieb	3.53	3.24574	0.28426
o6	Mizieb	4.69	3.58321	1.10679
o7	Mizieb	4.32	3.64606	0.67394
o8	Mizieb	3.87	3.70516	0.16484
o9	Mizieb	10.73	16.0635	-5.3335
o10	Mizieb	4.58	3.99428	0.58572
o11	Mizieb	3.14	3.81697	-0.67697
o12	Mizieb	2.53	3.78019	-1.25019
o13	Mizieb	3.76	3.99795	-0.23795
o14	Mizieb	2.75	3.48196	-0.73196
o15	Mizieb	19.44	14.013	5.427
o16	Mizieb	3.02	3.35526	-0.33526
o17	Mizieb	3.05	3.28337	-0.23337
o18	Mizieb	21.52	18.3397	3.1803
o19	Mizieb	3.78	5.3691	-1.5891
o20	Mizieb	4.65	5.77314	-1.12314
o21	Pwales	0.28	0.195118	0.084882
o22	Pwales	0.203	0.318315	-0.11532

Name	Group	Measured	Modelled	Residual
o23	Pwales	0.457	0.302177	0.154823
o24	Pwales	0.483	0.476477	0.006523
o25	Pwales	0.458	0.562794	-0.10479
o26	Pwales	0.254	0.604892	-0.35089
o27	Pwales	0.356	0.622838	-0.26684
o28	Pwales	0.407	0.49587	-0.08887
o29	Pwales	0.559	0.536885	0.022115
o30	Pwales	0.762	0.555606	0.206394
o31	Pwales	0.609	0.591875	0.017125
o32	Pwales	1.016	0.623208	0.392792
o33	Pwales	0.61	0.655743	-0.04574
o34	Pwales	1.219	0.685425	0.533575
o35	Pwales	0.66	0.711304	-0.0513
o36	Pwales	0.762	0.714908	0.047092
o37	Pwales	1.422	0.721643	0.700357
o38	Pwales	1.727	0.727658	0.999342
o39	Pwales	0.915	0.732172	0.182828
o40	Pwales	1.803	0.741329	1.061671
o41	Pwales	1.092	0.745162	0.346838
o42	Pwales	1.727	0.747398	0.979602
o43	Pwales	1.219	0.745602	0.473398
o44	Pwales	1.219	0.74371	0.47529
o45	Pwales	1.168	0.733067	0.434933
o46	Pwales	1.981	0.735787	1.245213
o47	Pwales	0.864	0.730435	0.133565
o48	Pwales	0.61	0.722745	-0.11275
o49	Pwales	0.686	0.714605	-0.02861
o50	Pwales	1.168	0.721344	0.446656
o51	Pwales	1.117	0.731033	0.385967
o52	Pwales	0.915	0.731232	0.183768
o53	Pwales	0.686	0.731515	-0.04552
o54	Pwales	0.788	0.740817	0.047183
o55	Pwales	0.66	0.716707	-0.05671
o56	Pwales	0.915	0.703073	0.211927
o57	Pwales	0.61	0.674994	-0.06499
o58	Pwales	0.762	0.635685	0.126315
o59	Pwales	1.524	0.562289	0.961711
o60	Pwales	6.096	0.541086	5.554914
o61	Pwales	4.267	0.236384	4.030616

Table 6. Comparison of observed and simulated heads (zone calibration).

PP calibration

In order to further evaluate hydraulic conductivity sensitivities, Pilot Points (PP) were introduced and a second round of calibration was undertaken applying the highly parametrized approach described in

Deliverable D4.1. Agricultural wells shown in Figure 34. Boundary conditions of MP model. were activated. The other parameters were kept unchanged from the previous calibration run.

PP sensitivities are reported in Figure 38. PP sensitivities, where it can be seen that the highest values of sensitivity is associated to PP50. The position of PP and relative associated sensitivity are shown in Figure 39. PP position and sensitivities (darker colors corresponds to higher sensitivities)..

The spatial distribution of the hydraulic conductivity field obtained in this steady state parameter adjustment is shown in Figure 40. Hydraulic conductivity distribution obtained from the PP value adjustments (in m/s)..

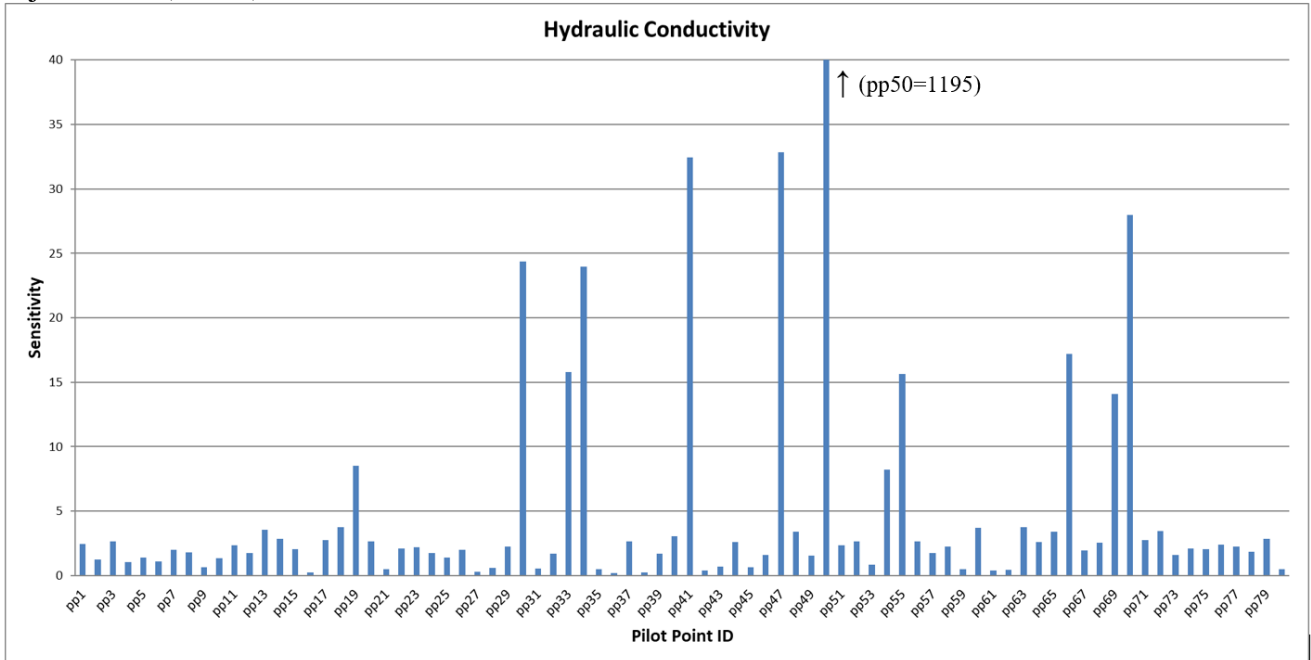


Figure 38. PP sensitivities.

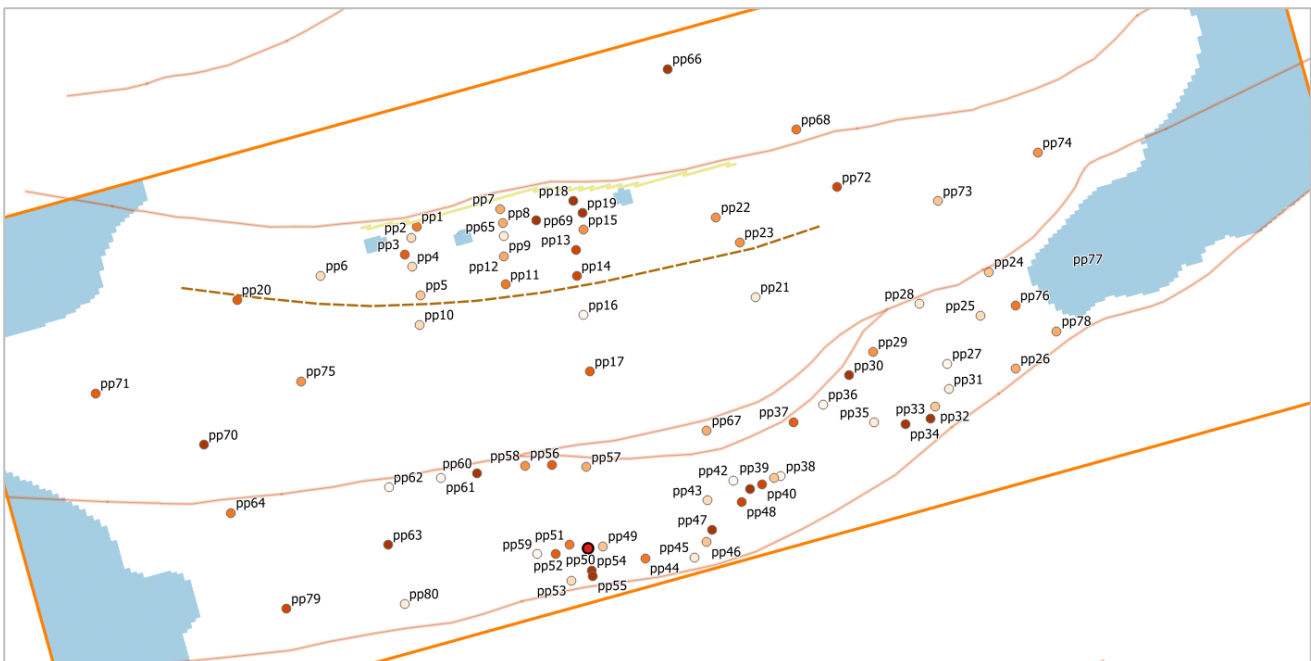


Figure 39. PP position and sensitivities (darker colors corresponds to higher sensitivities).



Figure 40. Hydraulic conductivity distribution obtained from the PP value adjustments (in m/s).

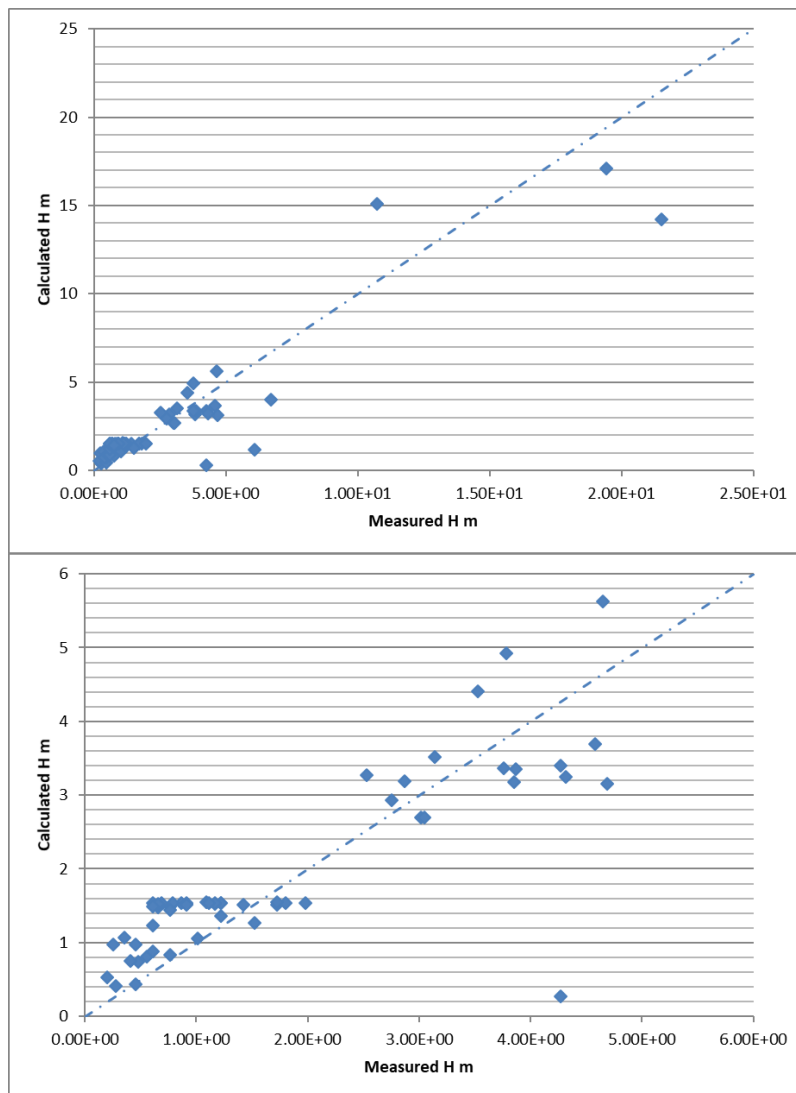


Figure 41. Scatterplot of Calculated and observed heads, whole model (above) and detail for heads lower than 6 m asl (below).

Name	Group	Measured	Modelled	Residual
o1	Mizieb	2.87E+00	3.190578	-0.32058
o2	Mizieb	3.85E+00	3.171655	0.678345
o3	Mizieb	4.27E+00	3.394478	0.875522
o4	Mizieb	6.72E+00	3.993952	2.726048
o5	Mizieb	3.53	4.411922	-0.88192
o6	Mizieb	4.69	3.148832	1.541168
o7	Mizieb	4.32	3.249635	1.070365
o8	Mizieb	3.87	3.357897	0.512103
o9	Mizieb	10.73	15.08321	-4.35321
o10	Mizieb	4.58	3.688798	0.891202
o11	Mizieb	3.14E+00	3.513713	-0.37371
o12	Mizieb	2.53E+00	3.27E+00	-0.74492
o13	Mizieb	3.76	3.36E+00	0.397515
o14	Mizieb	2.75	2.925301	-0.1753
o15	Mizieb	19.44	17.07248	2.36752
o16	Mizieb	3.02E+00	2.701128	0.318872
o17	Mizieb	3.05E+00	2.70E+00	0.353053
o18	Mizieb	21.52	1.42E+01	7.30672
o19	Mizieb	3.78	4.922093	-1.14209
o20	Mizieb	4.65E+00	5.625414	-0.97541
o21	Pwales	2.80E-01	0.407714	-0.12771
o22	Pwales	2.03E-01	0.533198	-0.3302
o23	Pwales	0.457	0.43294	0.02406
o24	Pwales	4.83E-01	0.739148	-0.25615
o25	Pwales	0.458	9.68E-01	-0.51026
o26	Pwales	2.54E-01	9.73E-01	-0.71916
o27	Pwales	0.356	1.065633	-0.70963
o28	Pwales	4.07E-01	0.753621	-0.34662
o29	Pwales	5.59E-01	0.813188	-0.25419
o30	Pwales	7.62E-01	0.836014	-0.07401
o31	Pwales	0.609	0.885345	-0.27635
o32	Pwales	1.02E+00	1.057896	-0.0419
o33	Pwales	6.10E-01	1.232789	-0.62279
o34	Pwales	1.219	1.361081	-0.14208
o35	Pwales	6.60E-01	1.478787	-0.81879
o36	Pwales	7.62E-01	1.491274	-0.72927
o37	Pwales	1.42E+00	1.511724	-0.08972
o38	Pwales	1.73E+00	1.51835	0.20865
o39	Pwales	9.15E-01	1.524471	-0.60947
o40	Pwales	1.803	1.533762	0.269238
o41	Pwales	1.092	1.54E+00	-0.45238
o42	Pwales	1.73E+00	1.54E+00	0.183737

Name	Group	Measured	Modelled	Residual
o43	Pwales	1.22E+00	1.540575	-0.32158
o44	Pwales	1.22E+00	1.538605	-0.31961
o45	Pwales	1.17E+00	1.523869	-0.35587
o46	Pwales	1.98E+00	1.540027	0.440973
o47	Pwales	8.64E-01	1.54E+00	-0.67323
o48	Pwales	6.10E-01	1.53E+00	-0.9223
o49	Pwales	6.86E-01	1.526466	-0.84047
o50	Pwales	1.17E+00	1.532461	-0.36446
o51	Pwales	1.117	1.537755	-0.42076
o52	Pwales	9.15E-01	1.54E+00	-0.62359
o53	Pwales	6.86E-01	1.53E+00	-0.84884
o54	Pwales	0.788	1.540584	-0.75258
o55	Pwales	0.66	1.527215	-0.86722
o56	Pwales	9.15E-01	1.517383	-0.60238
o57	Pwales	6.10E-01	1.495232	-0.88523
o58	Pwales	0.762	1.441872	-0.67987
o59	Pwales	1.524	1.263516	0.260484
o60	Pwales	6.096	1.186777	4.909223
o61	Pwales	4.267	0.27547	3.99153

Table 7. Comparison of observed and simulated heads (PP calibration).

Water budget and head distribution

The terms of the budget obtained in the steady state of Mizieb and Pwales are shown in m³/s and m³/y in

INFLOWS				OUTFLOWS				Water balance Mizieb aquifer (PP cal.)	
Storage	0	0	0	OLFX min	0	0	0	Inflows	
X min	0.000193819020989139	0.00608850709171664	0	OLFX max	0	0	0	Recharge (m ³ /y)	818472
X max	0.0109949978378552	0.00162783577397363	0	OLFY min	0	0	0	From aquifer boundaries	697173
Y min	0.00405087312356045	0.019410233198073	0	OLFY max	0	0	0	Outflows	
Y max	0.00686752752072262	0.0035568955517072	0	GW to DLF	0	0	0	From aquifer boundaries	967596
Top	0	0	0	DLF to GW	0	0	0	Sinkholes (GHB) (m ³ /y)	435051
Bottom	0	0	0	DLF CH	0	0	0	Breccia fault (DRAIN) (m ³ /y)	70668
Well	0	0.00135762002173578	0	DLF Source-Sink	0	0	0	Wells (agricultural) (m ³ /y)	42814
C.H.	0	0	0	Special Boundar	0	0	0		
GHB	0	0.013795386140373	0	DLF Recharge	0	0	0		
River	0	0	0	DLF Evap.	0	0	0		
Drain	0	0.00224087619790225	0	Interception Stor.	0	0	0		
Stream	0	0	0	Precipitation	0	0	0		
Recharge	0.0259535786398502	0	0	Evp. Canopy	0	0	0		
ET	0	0	0	Recharge to Grc	0	0	0		
Lake	0	0	0	Total PET Possil	0	0	0		
TOTAL	0.0480607961429775	0.048076147978945	-0.00082						
								Water balance Pwales aquifer (PP cal.)	
								Inflows	
								Recharge (m ³ /y)	439428
								From aquifer boundaries	909649
								Outflows	
								Sea (GHB) (m ³ /y)	593830
								Wells (agricultural) (m ³ /y)	37777

INFLOWS		OUTFLOWS			
Storage	0	0	0	OLF X min	From aquifer boundaries
X min	0.00163710980142895	0.0102809634435381	0	OLF X max	
X max	0.00258197371627666	0.00790920956562646	0	OLF Y min	
Y min	0.0118821790991888	0.00260765439452371	0	OLF Y max	
Y max	0.0127435255184771	0.00180791340316448	0	GW to OLF	
Top	0	0	0	OLF to GW	
Bottom	0	0	0	OLF CH	
Well	0	0.00119790001917863	0	OLF Source-Si	
C.H.	0	0	0	Special Bound	
GHB	0	0.0188302135436516	0	OLF Recharge	
River	0	0	0	OLF E.vap.	
Drain	0	0	0	Interception St	
Stream	0	0	0	Precipitation	
Recharge	0.0139341731686713	0	0	Evp. Canopy	
ET	0	0	0	Recharge to C	
Lake	0	0	0	Total PET Po	
TOTAL	0.0427789613040428	0.042633854369683	0.339		

Table 8. Aquifers water balances (PP calibration results).. Even if acceptable numerical stability of the model is confirmed by the low water budget discrepancy which is less than 1%, results needs to be carefully revised.

INFLOWS		OUTFLOWS			
Storage	0	0	0	OLF X min	Water balance Mizieb aquifer (PP cal.)
X min	0.000193819020989139	0.00608850709171664	0	OLF X max	
X max	0.0109949978378852	0.00162783577397363	0	OLF Y min	Recharge (m ³ /y)
Y min	0.00405087312356045	0.019410233198073	0	OLF Y max	818472
Y max	0.00686752752072262	0.00359568955517072	0	GW to OLF	From aquifer boundaries
Top	0	0	0	OLF to GW	697173
Bottom	0	0	0	OLF CH	<i>Outflows</i>
Well	0	0.00135762002173578	0	OLF Source-Sink	From aquifer boundaries
C.H.	0	0	0	Special Bound	967596
GHB	0	0.013795386140373	0	OLF Recharge	Sinkholes (GHB) (m ³ /y)
River	0	0	0	OLF E.vap.	435051
Drain	0	0.00224087619790225	0	Interception Stor.	Breccia fault (DRAIN) (m ³ /y)
Stream	0	0	0	Precipitation	70668
Recharge	0.0259535786398502	0	0	Evp. Canopy	Wells (agricultural) (m ³ /y)
ET	0	0	0	Recharge to Grc	42814
Lake	0	0	0	Total PET Possi	
TOTAL	0.0480607961429775	0.048076147978945	-0.00082		

INFLOWS		OUTFLOWS			
Storage	0	0	0	OLF X min	Water balance Pwales aquifer (PP cal.)
X min	0.00163710980142895	0.0102809634435381	0	OLF X max	
X max	0.00258197371627666	0.00790920956562646	0	OLF Y min	Recharge (m ³ /y)
Y min	0.0118821790991888	0.00260765439452371	0	OLF Y max	439428
Y max	0.0127435255184771	0.00180791340316448	0	GW to OLF	From aquifer boundaries
Top	0	0	0	OLF to GW	909649
Bottom	0	0	0	OLF CH	<i>Outflows</i>
Well	0	0.00119790001917863	0	OLF Source-Si	Sea (GHB) (m ³ /y)
C.H.	0	0	0	Special Bound	593830
GHB	0	0.0188302135436516	0	OLF Recharge	Wells (agricultural) (m ³ /y)
River	0	0	0	OLF E.vap.	37777
Drain	0	0	0	Interception St	From aquifer boundaries
Stream	0	0	0	Precipitation	712895
Recharge	0.0139341731686713	0	0	Evp. Canopy	
ET	0	0	0	Recharge to C	
Lake	0	0	0	Total PET Po	
TOTAL	0.0427789613040428	0.042633854369683	0.339		

Table 8. Aquifers water balances (PP calibration results).

The hydraulic head resulting from the steady state model and presumably reproducing the average situation in 1940-1960 is shown in Figure 42. Potentiometric surface with associated residuals in observation points (below; red: simulated higher than observed; blue: simulated lower than observed).. It is evident how the boundary condition control over the groundwater flow is dominant. Not negligible exchanges between the aquifers and the nearby systems arose (Table 8. Aquifers water balances (PP calibration results)). The volumes are surely overestimated and an improvement in the hydrogeological knowledge and data would provide more reliable results in terms of water balance. A different parameter combination would provide the same head distribution with a different water balance.

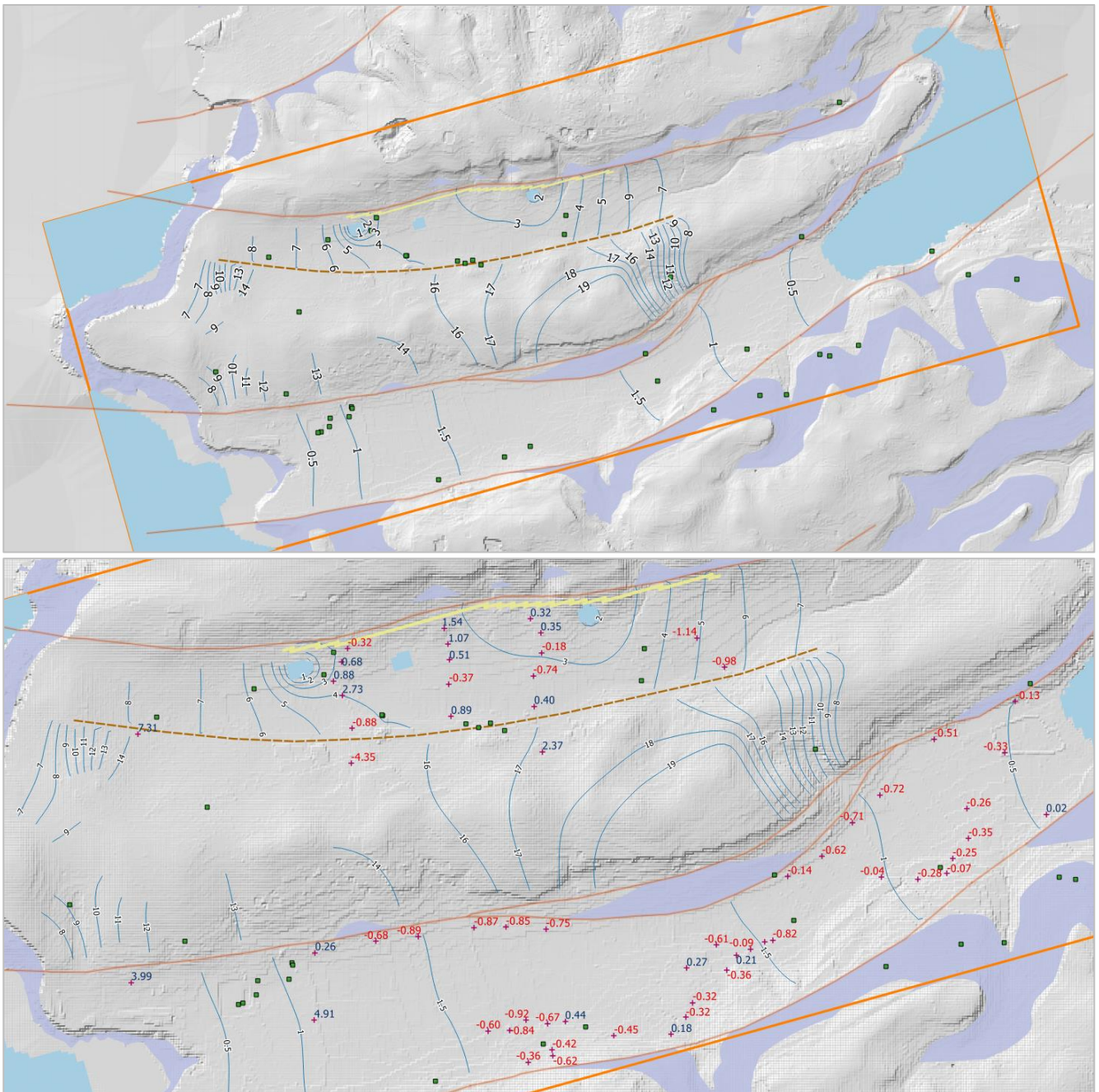


Figure 42. Potentiometric surface with associated residuals in observation points (below; red: simulated higher than observed; blue: simulated lower than observed).

These preliminary results, mostly based on assumptions, need to be revised as soon as further and updated data are made available. Nevertheless, some points can be commented:

-
- in order to calibrate the heads, the model adjust the parameters in order to get more water from outside the system, since it does not “receive” enough water from direct recharge;
 - this can be interpreted with an additional recharge provided by runoff over the Blue Clay and/or local discontinuities in BC and faults. The high sensitivity of the fault hfb5 (Figure 35. Initial hydraulic conductivity distribution.), the PP75 and PP63 (Figure 39. PP position and sensitivities (darker colors corresponds to higher sensitivities). and Figure 40. Hydraulic conductivity distribution obtained from the PP value adjustments (in m/s.) opposite tendency to adjust the K value, the impossibility to increase the head level in observations o60 and o61 (Table 7. Comparison of observed and simulated heads (PP calibration).) would suggest a lateral exchange from Mizieb to Pwales in that area.

Aquifer Management Scenario 1 (AM_S1)

The roughly calibrated model was used to qualitatively test some management actions in Pwales aquifer. The first scenario includes a MAR scheme through 4 injection BHs spread over the length of the valley (Figure 43. Position of the 4 MAR boreholes.). The injection discharge Q was iteratively adjusted with the use of the code PEST in prediction mode, setting the target heads equal to ground elevation minus 7 m. Results expressed as adjusted injection rates for each well and obtained new heads elevations is reported in Table 9. Results of the injection rate adjustment. and Figure 44. Potentiometric surface deformation due to the 4 injection wells..

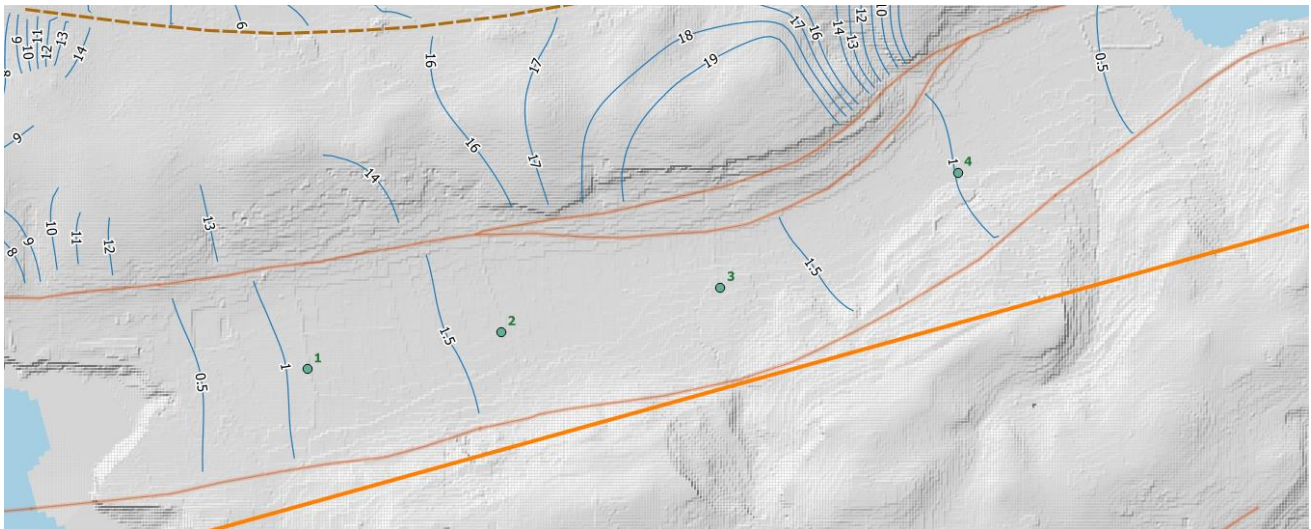


Figure 43. Position of the 4 MAR boreholes.

Borehole ID	Injection rate Q (m^3/s)	Initial h (m asl)	Target h (m asl)	New h (m asl)
W1	0.0108	1.18	13	12.96 (4 at 100 m)
W2	0.0131	1.52	5	5.05
W3	0.0033	1.53	5	4.53
W4	0.0001	0.98	2	2.00

Table 9. Results of the injection rate adjustment.

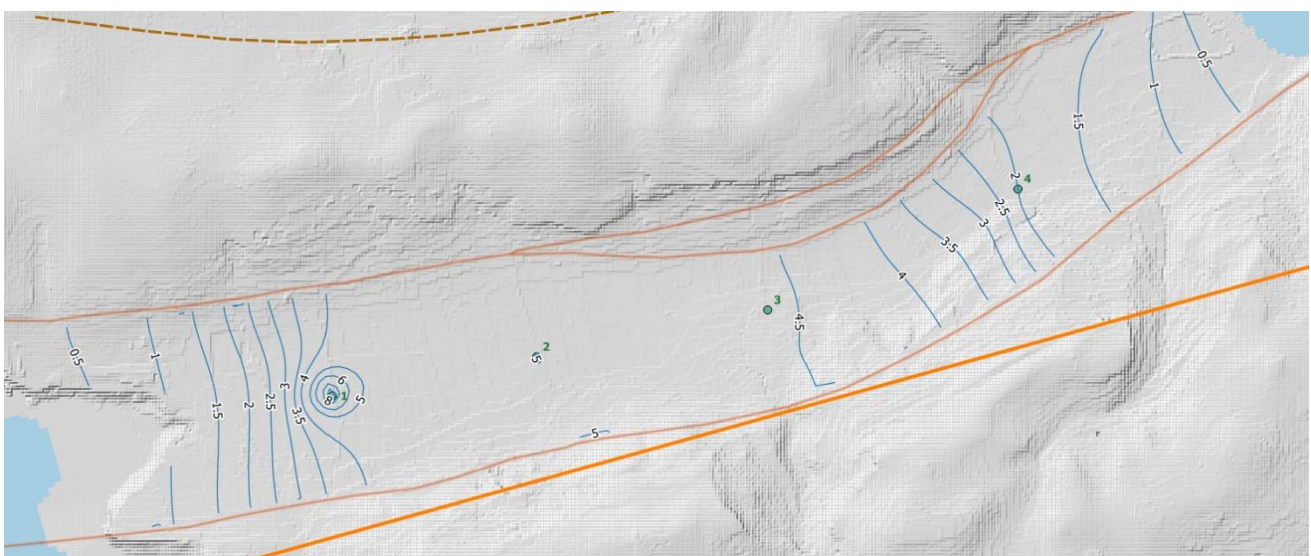


Figure 44. Potentiometric surface deformation due to the 4 injection wells.

Aquifer Management Scenario 2 (AM_S2)

The second scenario includes a MAR scheme through an injection gallery covering the length of about 3 km. The injection discharge Q was iteratively adjusted with the use of the code PEST in prediction mode, setting the target heads equal to ground elevation minus 7 m. Results expressed as adjusted injection rates for the 2 shafts of the gallery and obtained new heads elevations is reported in Table 10. Results of the injection rate adjustment. and Figure 46. Potentiometric surface deformation due to the injection gallery..

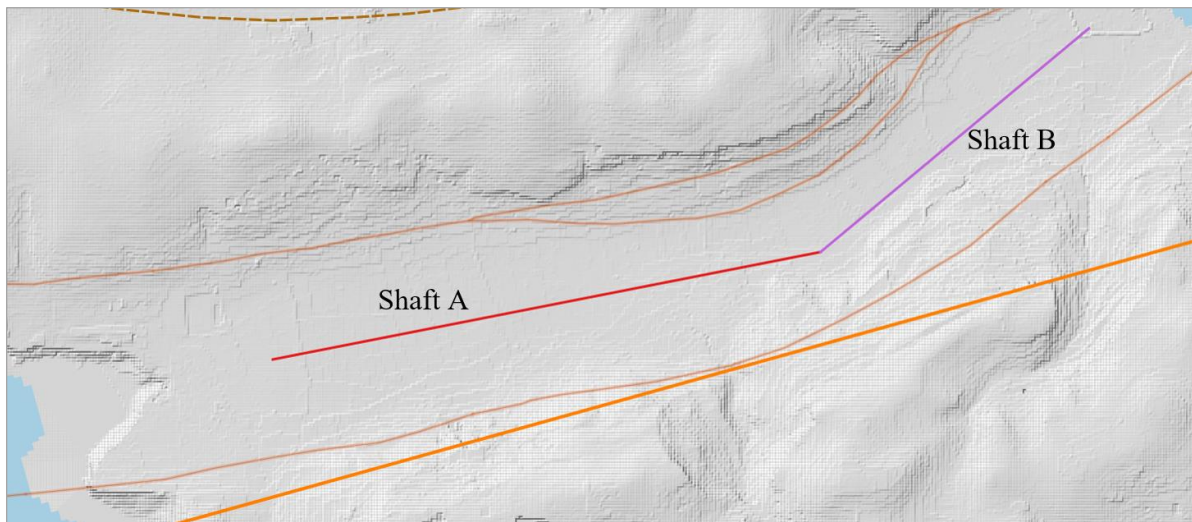


Figure 45. Injection gallery in Pwales.

Gallery shaft	Length (m)	Injection rate Q (m ³ /s)
Shaft A	1900	0.050
Shaft B	1100	0.0002

Table 10. Results of the injection rate adjustment.

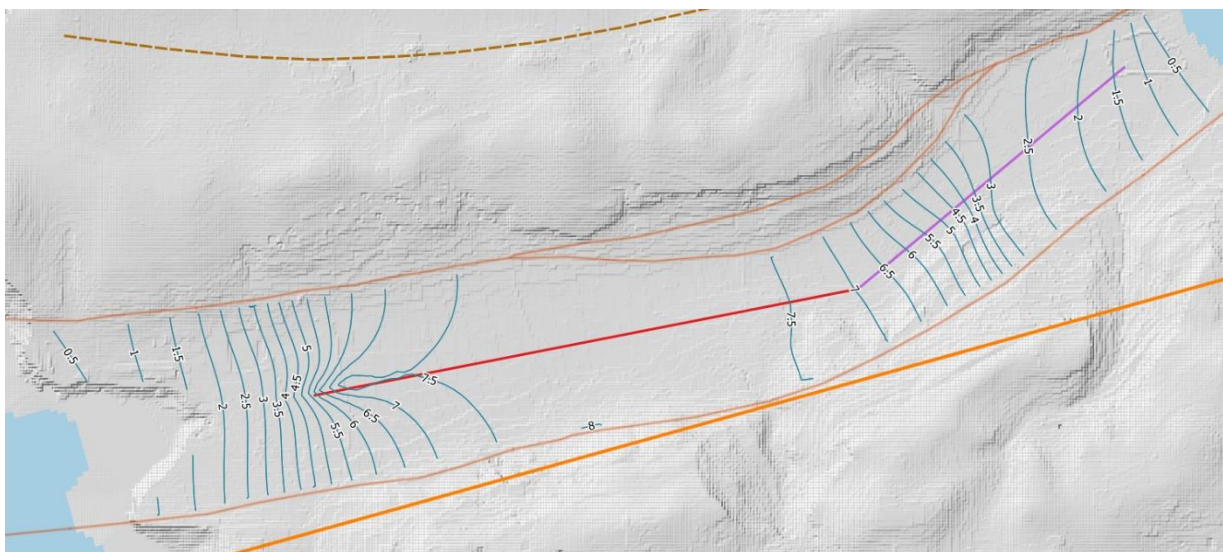


Figure 46. Potentiometric surface deformation due to the injection gallery.

Aquifer Management Scenario 3 (AM_S3)

A last scenario includes the same MAR scheme of AM_S2, but assuming that only the shaft A is developed (about 2 km). The injection discharge Q was iteratively adjusted with the use of the code PEST in prediction mode, setting the target heads equal to ground elevation minus 7 m. Results expressed as adjusted injection rates for the shaft A and obtained new heads elevations is reported in Table 11. Results of the injection rate adjustment, and Figure 47. Potentiometric surface deformation due to the injection gallery (only shaft A)..

Gallery shaft	Length (m)	Injection rate Q (m ³ /s)
Shaft A	1900	0.057
Shaft B	0	0

Table 11. Results of the injection rate adjustment.

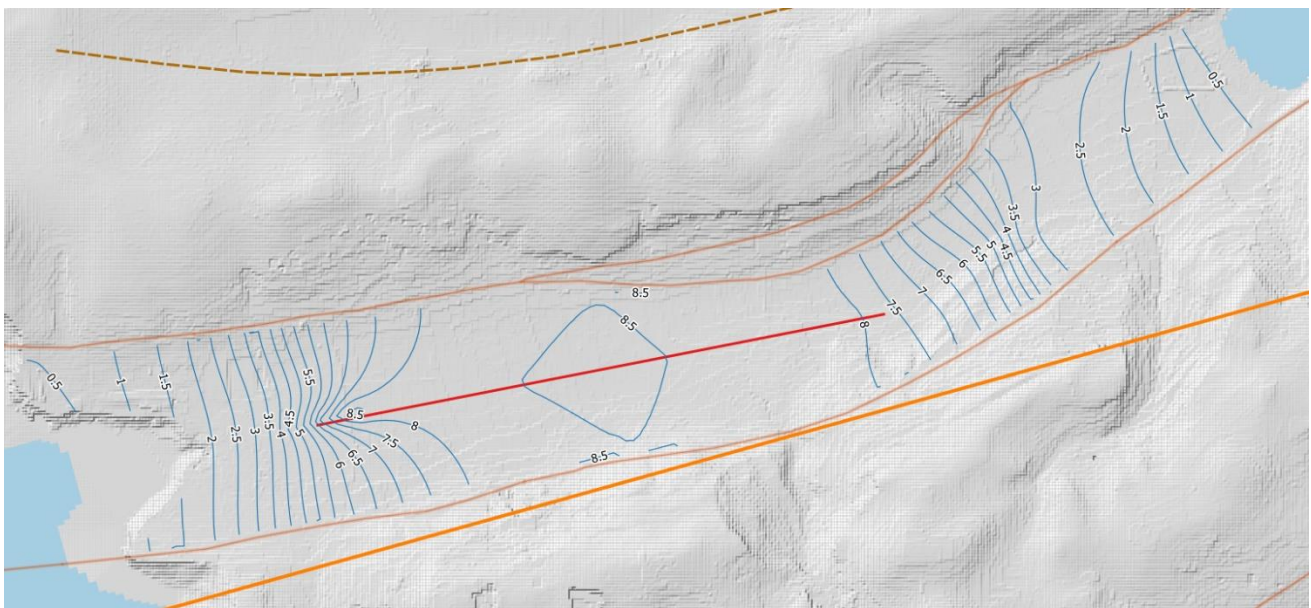


Figure 47. Potentiometric surface deformation due to the injection gallery (only shaft A).

Comments

The preliminary results obtained for the Mizieb-Pwales model are mostly based on assumptions and observations affected by a high uncertainty. The whole process needs to be revised as soon as further and updated data are made available. Nevertheless, some points can be commented both regarding the model calibration and the scenarios:

- in order to calibrate the heads, the model adjust the parameters in order to get more water from outside the system, since it does not “receive” enough water from direct recharge;
- this can be interpreted with an additional recharge provided by runoff over the Blue Clay and/or local discontinuities in BC and faults. The high sensitivity of the fault hfb5 (Figure 35. Initial hydraulic conductivity distribution.), the PP75 and PP63 (Figure 39. PP position and sensitivities (darker colors corresponds to higher sensitivities). and Figure 40. Hydraulic conductivity distribution obtained from the PP value adjustments (in m/s.) opposite tendency to adjust the K value, the impossibility to increase the head level in observations o60 and o61 (Table 7. Comparison of observed and simulated heads (PP calibration).) would suggest a lateral exchange from Mizieb to Pwales in that area;
- AM_S1: better than the reference situation, but the effect of single boreholes injection is strongly affected by the local hydraulic conductivity and degree of fracturing. If K is high, the raise in head would be small and spread in a wide area, if K is low the head would raise only locally, with little effect over wide areas. Furthermore, a critical K in points near the coast (for instance W4 in Figure 44. Potentiometric surface deformation due to the 4 injection wells.) would make the difference between creating a hydraulic barrier to seawater intrusion (hard to achieve) and throwing away freshwater to the sea (easier to happen).
- AM_S2: better than the reference situation and AM_S1. Shaft B, closer to the coast, does not play a fundamental role in the overall management, vice versa could increase the outflow of freshwater to the sea.
- AM_S3: better than the reference situation and AM_S1. It seems to be more efficient than AM_S2.

Part 2: Models for Gozo

Gozo Mean Sea Level Aquifer

Introduction

The reference model to start the scenarios simulation is the analogous of the Alternative Model (post-calibration adjustment) defined during Activity 4, but with a simplified time discretization as depicted in the Table 12. Time discretization for the reference model.. This allows to speed-up the model run and to consider input data averaged on a multi-year time range, so that simulations of current and future settings are made comparable.

SP	Start	End	SP Length (day)	State	n. of TS
1	01/01/1650	31/12/1940	105850	SS	1
2	01/01/1941	31/12/1980	14609	SS	1
3	01/01/1981	31/12/2015	12782	SS	1

Table 12. Time discretization for the reference model.

The meaning of the stress period selection is summarized hereafter:

- Stress Period 1: no groundwater exploitation.
- Stress Period 2: only public abstraction (no private wells active).
- Stress Period 3: adding private abstraction to public pumping infrastructure.

Modification of the time discretization implied a revision of the recharge multiplier set out during Activity 4: due to the large time frame of the stress periods, the multiplier values for stress period 2 and 3 slightly differ from the reference value of stress period 1 (Figure 48. Recharge multiplier for the new time discretization.).



Figure 48. Recharge multiplier for the new time discretization.

The settings to include public abstraction were revised as well, as reported in Figure 47.

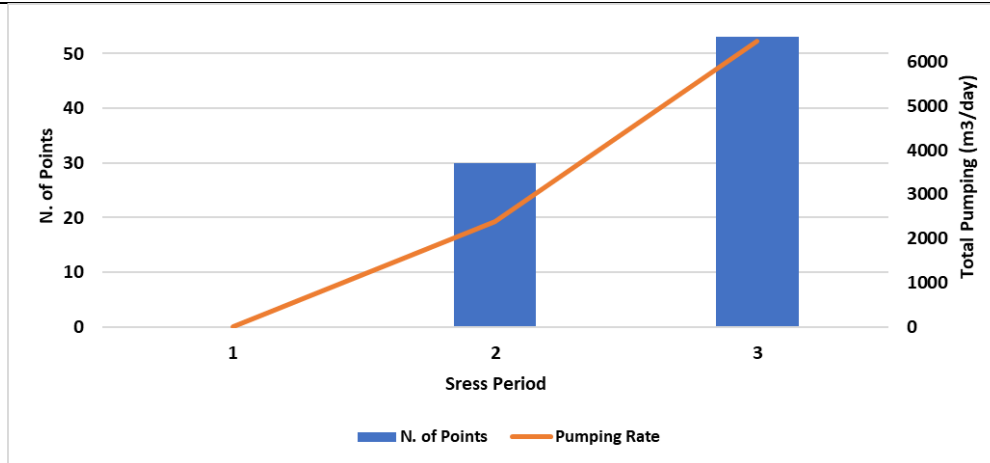


Figure 49. Public abstraction (accounting for boreholes and pumping stations) referred to the new time discretization.

Settings for other stresses in the model are taken as in the original version. They include: (i) General Head Boundary for mimic the flow exchange through the coastal line; (ii) Horizontal Flow Barrier to simulate the main faults.

Regarding the seawater intrusion, as introduced for Malta MSLA model, in this stage of modelling activity the saltwater interface is simulated by the Ghyben-Herzberg formula (Herzberg 1901) approximation, using 36 as coefficient.

The distribution of head simulated for the final stress period (SP3) is shown in Figure 48, while the corresponding elevation of the saltwater interface is reported in Figure 49. It is worth noting that in case of negative heads (as the one achieved in the south part of the aquifer), the interface is set to 0 m a.s.l. This zone should be considered as the *critical zone* where the interface might achieve the maximum level, namely all the abstracted water could be affected by salinization due a total shrinking of the freshwater lens.

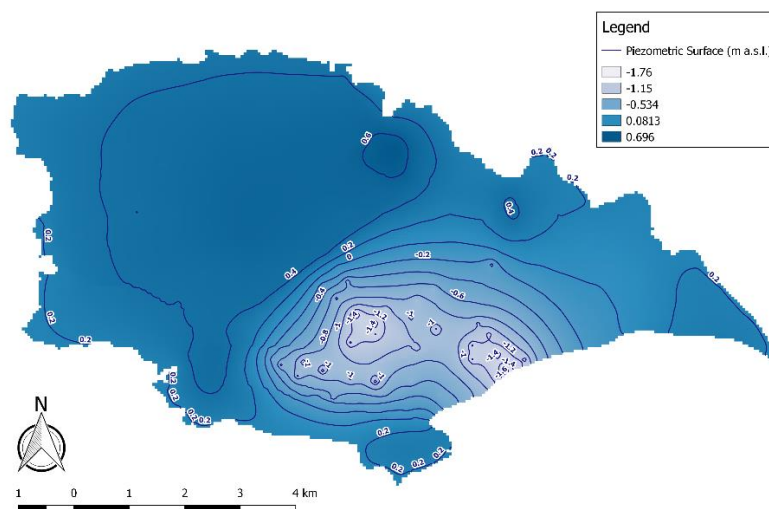


Figure 50. Piezometric surface simulated in SP3 of the reference model.

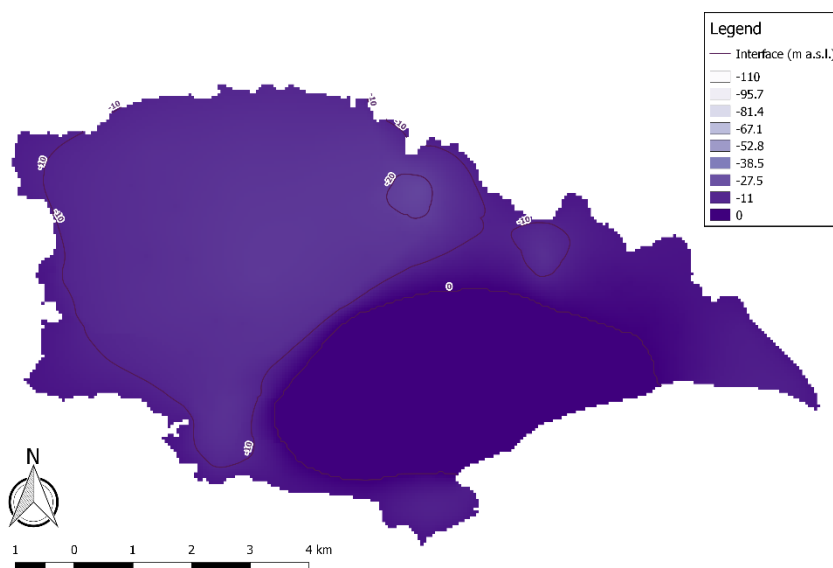


Figure 51. Saltwater interface in SP3 of the reference model.

Hydrogeological Scenario 1 (HG_S1)

This new model run features different Hydraulic Conductivity values, loosely based on the experience acquired by EWA from the operation of groundwater abstraction wells. In particular, the western zone of the island is now represented to have a conductivity halving the optimal value found through calibration for the entire northern part (i.e 5.43 m/day instead of 10.86 m/day). The new distribution of conductivity values is shown in Figure 50.

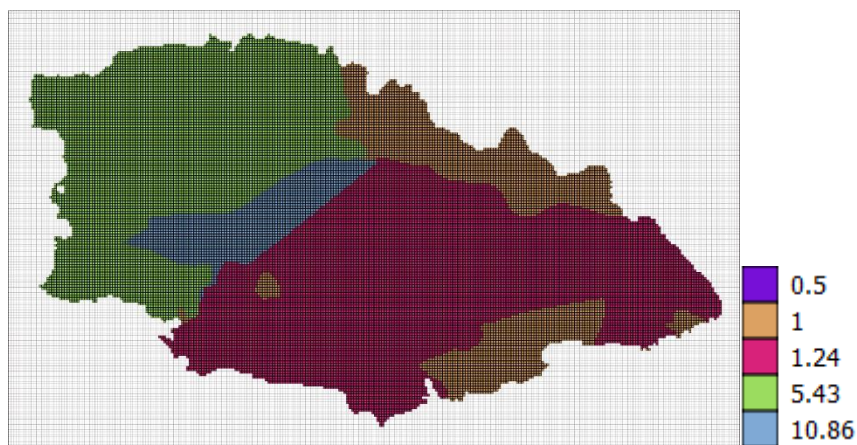


Figure 52. Zonation of hydraulic conductivity in model version HG_S1, expressed in m/day.

The reference model was run, obtaining a distribution of head and saltwater interface shown in Figure 51 and 52, respectively, at stress period 3. From a comparison of these maps with the reference ones, it is noted that the piezometry mainly changes in the northern part of the aquifer, as expected, while this difference slight influences the head elevation in the high exploitation zone (south part): the low

conductivity of the southern zone, the faults system and the greater exploitation level on this region do not allow this part of the aquifer to be so much influenced by the variation of conductivity in the northern part. In particular, the negative values of head level in some zones are confirmed to be there, even if a slightly improvement. Furthermore, this scenario confirms that the optimal value for the conductivity on the northern zone, found in Activity 4, cannot be changed so much, unless new observation points are placed in this part of the island, while currently the head measurements were made only on the central and southern zone.

In conclusion, model version HG_S1 confirms the suggestion (already pointed out in Deliverable D4.1) that additional investigations on transmissivity and piezometry level of the northern zone are needed to get a deeper understanding of the whole flow regime in Gozo MSLA.

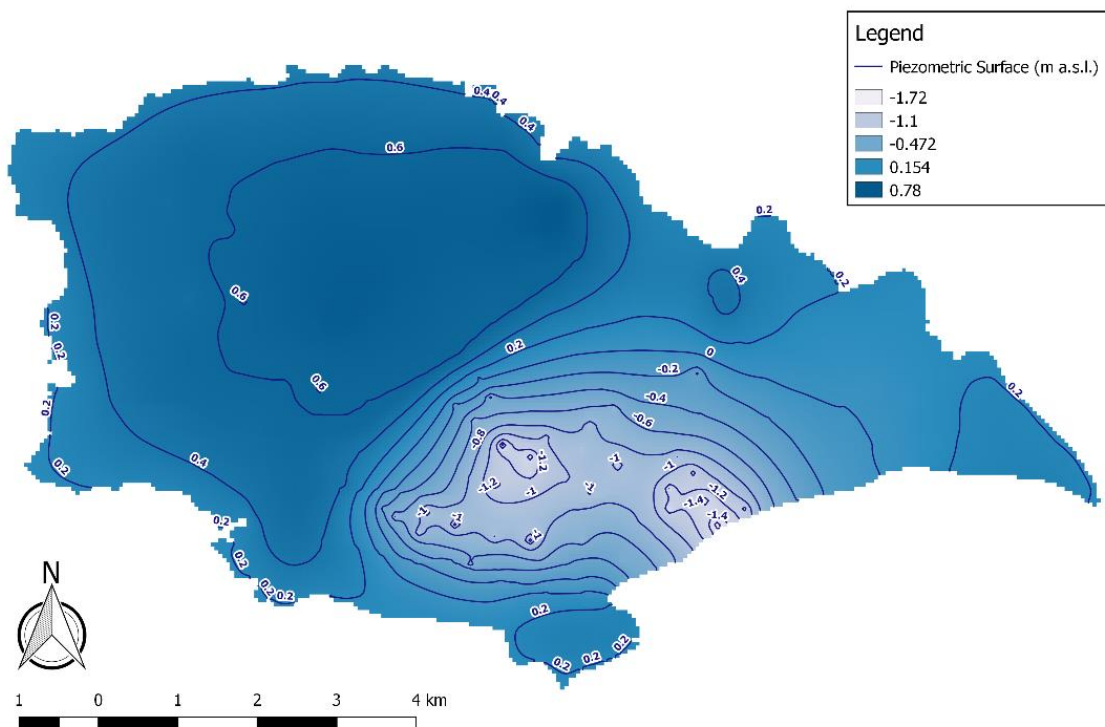


Figure 53. Piezometric surface simulated in SP3 of the model HG_S1.

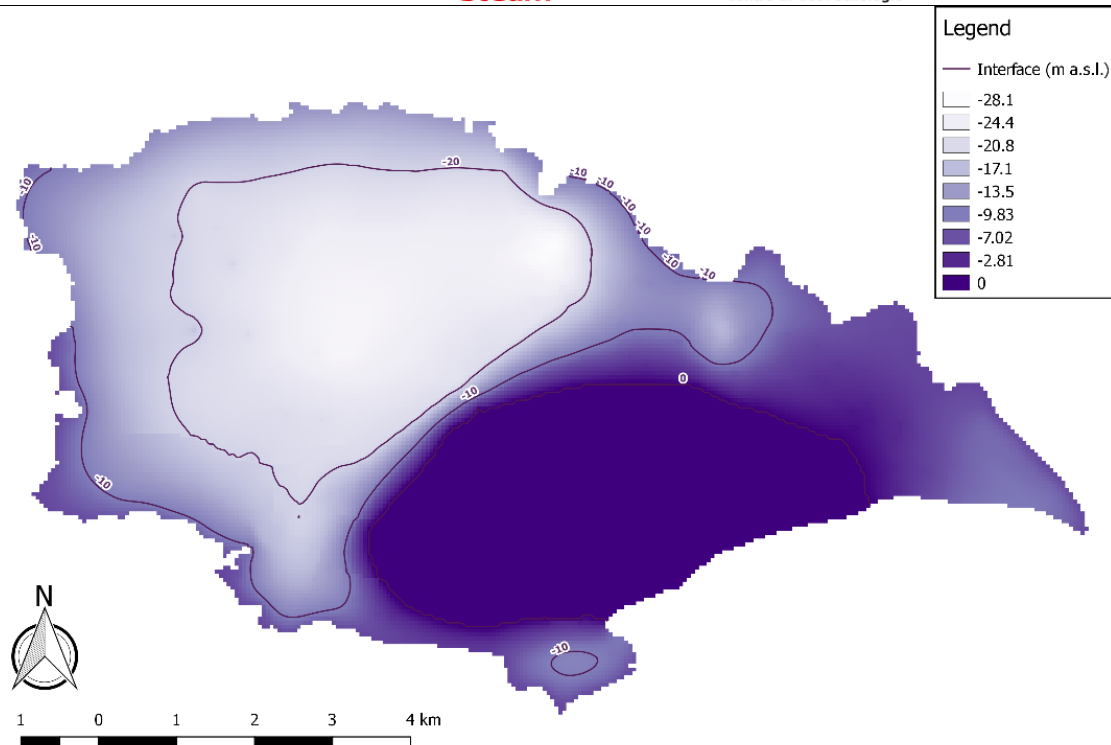


Figure 54. Saltwater interface simulated in SP3 of the model HG_S1.

Abstraction Scenario 1 (ABS_S1)

This model version includes an additional stress period, with a length of further 50 years (getting year 2065) to simulate the framework expected when applying the envisaged groundwater plan, as depicted in the 2nd Water Catchment Management Plan.

To this purpose, the abstraction conditions for private usage are taken the same as in last stress period (namely last 35 years), while the public abstraction (pumping stations and boreholes) is reduced by 3000 m³/day which will instead be sourced from the new RO desalination plant at Hondoq ir-Rummien. The lowering rate (3000 m³/day) was applied not uniformly to all the public abstraction points, but respecting the current proportionality at each point: the latter has been reduced according to the current percentage of withdrawal with respect to the whole public abstraction rate. The new total public abstraction rate is 3254 m³/day instead of 6254 m³/day.

This model version will be also the reference for other abstraction scenarios and the climate change scenario (see later on).

Results show that this abstraction setting is more sustainable than the current one (SP3): the piezometry level is always positive even in the high exploitation region (the minimum value is 0.161 m, see Figure 53), and even the saltwater interface is never reaching the critical value (maximum level is -5.31 m, see Figure 54).

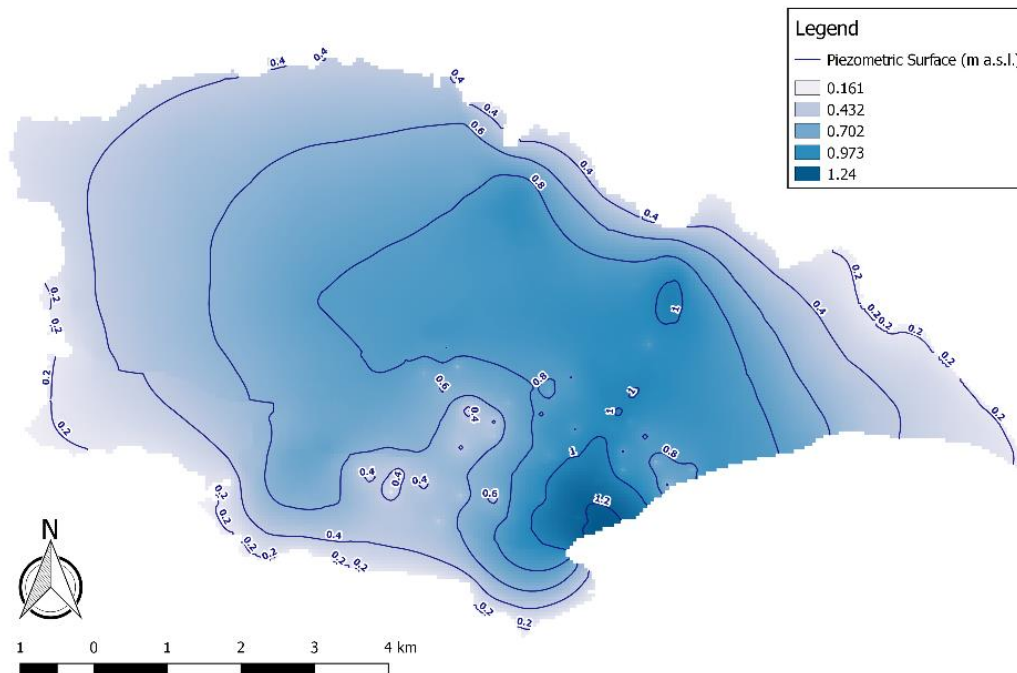


Figure 55. Piezometric surface simulated in SP4 of the model version ABS_S1.

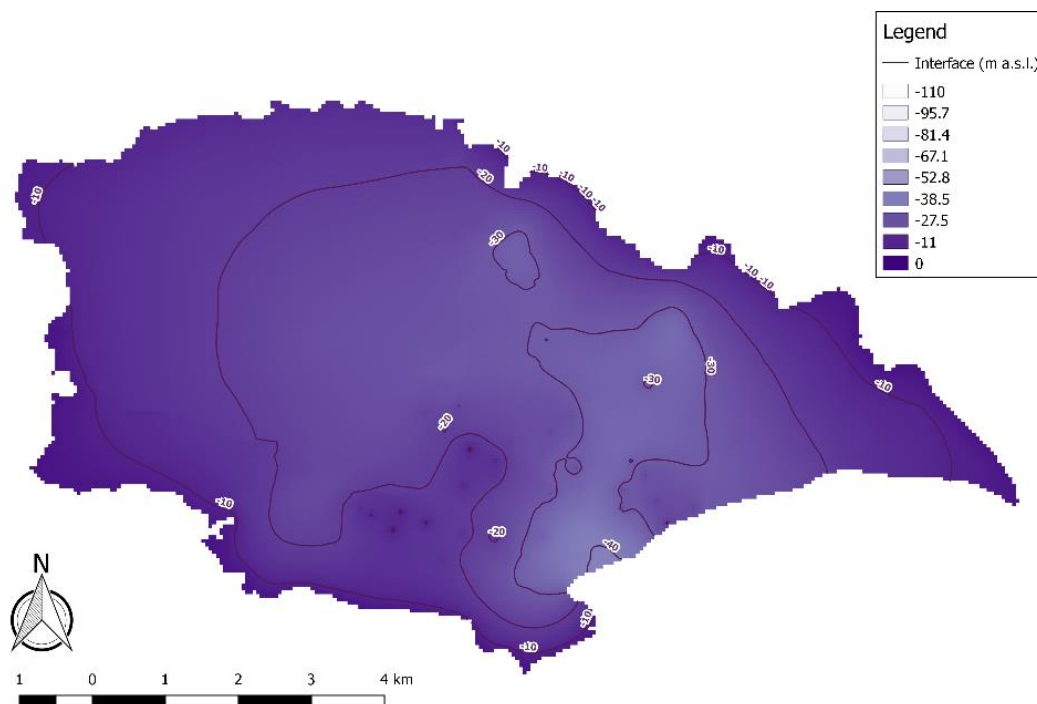


Figure 56. Saltwater interface simulated in SP4 of the model version ABS_S1.

Abstraction Scenario 2 (ABS_S2)

In this version, the private pumping is reduced by 25% with respect to ABS_S1, thus lowering also the private abstraction compared to the existing management. This reduction mimics the impact of the New Water project in Gozo, as well as the adoption of water storage techniques by farmers. It is evident that this further reduction of withdrawal will improve the status of MSLA, as shown in Figure 55 and Figure 56, especially for what concerns the distribution of drawdown zone (an of the interface, consequently), while the extreme values of piezometric levels are of the same order (Table 13. Level of head in different model version. Expressed as m asl).

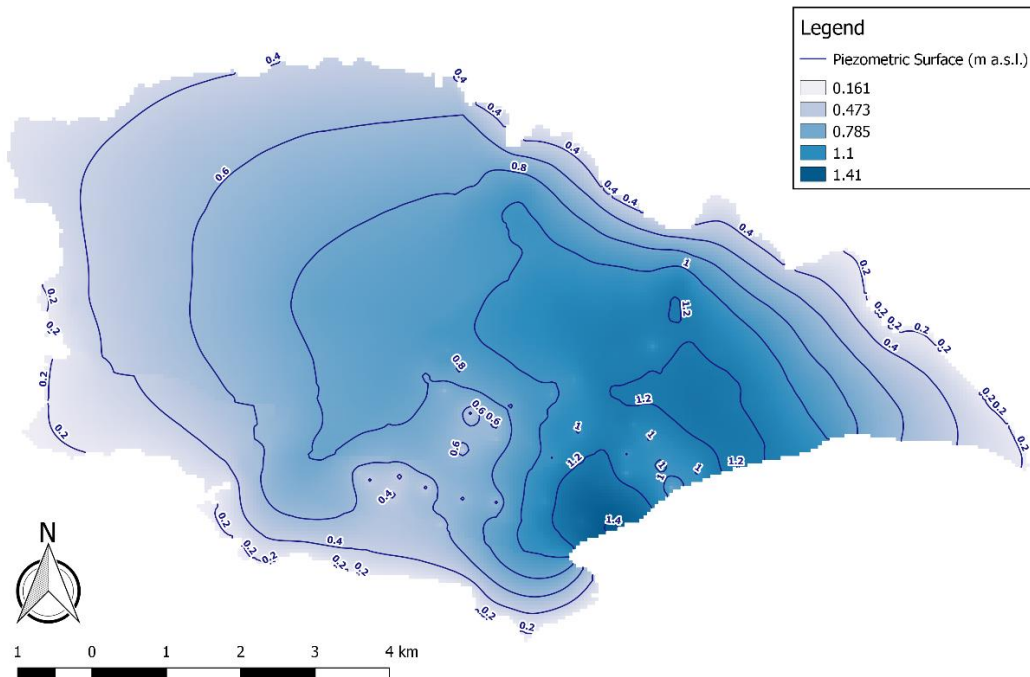


Figure 57. Piezometric surface simulated in SP4 of the model version ABS_S2.

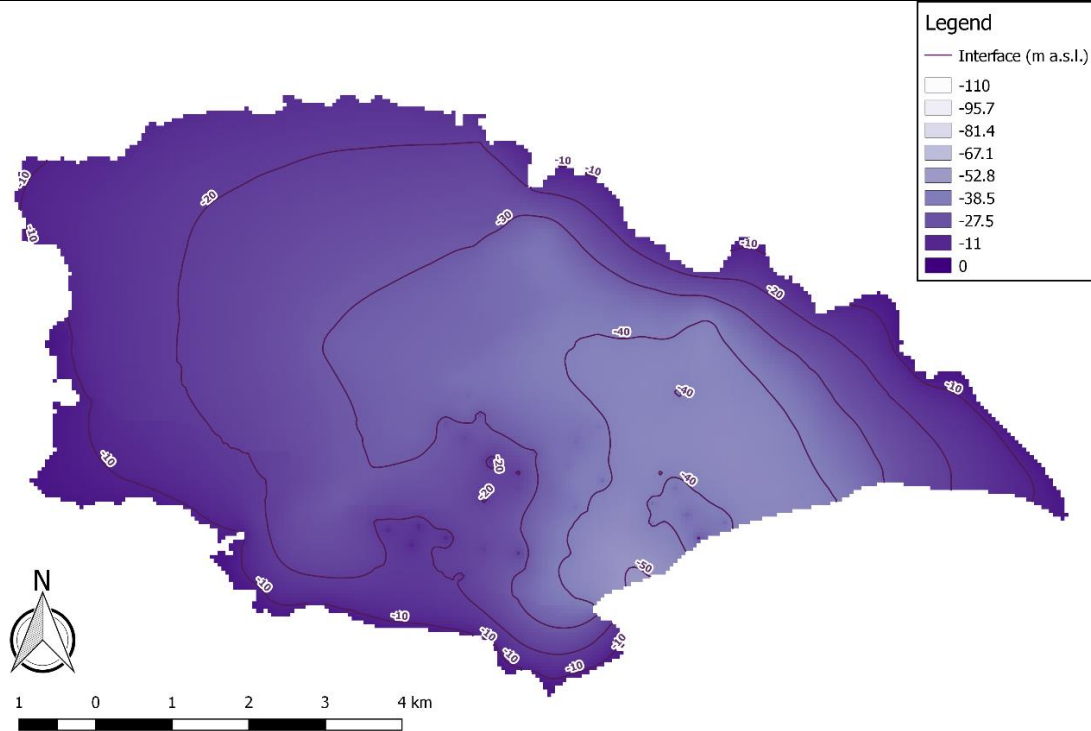


Figure 58. Saltwater interface simulated in SP4 of the model version ABS_S2.

Abstraction Scenario 3 (ABS_S3)

The last abstraction scenario deals with a complete stopping of abstraction for public purposes, allocating groundwater to the agricultural sector. This scenario is simulated by deleting public abstraction points, while doubling the rate imposed to the existing private wells. The latter setting could be thought also as a doubling of the number of wells keeping the same rate, namely an increase of abstraction points. This scenario shows, as expected, that the great impact on the aquifer is given by the public pumping, since in this case the depletion zone is vanishing (Figure 57), and no problems of seawater upcoming appear anymore (Figure 58).

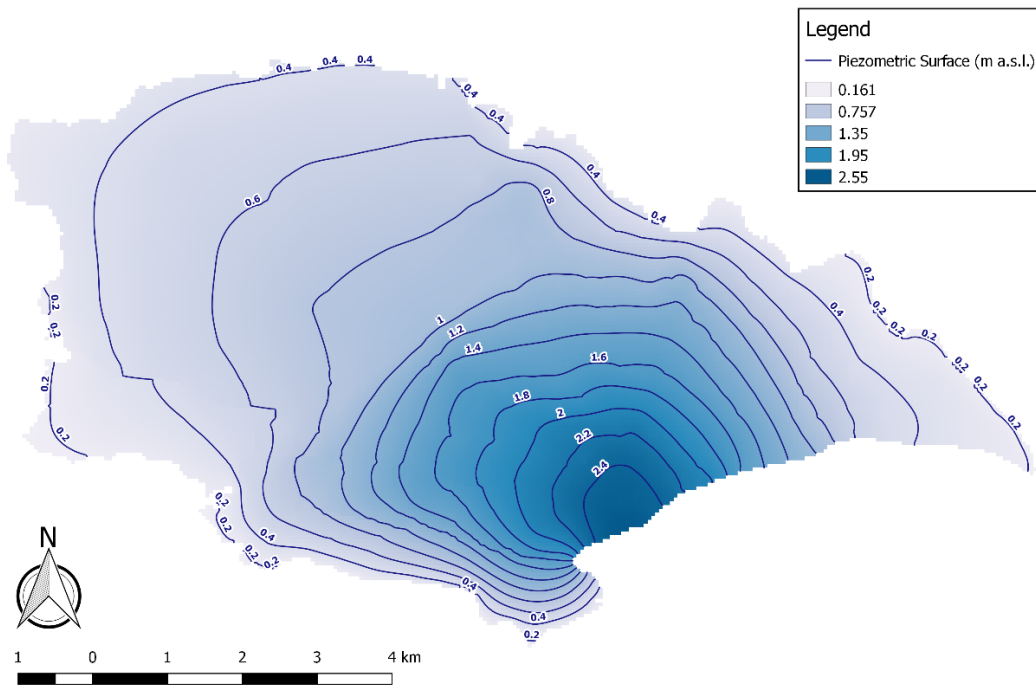


Figure 59. Piezometric surface simulated in SP4 of the model version ABS_S3.

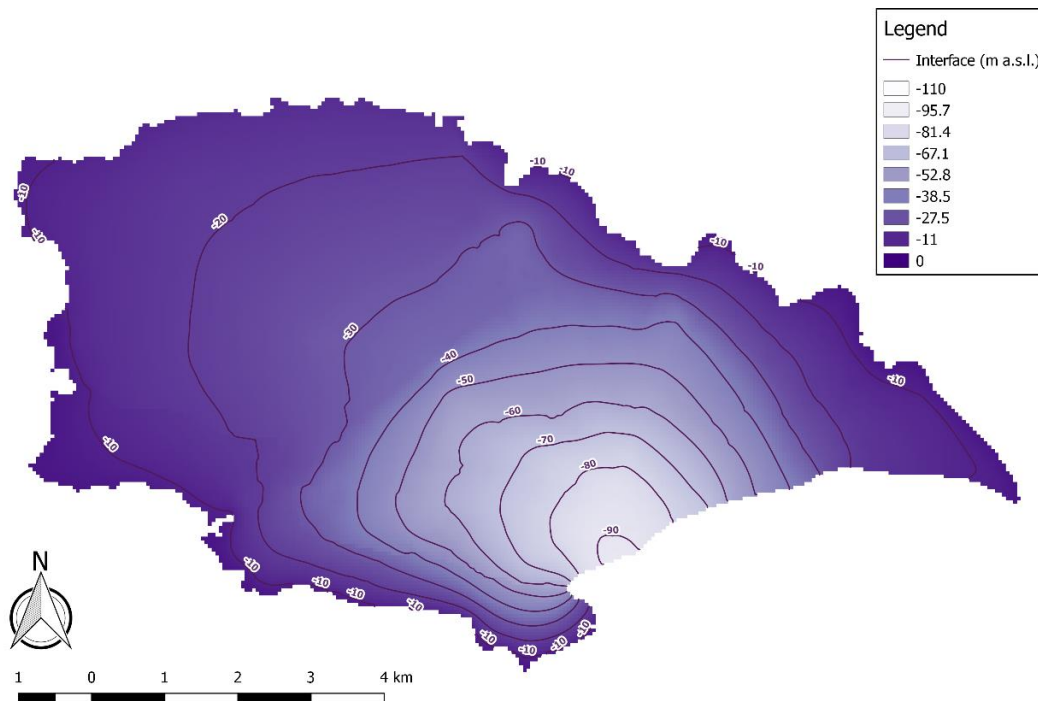


Figure 60. Saltwater interface simulated in SP4 of the model version ABS_S3.

Climate Change Scenario 1 (CC_S1)

This model version simulates the impact of reduction of recharge due to changing precipitation characteristics and higher evapotranspiration. This is represented by reducing the recharge term by 10%: more in detail, the foreseen (averaged) precipitation rates and temperatures provided by EWA, coming from projection to 2050, have an impact on the computation of the recharge term by a factor of 0.91. Such a coefficient was applied to the reference RCH term, while keeping all the other stresses as in ABS_S1. Results show (Figures 59-60 and Table 12) that even in this scenario the assumed management for public abstraction (as set out in ABS_S1) is still able to guarantee a status better than the existing one (reference model).

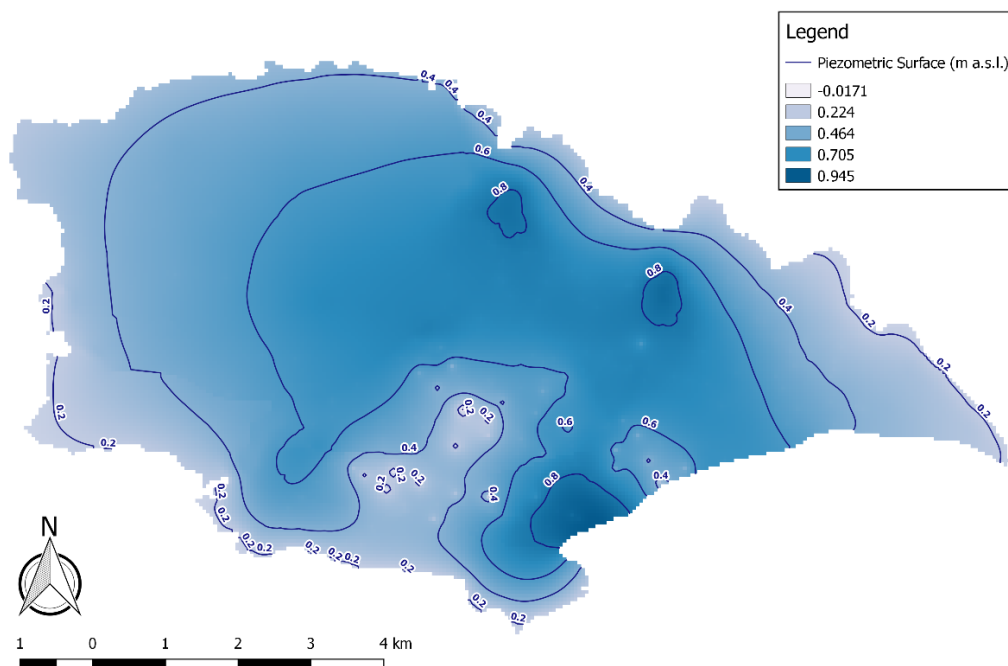


Figure 61. Piezometric surface simulated in SP4 of the model version CC_S1.

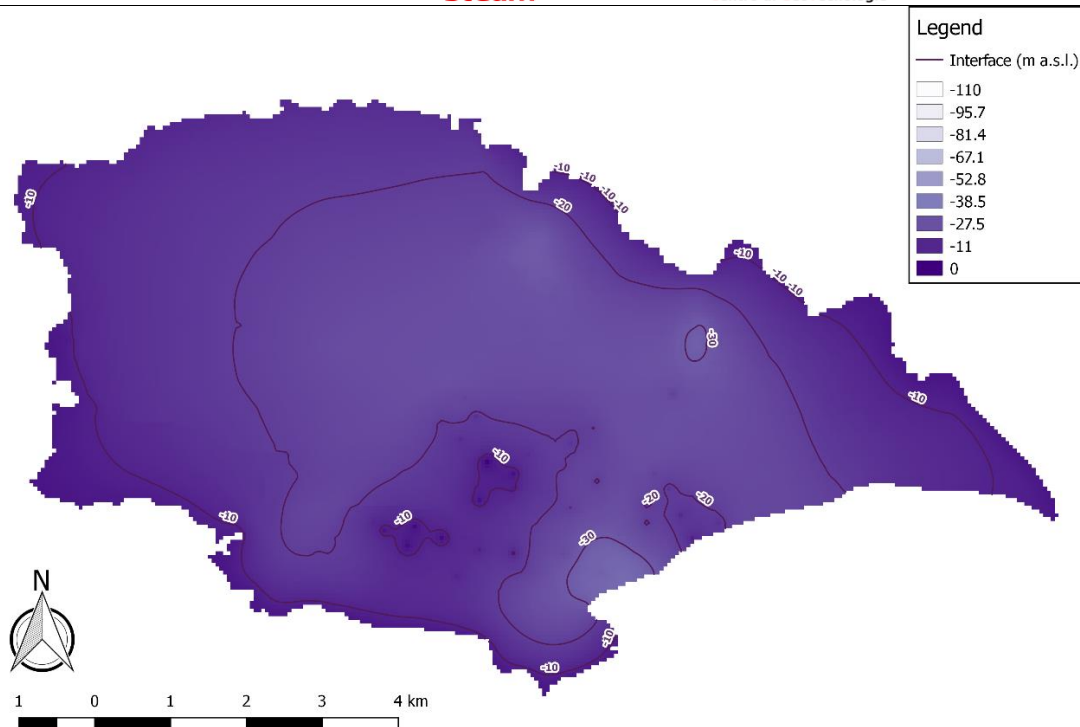


Figure 62. Saltwater interface simulated in SP4 of the model version CC_S1.

	Current (reference model)	ABS_S1	ABS_S2	ABS_S3	CC_S1
Maximum (m)	0.70	1.24	1.41	2.55	0.95
Average (m)	0.12	0.62	0.71	0.86	0.52
Minimum (m)	-1.76	0.16	0.16	0.16	-0.02

Table 13. Level of head in different model version. Expressed as m asl

Ghajnsielem Perched Aquifer

Introduction

Regarding the Ghajnsielem perched aquifer, the transient model provided in Activity 4 is used as reference. In particular, it is useful to recall that the model considers the following time discretization framework:

1. Period of no pumping, namely the years 1941-1960. This time range has been divided in two stress periods, since the reference spatial recharge rate is computed for the period 1941-1944. Therefore, two stress periods belong to this class:
 - a. Stress Period 1: 1941-1944.
 - b. Stress Period 2: 1945-1960.
2. Period of water gallery activation, with no private abstraction: Stress Period 3, 1961-1978 (see section *Abstraction*).
3. Period of no public pumping, but private abstraction active, divided in two stress periods:
 - a. Stress Period 4: 1979-2004.
 - b. Stress Period 5: 2005-2015.

The last stress period is used as reference for running an additional scenario (see below), and the head distribution regarding this period is reported in Figure 61.

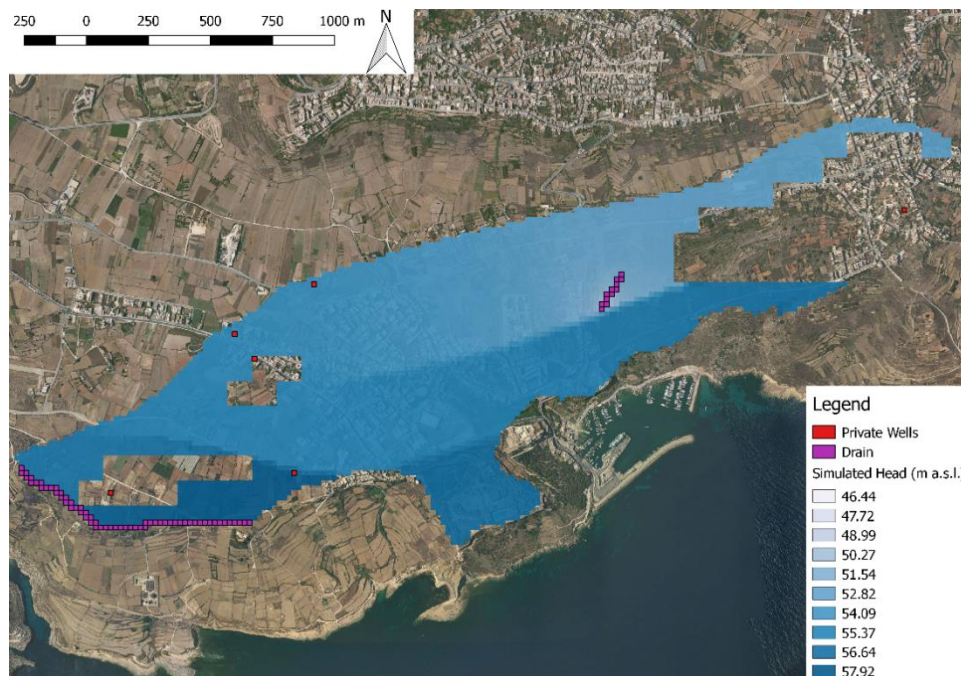


Figure 63. Piezometric surface simulated in SP5 of the reference model.

Abstraction Scenario 1 (ABS_S1)

This scenario simulates the impact of doubling the abstraction in future 50 years. Therefore, an additional stress period is added, in which the pumping rate assigned to existing private wells is doubled. All the other settings are taken as in the reference model (namely the previous stress period).

The simulated head is shown in Figure 62: the overall picture shows a reduction of about 4 m of the piezometric surface. Furthermore, the model suggests that this doubled pumping rate is not feasible for all the abstraction points: the one in the southern zone seems to create dry zone larger than in the reference scenario, namely the pumping rate might be too high for the water storage available. In the meantime, the northern part referred as *Through* in the region classification identified in (Costain, 1958) seems to be not negatively impacted by this increased withdrawal.

It is worth noting that all these arguments need to be taken from a qualitative point of view, due to the huge amount of assumptions were made in the model definition to cover the data gap.

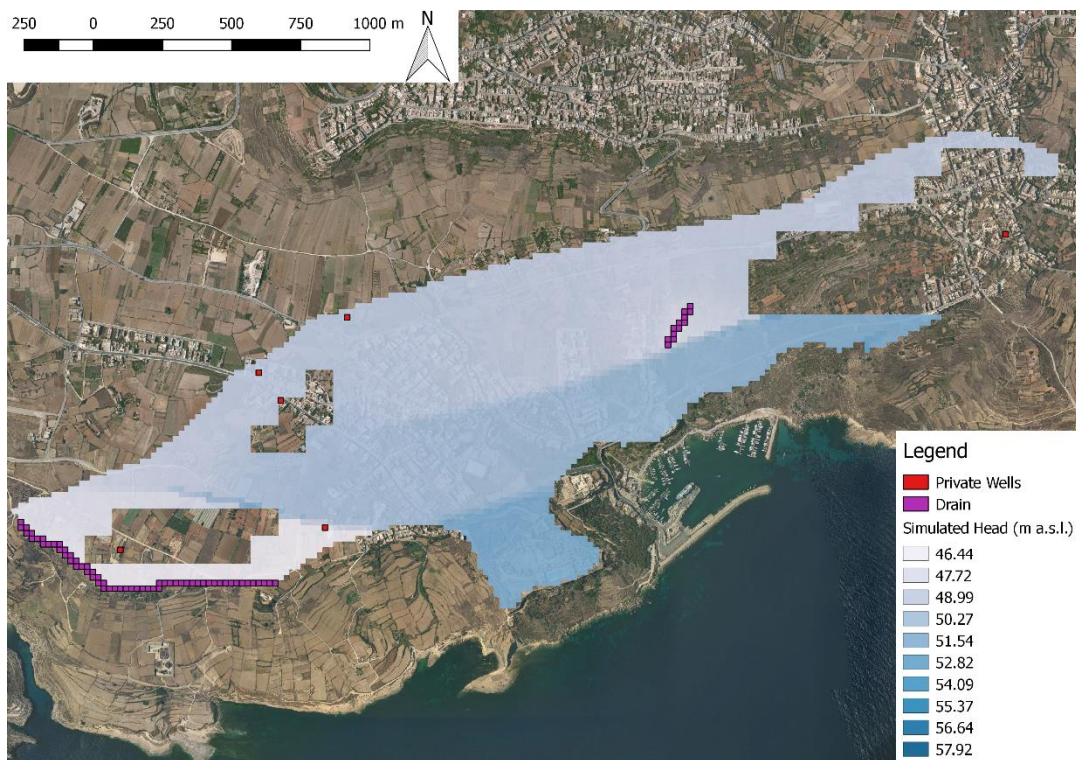


Figure 64. Piezometric surface simulated in SP6 of the model version ABS_S1.

References

- Carlsson A, Olsson T (1993). The analysis of fractures, stress and water flow for rock engineering projects. In: Hudson JA Ed, *Comprehensive Rock Engineering, Principle, Practice & Projects*. Pergamon, Oxford UK 2: 415–437.
- Dagan G. & Bear J. (1968). - Solving the problem of local interface upconing in a coastal aquifer by a method of small perturbations. *J. Hydr. Research*, 6: 15-44.
- Doherty J, Moore C (2017) Simple is Beautiful. NCGRT National Groundwater Modelling Uncertainty Workshop, Sydney, 10 July 2017. 1, <https://pdfs.semanticscholar.org/4c1a/5cba64559cbab50cdf90066f0f74b8a3b557.pdf>
- Hill M.C. and Tiedeman C.R. (2007). *Effective Groundwater Model Calibration: with Analysis of Data, Sensitivities, Predictions, and Uncertainty*, John Wiley and Sons, New York.
- Kruseman GP, de Ridder NA (1994). *Analysis and evaluation of pumping test data*. Second edition. International Institute for Land Reclamation and Improvement, Wageningen, The Netherlands, 377 pp
- Lee CH, Farmer I (1993). *Fluid flow in discontinuous rocks*. Chapman and Hall, London, 169 pp.
- Lewis DC, Burgoyne RH (1964). Hydraulic characteristics of fractured and jointed rock. *Ground Water* 2:4–9.
- Louis C (1974). Rock hydraulics. In: Muller L (ed) *Rock mechanics*. Springer Verlag, Berlin, pp 299–387.
- Meng Z, Zhang J, Wang R (2011). In situ stress, pore pressure and stress-dependent permeability in the southern Qinshui Basin. *Int J Rock Mech Min Sci* 48(1):122–131.
- Morris, T. O. (1952). *The water supply resources of Malta*. Valletta: Government Printing Office.
- Schirmer, Mario & Leschik, Sebastian & Musolff, Andreas. (2012). Current research in urban hydrogeology – A review. *Advances in Water Resources*. 51. 280-291. 10.1016/j.advwatres.2012.06.015.
- Schmorak, S., Mercado, A. (1969). Upconing of freshwater–seawater interface below pumping well. *Water Resources Res.*, 5, 1290-1311.
- Sharqawy MH, Lienhard VJH, Zubair SM (2010). Thermophysical properties of seawater: a review of existing correlations and data. *Desalination Water Treat* 16(1–3):354–380.
- Snow DT (1968). Rock fracture spacings, openings and porosities. *J Soil Mech Found Div Proc Am Soc Civil Eng* 94:73–91.
- Snow DT (1970) The frequency and apertures of fractures in rock. *Int J Rock Mech Min Sci Geomech Abstr* 7:23–40.
- Wei ZQ, Egger P, Descoeudres F (1995). Permeability predictions for jointed rock masses. *Int J Rock Mech Min Sci Geomech Abstr* 32:251–261.
- Zhang L (2013). Aspects of rock permeability. *Front Struct Civ Eng* 7(2):102–116.

Appendix 1 - Density of fresh and seawater

The Ghyben-Herzberg formula (Herzberg 1901) considers the measures of the elevation of the water level in the well and the ratio (α):

$$\alpha = \rho_f / (\rho_s - \rho_f)$$

where ρ_f and ρ_s are the densities of the “fresh” water and the salt water, respectively. The densities of the “fresh” water and the salt water can be slightly different in each point, depending on temperature and salinity. The value which has been estimated for the Malta Island is $\alpha=36$ (Morris, 1952).

Given the limited number of available measurements, the value used in the scenario processing is the reference one, nevertheless a check has been made considering the EC logs in deep boreholes and applying the relationship described in Sharqawy et al. (2010), which is based on water salinity and temperature:

$$\rho_{sw} = (a_1 + a_2t + a_3t^2 + a_4t^3 + a_5t^4) + (b_1S + b_2St + b_3St^2 + b_4St^3 + b_5S^2t^2)$$

where

$$a_1 = 9.999 \times 10^2, a_2 = 2.034 \times 10^{-2}, a_3 = -6.162 \times 10^{-3}, a_4 = 2.261 \times 10^{-5}, a_5 = -4.657 \times 10^{-8},$$

$$b_1 = 8.020 \times 10^2, b_2 = -2.001, b_3 = 1.677 \times 10^{-2}, b_4 = -3.060 \times 10^{-5}, b_5 = -1.613 \times 10^{-5}$$

Validity: ρ_{sw} in (kg/m³); $0 < t < 180$ °C; $0 < S < 0.16$ kg/kg

Accuracy: ± 0.1 %

For the “fresh” water, the salinity and water temperature values measured in the first meters of depth of the logs were considered. For the seawater, the salinity of the Mediterranean Sea water (39.42 g/L in Jiao & Post, 2019) and a temperature of 20 °C (equal to the average temperature found at the bottom of deep borehole).

The α ratio results to vary between 33.0 and 33.7 for the examined deep borehole (10024, 10075, 10366, 10429).

Site I.D.	Site Name	Date	Aquifer Level m asl	Temperature °C	EC mS/cm	TDS=0.612 EC (g/L)	"Salinity" kg/m ³	Density kg/m ³	ALFA
10075	Mosta Road	30-apr-02	2	19.1	0.930	569.16	0.000569	998.63	33.65
10075	Mosta Road	30-apr-02	1	19.1	0.932	570.384	0.00057	998.63	33.65
10024	Mriehel	14-mag-02	2	19.2	1.240	758.88	0.000759	998.76	33.80
10024	Mriehel	14-mag-02	1	19.2	1.228	751.536	0.000752	998.75	33.79
10366	Tal-Barrani 2	14-gen-03	2	19.1	0.995	608.94	0.000609	998.66	33.69
10366	Tal-Barrani 2	14-gen-03	1	19.1	0.995	608.94	0.000609	998.66	33.69
10429	Miaco 2	18-mar-03	2	19.3	0.928	567.936	0.000568	998.59	33.60
10429	Miaco 2	18-mar-03	1	19.4	0.922	564.264	0.000564	998.57	33.58
10024	Mriehel	22-apr-03	2.675	19.0	1.279	782.748	0.000783	998.81	33.87
10024	Mriehel	22-apr-03	2	19.0	1.280	783.36	0.000783	998.81	33.87
10024	Mriehel	22-apr-03	1	19.0	1.258	769.896	0.00077	998.80	33.85
10075	Mosta Road	24-apr-03	1.875	19.0	0.824	504.288	0.000504	998.60	33.61
10075	Mosta Road	24-apr-03	1	18.9	0.830	507.96	0.000508	998.62	33.64
10075	Mosta Road	07-lug-03	1.835	19.0	0.953	583.236	0.000583	998.66	33.68
10075	Mosta Road	07-lug-03	1	18.9	0.954	583.848	0.000584	998.68	33.71
10024	Mriehel	07-lug-03	2.605	19.2	1.279	782.748	0.000783	998.78	33.82

Site I.D.	Site Name	Date	Aquifer Level m asl	Temperature °C	EC mS/cm	TDS=0.612 EC (g/L)	"Salinity" kg/m ³	Density kg/m ³	ALFA
10024	Mriehel	07-lug-03	2	19.2	1.273	779.076	0.000779	998.77	33.82
10024	Mriehel	07-lug-03	1	19.2	1.259	770.508	0.000771	998.77	33.81
10366	Tal-Barrani 2	08-lug-03	2.144	19.1	0.991	606.492	0.000606	998.66	33.68
10366	Tal-Barrani 2	08-lug-03	2	19.1	0.991	606.492	0.000606	998.66	33.68
10366	Tal-Barrani 2	08-lug-03	1	19.0	0.993	607.716	0.000608	998.68	33.71
10429	Miaco 2	08-lug-03	2.162	19.5	0.918	561.816	0.000562	998.55	33.55
10429	Miaco 2	08-lug-03	1	19.4	0.928	567.936	0.000568	998.57	33.58
10075	Mosta Road	09-ott-03	2.015	19.0	0.957	585.684	0.000586	998.66	33.69
10075	Mosta Road	09-ott-03	2	18.9	0.958	586.296	0.000586	998.68	33.71
10075	Mosta Road	09-ott-03	1	18.9	0.960	587.52	0.000588	998.68	33.71
10024	Mriehel	09-ott-03	2.915	19.0	1.283	785.196	0.000785	998.82	33.87
10024	Mriehel	09-ott-03	2	19.0	1.283	785.196	0.000785	998.82	33.87
10024	Mriehel	09-ott-03	1	19.0	1.268	776.016	0.000776	998.81	33.86
10366	Tal-Barrani 2	09-ott-03	2.484	19.0	0.909	556.308	0.000556	998.64	33.66
10366	Tal-Barrani 2	09-ott-03	2	19.0	0.910	556.92	0.000557	998.64	33.66
10366	Tal-Barrani 2	09-ott-03	1	19.0	0.910	556.92	0.000557	998.64	33.66
10429	Miaco 2	09-ott-03	2.242	19.6	0.935	572.22	0.000572	998.53	33.54
10429	Miaco 2	09-ott-03	2	19.5	0.944	577.728	0.000578	998.56	33.57
10429	Miaco 2	09-ott-03	1	19.5	0.949	580.788	0.000581	998.56	33.57
10075	Mosta Road	15-giu-04	1.955	19.0	0.962	588.744	0.000589	998.66	33.69
10075	Mosta Road	15-giu-04	1	18.9	0.970	593.64	0.000594	998.69	33.72
10024	Mriehel	15-giu-04	2.605	19.0	1.339	819.468	0.000819	998.84	33.90
10024	Mriehel	15-giu-04	2	19.0	1.288	788.256	0.000788	998.82	33.87
10024	Mriehel	15-giu-04	1	19.0	1.288	788.256	0.000788	998.82	33.87
10429	Miaco 2	16-giu-04	2.192	19.5	0.947	579.564	0.00058	998.56	33.57
10429	Miaco 2	16-giu-04	2	19.4	0.955	584.46	0.000584	998.58	33.60
10429	Miaco 2	16-giu-04	1	19.4	0.957	585.684	0.000586	998.58	33.60
10366	Tal-Barrani 2	16-giu-04	2.184	19.1	1.010	618.12	0.000618	998.67	33.69
10366	Tal-Barrani 2	16-giu-04	2	19.1	1.012	619.344	0.000619	998.67	33.69
10366	Tal-Barrani 2	16-giu-04	1	19.0	1.012	619.344	0.000619	998.69	33.72
10024	Mriehel	28-ott-04	2.755	19.1	1.316	805.392	0.000805	998.81	33.86
10024	Mriehel	28-ott-04	2	19.0	1.311	802.332	0.000802	998.83	33.88
10024	Mriehel	28-ott-04	1	19.0	1.291	790.092	0.00079	998.82	33.87
10075	Mosta Road	28-ott-04	2.062	18.9	0.971	594.252	0.000594	998.69	33.72
10075	Mosta Road	28-ott-04	1	18.9	0.976	597.312	0.000597	998.69	33.72
10366	Tal-Barrani 2	28-ott-04	2.274	19.1	0.996	609.552	0.00061	998.66	33.69
10366	Tal-Barrani 2	28-ott-04	2	19.1	0.998	610.776	0.000611	998.66	33.69
10366	Tal-Barrani 2	28-ott-04	1	19.0	0.998	610.776	0.000611	998.68	33.71
10429	Miaco 2	28-ott-04	2.312	19.4	0.937	573.444	0.000573	998.58	33.59
10429	Miaco 2	28-ott-04	2	19.4	0.943	577.116	0.000577	998.58	33.59
10429	Miaco 2	28-ott-04	1	19.4	0.953	583.236	0.000583	998.58	33.59
10429	Miaco 2	03-nov-05	2.192	19.9	0.193	118.116	0.000118	998.13	33.07

Site I.D.	Site Name	Date	Aquifer Level m asl	Temperature °C	EC mS/cm	TDS=0.612 EC (g/L)	"Salinity" kg/m ³	Density kg/m ³	ALFA
10429	Miaco 2	03-nov-05	2	19.9	0.926	566.712	0.000567	998.47	33.46
10429	Miaco 2	03-nov-05	1	19.9	0.927	567.324	0.000567	998.47	33.47
10366	Tal-Barrani 2	03-nov-05	2.274	19.5	1.004	614.448	0.000614	998.59	33.60
10366	Tal-Barrani 2	03-nov-05	2	19.5	1.003	613.836	0.000614	998.59	33.60
10366	Tal-Barrani 2	03-nov-05	1	19.5	1.003	613.836	0.000614	998.59	33.60
10075	Mosta Road	03-nov-05	1.955	19.4	0.902	552.024	0.000552	998.56	33.57
10075	Mosta Road	03-nov-05	1	19.4	0.969	593.028	0.000593	998.59	33.60
10024	Mriehel	03-nov-05	2.595	19.5	1.288	788.256	0.000788	998.72	33.76
10024	Mriehel	03-nov-05	2	19.4	1.282	784.584	0.000785	998.74	33.78
10024	Mriehel	03-nov-05	1	19.4	1.259	770.508	0.000771	998.73	33.76
10075	Mosta Road	23-mar-06	2.185	19.3	0.943	577.116	0.000577	998.60	33.61
10075	Mosta Road	23-mar-06	2	19.3	0.962	588.744	0.000589	998.61	33.62
10075	Mosta Road	23-mar-06	1	19.3	0.967	591.804	0.000592	998.61	33.62
10024	Mriehel	23-mar-06	3.005	19.4	1.307	799.884	0.0008	998.75	33.79
10024	Mriehel	23-mar-06	3	19.4	1.307	799.884	0.0008	998.75	33.79
10024	Mriehel	23-mar-06	2	19.4	1.309	801.108	0.000801	998.75	33.79
10024	Mriehel	23-mar-06	1	19.4	1.277	781.524	0.000782	998.74	33.77
10429	Miaco 2	23-mar-06	2.302	19.7	0.911	557.532	0.000558	998.50	33.50
10429	Miaco 2	23-mar-06	2	19.8	0.918	561.816	0.000562	998.49	33.48
10429	Miaco 2	23-mar-06	1	19.8	0.924	565.488	0.000565	998.49	33.49
10075	Mosta Road	04-lug-06	2.115	19.4	0.955	584.46	0.000584	998.58	33.60
10075	Mosta Road	04-lug-06	2	19.3	0.961	588.132	0.000588	998.61	33.62
10075	Mosta Road	04-lug-06	1	19.3	0.964	589.968	0.00059	998.61	33.62
10024	Mriehel	06-lug-06	2.645	19.6	1.319	807.228	0.000807	998.72	33.75
10024	Mriehel	06-lug-06	2	19.4	1.268	776.016	0.000776	998.73	33.77
10024	Mriehel	06-lug-06	1	19.4	1.250	765	0.000765	998.72	33.76
10429	Miaco 2	06-lug-06	2.192	20.3	0.875	535.5	0.000536	998.37	33.34
10429	Miaco 2	06-lug-06	2	20.0	0.913	558.756	0.000559	998.44	33.43
10429	Miaco 2	06-lug-06	1	19.9	0.915	559.98	0.00056	998.47	33.46
SEA			Bottom of boreholes	20.0			0.03942	1028.31	

Table 14 Estimate of ALFA starting from the available data of EC and temperature at the top of the aquifer.